AD-A045 769 MASSACHUSETTS INST OF TECH CAMBRIDGE DEPT OF OCEAN E--ETC F/G 20/4
AN EXPERIMENTAL INVESTIGATION OF WALL EFFECTS ON SUPERCAVITATIN--ETC(U)
JUL 77 M R MAIXNER
UNCLASSIFIED 83481-3 N00014-76-C-0358
NL

1 OF 2
AD
A045769

AN EXPERIMENTAL INVESTIGATION OF WALL EFFECTS ON SUPERCAVITATING HYDROFOILS OF FINITE SPAN

by

MICHAEL REX MAIXNER

Report No. 83481-3

July 1977

This research was carried out under the
Naval Ship Systems Command General Hydrodynamics
Research Program Subproject SR 009 01 01
administered by the David W. Taylor Naval Ship Research and
Development Center Contract N00014-76-C-0358

Department of Ocean Engineering

Massachusetts Institute of Technology
Cambridge, Massachusetts 02139

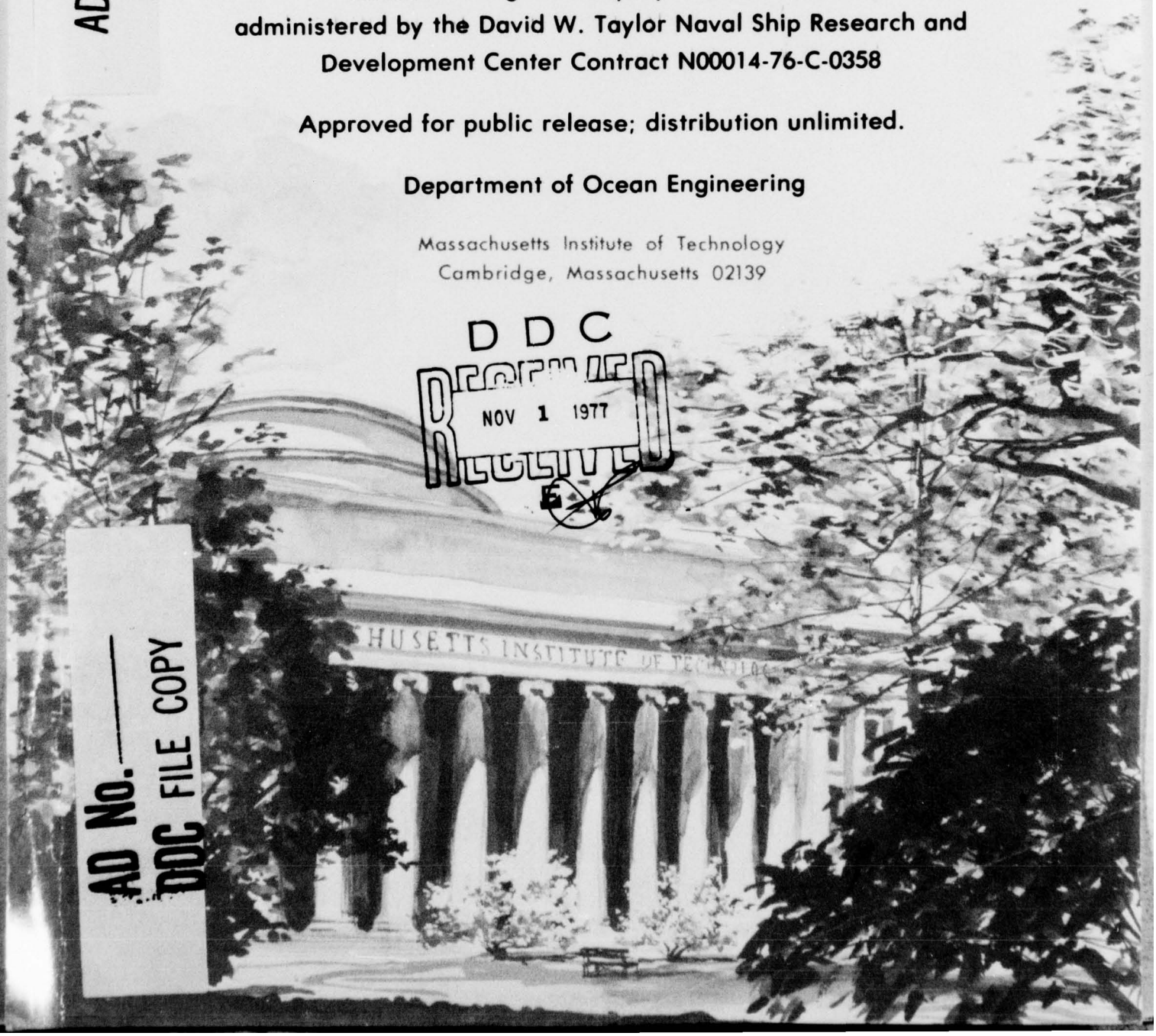

AN EXPERIMENTAL INVESTIGATION OF WALL EFFECTS ON SUPERCAVITATING HYDROFOILS OF FINITE SPAN

by

MICHAEL REX MAIXNER

Report No. 83481-3

July 1977

This research was carried out under the
Naval Ship Systems Command General Hydrodynamics
Research Program Subproject SR 009 01 01
administered by the David W. Taylor Naval Ship Research and
Development Center Contract N00014-76-C-0358

Department of Ocean Engineering
Massachusetts Institute of Technology
Cambridge, Massachusetts 02139

UNCLASSIFIED

SECURITY CLASSIFICATION OF THIS PAGE (When Data Entered)

REPORT DOCUMENTATION PAGE	READ INSTRUCTIONS BEFORE COMPLETING FORM
1. REPORT NUMBER (14) 83481-3 ✓	2. GOVT ACCESSION NO. / 3. RECIPIENT'S CATALOG NUMBER
4. TITLE (and Subtitle) (6) AN EXPERIMENTAL INVESTIGATION OF WALL EFFECTS ON SUPERCAVITATING HYDROFOILS OF FINITE SPAN,	5. TYPE OF REPORT & PERIOD COVERED (9) Technical rept. Oct. 76 — Sep 77
	6. PERFORMING ORG. REPORT NUMBER None
7. AUTHOR(s) (10) Michael Rex Maixner	8. CONTRACT OR GRANT NUMBER(s) (15) N00014-76-C-0358
9. PERFORMING ORGANIZATION NAME AND ADDRESS Massachusetts Institute of Technology Department of Ocean Engineering ✓ Cambridge, Massachusetts 02139	10. PROGRAM ELEMENT, PROJECT, TASK AREA & WORK UNIT NUMBERS SR 009 01 01 — no PE
11. CONTROLLING OFFICE NAME AND ADDRESS David W. Taylor Naval Ship R&D Center Department of the Navy Bethesda, Md 20084	12. REPORT DATE (11) Jul 77
	13. NUMBER OF PAGES ~~100~~ (12) 133 p.
14. MONITORING AGENCY NAME & ADDRESS (if different from Controlling Office) Office of Naval Research 800 N. Quincy Street Arlington, Va 22217	15. SECURITY CLASS. (of this report) Unclassified
	15a. DECLASSIFICATION/DOWNGRADING SCHEDULE

16. DISTRIBUTION STATEMENT (of this Report)

Approved For Public Release: Distribution Unli[illegible]

17. DISTRIBUTION STATEMENT (of the abstract entered in Block 20, if different from Report)

18. SUPPLEMENTARY NOTES Sponsored by the Naval Sea Systems Command General Hydromechanics Research Program administered by the David W. Taylor Naval Ship R&D Center, Code 1505, Bethesda, Md 20084. Presented at the 18th American Towing Tank Conference, Annapolis, Maryland (22-25 August 1977)

19. KEY WORDS (Continue on reverse side if necessary and identify by block number)

Cavity Flow

Hydrofoils

Wall Effects

20. ABSTRACT (Continue on reverse side if necessary and identify by block number)

A geometrically similar family of three supercavitating hydrofoils was tested in the M.I.T. variable pressure water tunnel. The half-span foils were of elliptical planform; the ratio of foil half-span to tunnel height was 1/4 for the small foil, 1/2 for the medium foil, and 3/4 for the largest foil. The tunnel was of square cross section. Lift, drag, moment, tunnel speed, ambient pressure, and cavity pressure were measured for attack

(Over)

DD FORM 1 JAN 73 1473 EDITION OF 1 NOV 65 IS OBSOLETE S/N 0102-014-6601

UNCLASSIFIED

SECURITY CLASSIFICATION OF THIS PAGE (When Data Entered)

406856

angles from 8 to 21 degrees and a variety of ambient pressure settings; cavity length measurements were obtained from photographs. Results were compared with theoretical results obtained by Leehey, and also with a more detailed numerical lifting surface procedure developed by Jiang and Leehey. For the small and medium foils, it was sufficient to correct only for the effect on downwash of the images of the trailing vortices. The large foil data, however, required further correction; upon application of the same corrections which were applied to the data for the two smaller foils, the force and moment data for the large foil plotted slightly lower than did the data for the two smaller foils, while the cavity length data for the large foil indicated cavity lengths significantly larger than for either of the theoretical predictions or the cavity length data for the two smaller foils. Through the application of existing two-dimensional corrections, the force data for the large foil were brought into close agreement with the force data for the two smaller foils, but no suitable correction factors exist for the cavity length data.

AN EXPERIMENTAL INVESTIGATION OF WALL EFFECTS ON SUPERCAVITATING HYDROFOILS OF FINITE SPAN

by

MICHAEL REX MAIXNER

ABSTRACT

A geometrically similar family of three supercavitating hydrofoils was tested in the M.I.T. variable pressure water tunnel. The half-span foils were of elliptical planform; the ratio of foil half-span to tunnel height was 1/4 for the small foil, 1/2 for the medium foil, and 3/4 for the largest foil. The tunnel was of square cross section. Lift, drag, moment, tunnel speed, ambient pressure, and cavity pressure were measured for attack angles from 8 to 21 degrees and a variety of ambient pressure settings; cavity length measurements were obtained from photographs. Results were compared with theoretical results obtained by Leehey, and also with a more detailed numerical lifting surface procedure developed by Jiang and Leehey. For the small and medium foils, it was sufficient to correct only for the effect on downwash of the images of the trailing vortices. The large foil data, however, required further correction; upon application of the same corrections which were applied to the data for the two smaller foils, the force and moment data for the large foil plotted slightly lower than did the data for the two smaller foils, while the cavity length data for the large foil indicated cavity lengths significantly larger than for either of the theoretical predictions or the cavity length data for the two smaller foils. Through the application of existing two-dimensional corrections, the force data for the large foil were brought into close agreement with the force data for the two smaller foils, but no suitable correction factors exist for the cavity length data.

ACKNOWLEDGMENTS

This research was carried out under the Naval Sea Systems Command, General Hydromechanics Research Program, Subproject SR 009 01 01, administered by the David W. Taylor Naval Ship Research and Development Center, Contract Number N00014-76-C-0358. The author is exceedingly grateful to Professor Patrick Leehey of the Department of Ocean Engineering at the Massachusetts Institute of Technology for his inspiration, suggestions, and guidance. Special thanks are also due to S. Dean Lewis and C. W. Jiang, also from M.I.T., who rendered valuable assistance in the performance of the experiments, and to Miss Cheryl Gibson for typing the various drafts and for enduring countless errors. Finally, the author is indebted to his wife, Gretchen, for her unfailing support and encouragement and for the many sacrifices endured by her during the preparation of this report.

TABLE OF CONTENTS

LIST OF FIGURES

NOMENCLATURE

a	foil leading edge bevel length; see Fig. 2
A	aspect ratio = $2s^2/S$
c	foil mean chord, measured at centroid position
C	foil root chord
δ	tunnel correction factor for influence of images of trailing vortex system
C_D	drag coefficient = $\frac{\text{total drag}}{(1/2)\rho U^2 S} = C_{D_{uncor}} + \Delta C_{D_i}$
$C_{D_{uncor}}$	uncorrected drag coefficient, as calculated from the raw experimental data = $\frac{\text{measured drag}}{(1/2)\rho U^2 S}$
C_D'	drag coefficient, corrected for blockage; see equation (1)
ΔC_{D_i}	change in induced drag due to effect of images of trailing vortex system
C_L	lift coefficient = $\frac{\text{measured lift}}{(1/2)\rho U^2 S}$
$C_{L_{2D}}$	two-dimensional lift coefficient; see equation (II-5)
C_M	moment coefficient about the midchord point = $\frac{\text{moment}}{(1/2)\rho U^2 Sc}$
H	tunnel height = 51 cm
$\ell(z)$	cavity length as a function of spanwise position; measured from leading edge
L	cavity length at centroid position; measured from midchord
p_b	minimum pressure along tunnel wall in vicinity of cavity

p_c	measured cavity pressure
p_∞	upstream tunnel static pressure at the spanwise position of the foil centroid
p_v	vapor pressure of water
$\tilde{p}$	tunnel static pressure controller setting
$p_{U,D}$	static pressure signal to controller from upstream, downstream tunnel static pressure taps; see Fig. 3
q_{ij}	strength of discrete source located in the (i,j)-th element
$q(x,z)$	source strength at (x,z)
s	foil half-span
Δs_{ij}	element length for (i,j)-th element
S	planform area of half-span model
S_o	tunnel test section cross-sectional area
t	thickness of hydrofoil
u,v	perturbation velocities in the x,y-directions
U	water velocity one meter upstream of dynamometer shaft axis
V	maximum water velocity (at point of minimum pressure, p_b) in vicinity of cavity
$x_\ell(z)$	chordwise coordinate of leading edge as a function of spanwise position
X_T	distance of cavity pressure tap from midchord
x,y,z	foil coordinates; see Fig. 2
Z_C	distance of centroid of half-span foil model from midspan
Z_T	distance of cavity pressure tap from midspan

α	geometric angle of attack with reference to tunnel side wall; when used in Appendices II and III, α indicates angle of attack in a free stream
α_T	"true" angle of attack, as corrected for effects of images of trailing vortices = $\alpha + \Delta\alpha_i$
$\Delta\alpha_i$	change in angle of attack due to effect of images of trailing vortices
γ	arctan $(2\alpha/\sigma_c)$
γ_{ij}	strength of discrete vortex located in (i,j)-th element
$\gamma(x,z)$	vortex strength at (x,z)
λ	ratio of foil frontal width to tunnel width; see equation (3)
λ_{3D}	ratio of foil frontal area to tunnel cross-sectional area (without foil); see equation (4)
ξ,ζ	dummy variables in the x,z-directions
ρ	density of water
σ_c	cavitation number based on measured cavity pressure = $\frac{p_\infty - p_c}{(1/2)\rho U^2}$
σ_v	cavitation number, based on vapor pressure = $\frac{p_\infty - p_v}{(1/2)\rho U^2}$
σ'	cavitation number, corrected for blockage; see equations (2) and (5)
σ''	cavitation number, based on p_b, p_c, and V, the maximum water velocity = $\frac{p_b - p_c}{(1/2)\rho V^2}$

INTRODUCTION

Corrections for water tunnel wall effects during the testing of subcavitating hydrofoils are essentially the same corrections developed fifty years ago for use in wind tunnel testing of airfoils; references [1] and [2] are standard texts in this area. Only within the last twenty years have wall effects been considered in the case of supercavitating hydrofoils, with the majority of theoretical and experimental work concentrated on two-dimensional hydrofoils. The problem of blockage can be significant; the shape of the foil and cavity combination must be known in order to apply a blockage correction of the type utilized in subcavitating flow. Unfortunately, this proves to be an area of great difficulty in the various theories. Corrections to drag coefficient and cavitation number for the two-dimensional pure-drag case are given in references [3] through [7]; a nonlinear theoretical model of the two-dimensional lifting problem is formulated in reference [6]. In reference [8], Baker converts this model into a computer program which numerically calculates the wall effect on two-dimensional hydrofoils of arbitrary shape. It was hoped by Baker that these results would prove adequate for application to flows over high aspect ratio hydrofoils. Prior to the current research, a systematic series of experiments which exhibit

wall effects on a geometrically similar family of hydrofoils had not been carried out in either the two- or three-dimensional case. The purpose of the present research is to make available data on a geometrically similar family of three supercavitating hydrofoils of finite span, and to apply existing two-dimensional corrections in an attempt to bring the data into agreement with three-dimensional, unbounded flow theory.

EXPERIMENTAL APPARATUS AND PROCEDURE

Apparatus

The experiments were conducted in the M.I.T. recirculating, variable pressure water tunnel (Fig. 1). The test section is 51 cm square in cross-section, and 147 cm long. Test section velocity was continuously variable between 0 and 9.1 m/sec; a manometer indicated the difference in pressure across a contraction in the tunnel one meter upstream of the dynamometer axis. This manometer had been previously calibrated using a pitot tube in the test section. The assumption was made that the blockage caused by the foil and cavity combination did not affect the manometer appreciably. Test section static pressure was variable between 60 mm Hg absolute and atmospheric pressure; static pressure readings were taken using a mercury manometer connected to either or both of two taps on the centerline of a side wall of the test section. These taps were located 62 cm upstream and downstream of the hydrofoil dynamometer, which was located at the center of the test section.

Foil dimensions are given in Fig. 2. The three half-span, aspect ratio five foils had sharp leading edges. Geometrically similar elliptical planforms were chosen even though foils of this type were more difficult to fabricate than, for example, foils of rectangular planform; elliptical

planform foils exhibit less tip loading effect than do rectangular planform foils, thereby rendering them more amenable to analysis. Each foil was drilled with a hole terminating in a pressure tap on the cavity side of the foil. The medium-sized foil was the aspect ratio five foil utilized by Leehey and Stellinger [9], except that the cavity pressure tap was relocated to a position nearer the tip. The composition of the medium foil was of type 304 stainless steel, while that of the small and large foils was of type 614 aluminum bronze. Each foil was welded to its own 10.16 cm diameter mounting plate; the mounting plates, in turn, were bolted to the dynamometer so that the small, medium, and large foils protruded 1/4, 1/2, and 3/4 of the way, respectively, downward from the top window into the test section.

The dynamometer was capable of measuring three moment and three force components, but only the moment about midchord and the forces tangential to and perpendicular to the span and chord were measured. Zero geometrical angle of attack was set by aligning the flat (wetted) side of each foil with the test section side wall. Upon alignment, a sighting telescope, which was attached to the dynamometer, was aligned with a scale on the laboratory wall; this scale, graduated in increments of 0.05 degree, was utilized in setting the geometrical angle of attack.

Procedure

Before test runs were begun on any one day, the tunnel was operated at medium velocity for twenty minutes at a pressure of 300 mm Hg absolute; this removed almost all of the air trapped in remote locations of the tunnel. Prior to each test run, the bubble chamber shown in Fig. 3 was utilized to collect and draw off any gases or air which may have been trapped in the static pressure sensing line; once cleared of gases, the bubble chamber was merely a reservoir of common pressure. On the other hand, small amounts of air were bled intermittently into the cavity pressure sensing line during testing in order to keep it free of moisture.

Each foil was tested at a variety of attack angles from 8 to 21 degrees. The lower limit of 8 degrees was chosen so that the cavities would not terminate on the foil. For all test runs, the test section velocity was set at 8.5 m/sec, whereupon static pressure was reduced until a cavity covered the entire planform. Readings were taken of lift, drag, moment, static pressure (with pressure taps U and D open; see Fig. 3), cavity pressure, and velocity. A Polaroid photograph was taken of the foil and cavity from the wetted side of the foil, utilizing an exposure time of 1/40 second with bottom flood lighting. Pressure tap D was then closed, and the same readingstaken; reopening pressure tap D and closing pressure tap U, the same series of readings was repeated once more. (Photographs were not

taken for these last two pressure tap combinations since hardly any variation in cavity shape or length was noted when compared to the situation where both pressure taps were open.) This completed the measurement of three data points at one controller setting. Both pressure taps were then opened, and the static pressure was reduced by 20 to 30 mm Hg, whereupon the above procedure was repeated. The static pressure was reduced in this fashion until an excessive number of recirculated cavitation bubbles resulted in either extremely poor conditions for photography or rapidly fluctuating instrument readings. Prior to and immediately following a run of this type, the room and water temperatures were recorded, as were the tares on the instrumentation.

A computer program was utilized in the data reduction. Wetted surface frictional drag (for each foil and its mounting plate) and dynamometer shaft twist were taken into account, and test section static pressure readings were modified for static head difference to give the static pressure at the vertical position of the foil centroid. (Gravity effects were otherwise neglected.) Cavitation number was computed using measured cavity pressure, and also by using vapor pressure at the ambient water temperature (computed using equation (2) on page 151 of reference [10]). Lift, drag, and moment coefficients

were also calculated. Standard wind tunnel corrections (as described in Appendix I) were applied to the data to account for the effect of the images of the trailing vortices; this resulted in an increase in drag coefficient and also in an increase in effective angle of attack. Utilizing the photographs, cavity lengths were measured from the midchord at the centroid position.

RESULTS

Experimental results were compared with predictions from Leehey's linearized theory [11], which utilizes the method of matched asymptotic expansions; the theory is valid to first order in angle of attack, and to second order in the reciprocal of aspect ratio. Comparisons were also made with a more detailed linear lifting surface calculation developed by Jiang and Leehey [12]. This numerical theory is expected to be more accurate at the lower values of σ_c/α_T, where the cavity length is the same size as the foil span or longer; it should also be more accurate, in general, for prediction of moment coefficients. Synopses of the theories developed in references [11] and [12] are given in Appendices II and III, respectively; the experimental data are given in Appendix IV, both in raw form and with standard wind tunnel corrections (Appendix I) applied.

The wall boundary layer momentum thickness was approximately 1.9 mm, as inferred from measurements by Stellinger under similar conditions [9]. Since less than two percent of the wetted surface area of the small foil was within 1.9 mm of the upper wall, the upper wall boundary layer was assumed to have negligible effect on the force and moment coefficients of all three of the foils tested.

It should be noted that the only correction for wall effect which has been applied to the data in Figs. 4 through 30 is the correction for the effects of the images of the trailing vortices (Appendix I). Also worthy of note is the fact that the supercavitating condition was never achieved for the small foil at an angle of attack of 8 degrees. This fact bears upon the lack of scaling evident in the force and moment data of Figs. 4, 12, and 20 for this foil. This matter will be considered again in the subsequent discussion section.

Lift (Figs. 4 through 11)

There was very good agreement, overall, between theoretical predictions and the experimental data. For small values of the similarity parameter σ_c/α_T (i.e., for long cavities), there was much better agreement with the numerical theory than with the asymptotic theory; in this case, the foil and cavity combination no longer has a large aspect ratio. For the higher values of σ_c/α_T, Leehey's theory appears to underpredict, especially at the higher angles of attack. This is in apparent contradiction with Fig. 4 of reference [9]; it should, however, be noted that the data of reference [9] were based on cavitation numbers calculated with vapor pressure rather than with measured cavity pressure. It can be seen from Figs. 32

through 35 of the present work that, when based on measured cavity pressure, the cavitation number will be smaller, so that the above contradiction is only apparent. The small and medium foil data plotted almost on top of one another, whereas the large foil data plotted lower than did the small and medium foil data, especially at attack angles greater than 11 degrees.

Drag (Figs. 12 through 19)

When the effects of streamwise foil or flow curvature are negligible, linear theory predicts $C_D = \alpha_T C_L$, so that the drag data are plotted as C_D/α_T^2 vs. σ_c/α_T. C_D/α_T^2 plotted somewhat higher than the theoretical predictions except for very long or for very short cavities. As with the lift data, the small and medium foil data plotted together, with the large foil data plotting somewhat below these, the effect becoming more pronounced at the higher angles of attack.

Moment (Figs. 20 through 27)

The moment coefficient was taken about the midchord consistent with the right-hand rule. As pointed out by Leehey and Stellinger [9], Leehey's matched asymptotic expansion theory neglects lifting surface corrections (third order in the reciprocal of aspect ratio) for the moment coefficient. It is not surprising, therefore, that

the current experimental data agreed best with the more detailed lifting surface theory of Jiang and Leehey [12]. The load cell utilized for moment measurements on the small foil was of inadequate sensitivity, and consequently, much of the small foil data at the smaller attack angles may be less accurate than the data for the medium and large foils; comparisons must therefore be made between the large and the medium foil data. Once again, the large foil data plotted below that of the medium foil, especially at the larger attack angles.

Cavity Length (Figs. 28 through 31)

As mentioned previously, cavity lengths were measured from midchord at the centroid position rather than from the leading edge, since this convention was utilized by Leehey [11]. Cavity length (L) was nondimensionalized on the foil mean chord (c). The cavity length data for the small and medium foils plotted on top of one another (Figs. 28 and 29); in both cases, the cavity lengths were slightly less than those predicted by theory, but the overall agreement with theory was good. In contrast, there was a marked deviation in the large foil cavity length (Fig. 30) and shape (Fig. 31), especially at the root, where local blockage was the worst. The tip vortices seen in the photographs had no evident effect upon the force or moment coefficients. Neither

Leehey's matched asymptotic expansion theory nor the numerical lifting surface theory developed by Jiang and Leehey accounts for the roll-up effects which produced these isolated trailing vortices in the wake.

Representative photographs of the large, medium, and small foils at the same angle of attack and at approximately the same cavitation number are shown in Fig. 31. The cavity shapes shown were averaged over the exposure time of 1/40 second; visual observations showed that the instantaneous cavity shape was highly unsteady. For the small and medium foils, the general outline of the cavity was elliptical, as predicted by theory; the cavity length was undoubtedly reduced toward the tip due to the hydrostatic pressure gradient existing in the tunnel.

Cavitation Number (Figs. 32 through 35)

Below a cavitation number of approximately 0.4, there was almost no difference between cavitation number calculated with measured cavity pressure or with vapor pressure. It should be noted that in this region there exists a large variation in cavity length from very short to very long. This indicates that for even short cavities, where ram effects of the re-entrant jet from the cavity end have heretofore been thought to have a pronounced effect on measured cavity pressure, the actual cavity pressure was approximately equal to the vapor pressure of the water.

Above a cavitation number of 0.4, the disparity between σ_v and σ_c increased with increasing cavitation number; the data in this region, however, were only for large angles of attack and small cavity lengths, indicating that there may indeed have been some effect caused by the impinging of the re-entrant jet on the cavity pressure tap.

After the series of basic experiments was completed, ram effects were further investigated on the large foil by Jiang and Leehey, this time utilizing a total head tube for cavity pressure measurement. The L-shaped total head tube protruded downwards into the cavity from the upper tunnel wall so that it was parallel to the foil wetted surface and pointed towards the leading edge and away from the impinging re-entrant jet. Cavity pressure readings were taken with both the standard foil surface pressure tap previously utilized and the total head tube, and vapor pressure was calculated as was done previously; results are shown in Fig. 35. For the larger attack angles and shorter cavities (higher cavitation numbers), use of the total head tube significantly reduced re-entrant jet effects; the result was that cavitation numbers calculated with total head tube data were as much as 5 to 8 percent higher than cavitation numbers calculated with data obtained from the previously used foil surface tap. Although a similar check was not made on the small and medium foils, it can be assumed that the same general trend would occur. It should

be noted, however, that data points in Figs. 32 and 33 exhibit a more pronounced downward "hook" at higher cavitation numbers than do the large foil data (Figs. 34 and 35), a fact which accounts for the noticeable "hooks" in the lift and moment data at the higher angles of attack (see, for example, Figs. 10, 11, 26, and 27). If the total head tube had been utilized throughout the entire series of experiments, these deviations from theory at high attack angles and short cavities would probably have been less.

Influence of Static Pressure Controller

As stated earlier, readings were taken for the various combinations of the two static pressure taps; this was done in order to determine the effect of blockage on pressure and velocity at the two different tap positions. It was anticipated that this variation in static pressure tap combination would have no effect on the forces and moments experienced by the foil. Due to the location within the system of the static pressure controller (Fig. 3) (which was inadvertently overlooked), the forces and moments varied significantly when the combination of static pressure taps was changed. The explanation for this is as follows. Before data were taken, both static pressure taps were opened and the controller setting reduced to $\tilde{p}$; the actual static pressure in the tunnel was decreased by the control system

until the combined signal from both taps was $\tilde{p}$. When the instrument readings settled out, data were taken. The downstream static pressure tap was then closed, so that the only signal to the controller was p_U, which was greater than the controller setting, $\tilde{p}$. The controller therefore lowered the actual static pressure in the tunnel until p_U equaled $\tilde{p}$. Consequently, the effective cavitation number (as seen by the foil) decreased, causing the cavity to grow. This reduced the effective camber of the foil and cavity combination; this loss of effective camber resulted in a reduction of the force and moment coefficients from their previous values. On the other hand, the measured cavitation number increased slightly due to a small decrease in measured cavity pressure; the presence of the controller prevented the measured static pressure from changing significantly. The opposite effect was observed with the upstream tap open and the downstream tap closed (i.e., an increase in force and moment coefficients, an increase in effective cavitation number, and a slight decrease in measured cavitation number when compared to the case when both pressure taps were open); there were only a few of these data points taken.

Although the desired pressure readings were not obtained in the current experiment (i.e., the actual tunnel static pressure was different for each of the tap combinations), the results do show the significance of the blockage. When

comparing the results obtained with the different tap combinations for the small and medium foils, there was very little change in the plotted data points; the increased blockage in the case of the large foil resulted in significantly different force and moment data. For the sake of clarity, the data for the different tap combinations are shown only for the large foil at an angle of attack of 14 degrees. Unless otherwise specified, further remarks concerning foil data will be for the data obtained with both static pressure taps open.

The general trend of the data agrees with the experimental results obtained by Kermeen (see page 37 of reference [13]); he observed that the longer the cavity in supercavitating flow, the smaller the force coefficients. The same conclusion follows from the theoretical results of Leehey, as may be seen from Fig. 4 of reference [9].

At a later time, the system indicated by the dashed lines in Fig. 3 will be utilized to obtain data on the large foil; the present system would be operated with only tap U open to provide an indication of static pressure at "infinity" to the controller. This configuration will allow pressure measurements to be made without affecting the input signal to the static pressure controller.

DISCUSSION

For the small and medium foils, it appears to be necessary to correct only for the effects of the images of the trailing vortices in accordance with standard wind tunnel procedure. These corrections to drag coefficient and effective angle of attack brought the data into good agreement with theory; the lift, moment, and cavity length data also agreed well with theoretical predictions. For the most part, the plots for the small and medium foils were very close to each other.

Upon application of the same corrections to the large foil data, good agreement with theory was seen for the force and moment coefficients; they were, however, generally lower than the data for the smaller foils, especially at higher attack angles. The plot of cavity length for the large foil, however, showed substantially longer cavities than predicted by either of the two theoretical models used for comparison. The most pronounced deviations in cavity length occurred for the long cavity (lower σ_c/α_T) data.

When compared with the data obtained from the two smaller foils, the general trend of the large foil data is in agreement with Baker's predictions for wall effects on two-dimensional supercavitating hydrofoils [8]. Baker makes the point that the wall effect is negligible for tunnel

height-to-foil chord ratios (H/c) greater than 10 for cambered foils. Although he makes no such generalizations concerning supercavitating flat plates, (i.e., the case applicable to the current research), it is seen from Figs. 4 through 27 that the effect of blockage on the force and moment coefficients is not exceedingly large. The following line of reasoning explains why the force and moment data for the large foil were somewhat lower than for the two smaller foils. For the three foils at the same cavitation number and at the same angle of attack, the magnitude of the velocity on the cavity wall of all three foils is $\sigma_c/2$ (from linearized theory); consequently, all three foils have identical pressure coefficients on the cavity. The largest foil experiences significantly more blockage than does either of the smaller foils, so that the velocity on the wetted surface of the large foil is much higher than for either of the smaller foils; the pressure coefficient on the wetted surface of the largest foil is therefore the least of all three foils, resulting in smaller lift, drag, and moment coefficients than for either of the smaller foils. It is interesting to note that this overall effect is contrary to blockage effects experienced in subcavitating water tunnel or wind tunnel testing, where force and moment coefficients are increased.

Baker also questions the sharp increase in wall effect predicted by Wu, Whitney, and Lin [6] for thin symmetric wedges or for small attack angles in the lifting flow case. The results of the present work do not show a marked increase in wall effect on force and moment coefficients at the lower angles of attack, in agreement with Baker.

Conversely, Baker's results indicate that the wall effect on the cavity plus wake can be tremendous. In the current research, this is, in fact, the most significant departure of the large foil data from the theoretical predictions and from the data of the two smaller foils (Figs. 28 through 30).

Several attempts were made to bring the large foil data into closer agreement with the small and medium foil data by using existing two-dimensional blockage corrections. Wu, Whitney, and Brennen [4] derive wall effect corrections for the two-dimensional pure-drag (wedge) case, employing the open-wake and Riabouchinsky models. Wu, Whitney, and Lin [6] consider wall effects in two-dimensional lifting cavity flows, a situation more applicable to the current research; Baker [8] utilizes a computer program to translate this into information which could be readily applied to correct experimental data.

The pure-drag, open-wake model employs corrections to both drag coefficient and cavitation number. The drag coefficient corrected for blockage, C_D', can be expressed as

$$C_D' = \left[\frac{1+\sigma'}{1+\sigma_c}\right] C_D + O(\lambda^2), \tag{1}$$

where σ', the cavitation number corrected for blockage, is given by

$$\sigma' = \sigma_c - \left[\frac{1+\sigma_c}{\sigma_c}\right] C_D\lambda + O(\lambda^2), \tag{2}$$

where σ_c is the measured cavitation number, C_D is the drag coefficient as defined in the nomenclature, and λ is the ratio of foil frontal width to tunnel width, which may be expressed as

$$\lambda = \frac{\text{(mean chord) x sin}(\alpha)}{\text{tunnel width}}. \tag{3}$$

For the large foil with λ defined in this fashion, $\lambda \cong 0.30$ sin (α). Application of the above corrections to the large foil data shifted the data points down and to the left on the plots of C_D/α_T^2 vs. σ_c/α_T (Figs. 12 through 19) but did not bring the data into any closer agreement with the small and medium foil data. When the cavity length data for the

large foil were replotted using the corrected cavitation numbers, the data points in Fig. 30 were moved downward; this downward movement was not sufficient, however, to bring the large foil cavity lengths into agreement with either theory or the small and medium foil data.

Actually, the straightforward application of such a two-dimensional correction to the case of a finite-span wing should overcorrect for blockage, making λ much larger than it should be. Perhaps a better representation of λ for the finite-span case would be

$$\lambda_{3D} = \frac{\text{foil frontal area}}{\text{tunnel cross-sectional area (without foil)}} = \frac{\text{(foil planform area) x sin } (\alpha)}{\text{tunnel cross-sectional area (without foil)}} . \quad (4)$$

Recalculating the corrections using λ_{3D} in place of λ in equations (1) and (2) would make the corrections even smaller than previously calculated. Since the previous corrections proved to be inadequate, there is no reason to believe that the modified corrections should be any better.

To correct measured cavitation number and measured drag coefficient utilizing the Riabouchinsky model, it is necessary to obtain p_b, the minimum pressure reading along the wall in the region of the cavity. Equation (1) is again

used to correct the drag coefficient, but now the corrected cavitation number is calculated as

$$\sigma' = (2/3)\sigma_c + (1/3)\sigma'' \qquad (5)$$

where σ'' is the cavitation number based on p_c, p_b, and maximum velocity, V, and where σ_c is the cavitation number based on p_c, p_∞, and upstream velocity, U. It had orginally been hoped that a reasonably close measurement of the minimum pressure could be obtained by using only the downstream tap (tap D in Fig. 3); as was shown earlier, the interaction of the static pressure controller precluded making this measurement accurately. In an attempt to apply the correction based on the Riabouchinsky model, the gross assumption was made that the maximum frontal area of the cavity was approximately the same as the frontal area of the foil; utilizing a continuity argument and the steady-flow Bernoulli equation, the pressure minimum was estimated, thus allowing application of the wall effect correction based on the Riabouchinsky model. Unfortunately, this procedure gave results which were comparable to those obtained using the open-wake model. The failure of both models in the current application should not be surprising since they were designed for two-dimensional, pure-drag cavity flows, and not for three-dimensional, lifting cavity flows.

Whereas the pure-drag wall effect corrections changed both drag coefficient and cavitation number, the results of Baker's computerization of the two-dimensional Wu, Whitney, and Lin [6] lifting case wall effect model are presented in terms of a change to the force coefficients (i.e., drag and lift coefficients in this case), referenced to the uncorrected measured cavitation number, σ_c. Accordingly, Baker's corrections to the lift and drag coefficients are expressed as a percentage difference from the free stream condition. He presents data for only one ratio of tunnel height-to-arclength (i.e., chord length), H/c = 4. Calculating this ratio using the mean chord of the large foil gives H/c $\tilde{=}$ 3.33; recalculating H/c as the ratio of tunnel cross-sectional area to foil area, H/c $\tilde{=}$ 4.48 is obtained. It was concluded, therefore, that the H/c = 4 corrections given by Baker should be suitable for correction of the large foil data. Upon application of these additive corrections to both lift and drag data, it was found to bring the large foil data into close agreement with the small and medium foil data.

Because an infinite wake model is utilized in reference [8], Baker's results give no correction for the extremely large cavity lengths recorded for the large foil. His results do show, however, that as blockage increases,

the nondimensional cavity thickness increases. This was borne out nicely when the cavitation characteristics of the three foils utilized in the current research were compared at an angle of attack of 8 degrees. On the small foil, which produced the least blockage, supercavitation was never totally achieved, no matter how low the static pressure was brought. For the medium and large foils, which produced more blockage than did the small foil, cavity termination was achieved behind the foil over a range of static pressures.

CONCLUSIONS

As a general rule, the agreement of the experimental data with unbounded flow theory was good for the small and medium foils, whose ratios of half-span to tunnel width were 1/4 and 1/2, respectively, and whose ratios of tunnel height to mean chord were approximately 10 and 5, respectively. It appeared that in order to bring the small foil and medium foil data into agreement with theory, it was necessary to apply only standard wind tunnel procedures in correcting for the effects of the images of the trailing vortices.

Of the three geometrically similar aspect ratio five foils, the largest foil, which protruded 3/4 of the way into the tunnel, and which had a ratio of tunnel height to mean chord of approximately 3.33, had force and moment data which were close to the small and medium foil data, although slightly lower; the cavity length data for the large foil differed greatly from the small and medium foil data, showing much longer cavities for the same ratio of cavitation number to angle of attack. It is evident that blockage corrections are required in addition to the standard wind tunnel down-wash corrections.

Application and modification of blockage corrections based on various two-dimensional pure-drag cavity flow models failed to bring the large foil data into agreement with the

data for the two smaller foils. It was found, however, that corrections based on a two-dimensional lifting cavity flow model brought the large foil force coefficient data into much closer agreement with the small and medium foil data. While these force coefficient corrections were found to give an "engineering order of accuracy," no corrections have been found which give adequate corrections to the large foil cavity length data; it is clearly evident that further analytical work is necessary in this area.

It is recommended that for future experiments, a static pressure measuring system similar to that depicted in Fig. 3 be utilized.

REFERENCES

1. Pope, A., and Harper, J.J., Low Speed Wind Tunnel Testing. Wiley, New York, 1969.

2. Pankhurst, R.C., and Holder, D.W., Wind-Tunnel Technique. Sir Isaac Pitman & Sons, Ltd., London, 1965.

3. Whitney, A.K., "A Simple Correction Rule for Wall Effect in Two Dimensional Cavity Flows," Cavitation State of Knowledge, ASME, New York, 1969, p. 138.

4. Wu, T.Y., Whitney, A.K., and Brennen, C., "Cavity-Flow Wall Effects and Correction Rules," Journal of Fluid Mechanics, Vol. 49, Part 2, 1971, p. 223.

5. Wu, T.Y., Whitney, A.K., and Brennen, C., "Wall Effects in Cavity Flows and Their Correction Rules," Non-Steady Flow of Water at High Speeds, Proceedings of the IUTAM Symposium in Leningrad, June 22-26, 1971, Nauka Publishing House, Moscow, 1973, p. 461.

6. Wu, T.Y., Whitney, A.K., and Lin, J.D., "Final Report: Wall Effects in Cavity Flows," Calif. Inst. of Tech. Div. of Eng. & App. Sci. Report No.E-111A.5, 1969.

7. Whitney, A.K., Brennen, C., and Wu, T.Y., "Experimental Verification of Cavity-Flow Wall Effects and Correction Rules," Calif. Inst. of Tech. Div. of Eng. & App. Sci. Report No. E-97A-18, 1970.

8. Baker, E., "Analytical Prediction of Wall Effect on Fully Cavitating Lifting Foils Using Nonlinear Theory," NSRDC Report 3688, 1972.

9. Leehey, P. and Stellinger, T.S., "Force and Moment Measurements of Supercavitating Hydrofoils of Finite Span with Comparison to Theory," Journal of Fluids Engineering, Vol. 97, No. 4, December 1975, p. 453.

10. Smith, L.B., Keyes, F.G., and Gerry, H.T., "The Vapor Pressure of Water, Part II, Steam Research Program," Proceedings of the American Academy of Arts and Sciences, published by the Society, Boston, Vol. 69, 1934, p. 137.

11. Leehey, P., "Supercavitating Hydrofoil of Finite Span," Non-Steady Flow of Water at High Speeds, Proceedings of the IUTAM Symposium in Leningrad, June 22-26, 1971, Nauka Publishing House, Moscow, 1973, p. 277.

12. Jiang, C.W., and Leehey, P., "A Numerical Method for Determining Forces and Moments on Supercavitating Hydrofoils of Finite Span," Proceedings of the Second International Conference on Numerical Ship Hydrodynamics, September 1977 (to be published).

13. Kermeen, R.W., "Experimental Investigations of Three-Dimensional Effects on Cavitating Hydrofoils," Journal of Ship Research, Vol. 5, No. 2, September 1961, p. 22.

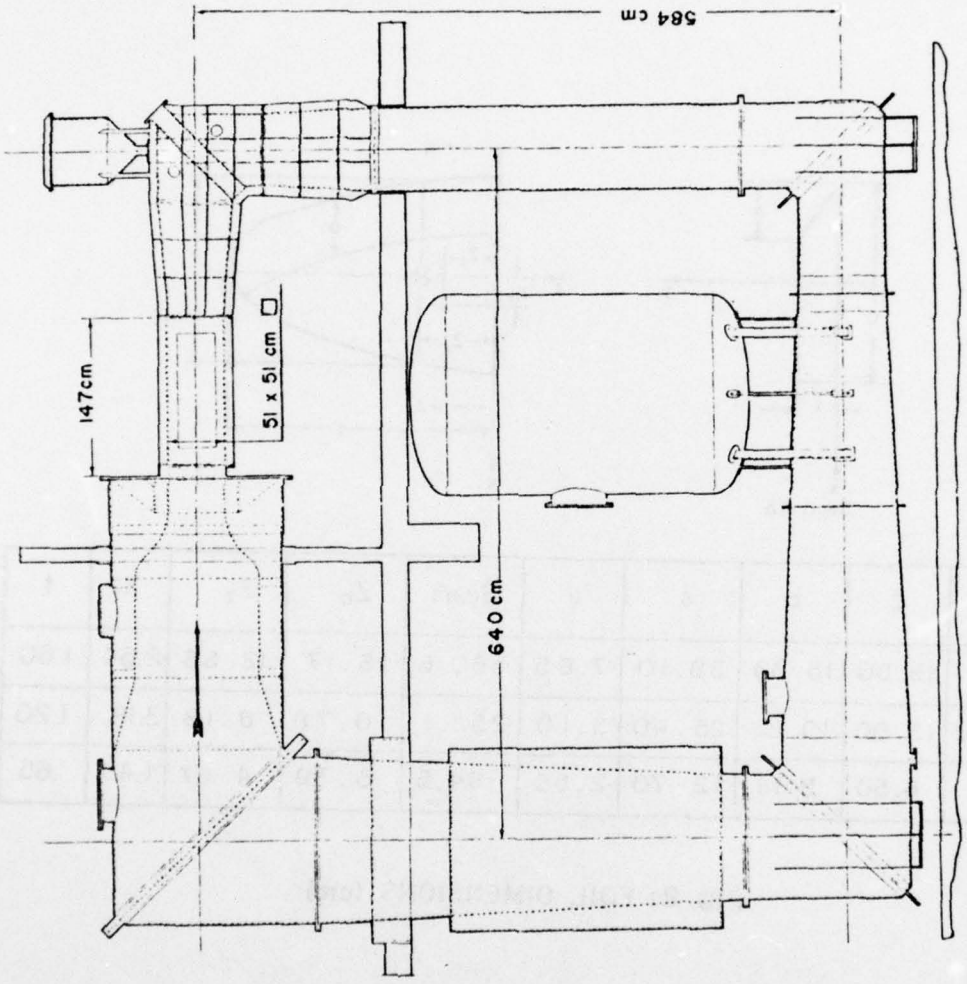

FIG. 1 : M.I.T. TEST FACILITY

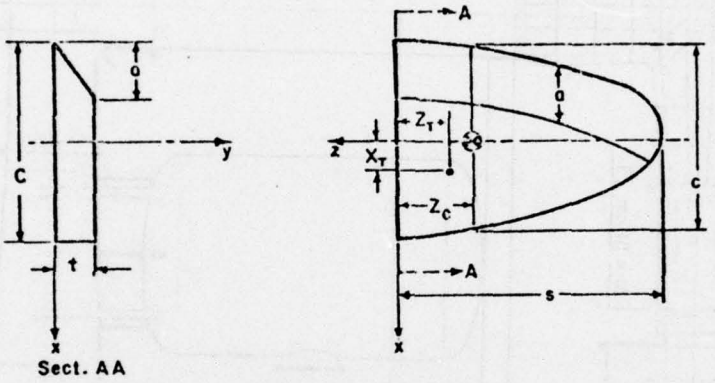

FOIL	C	c	s	a	S(cm²)	Z_C	Z_T	X_T	t
LARGE	19.50	15.33	38.10	7.65	580.6	16.17	12.55	2.54	1.60
MEDIUM	13.00	10.22	25.40	5.10	258.1	10.78	8.18	3.18	1.20
SMALL	6.50	5.11	12.70	2.55	64.5	5.39	4.67	1.43	.65

FIG. 2: FOIL DIMENSIONS (cm)

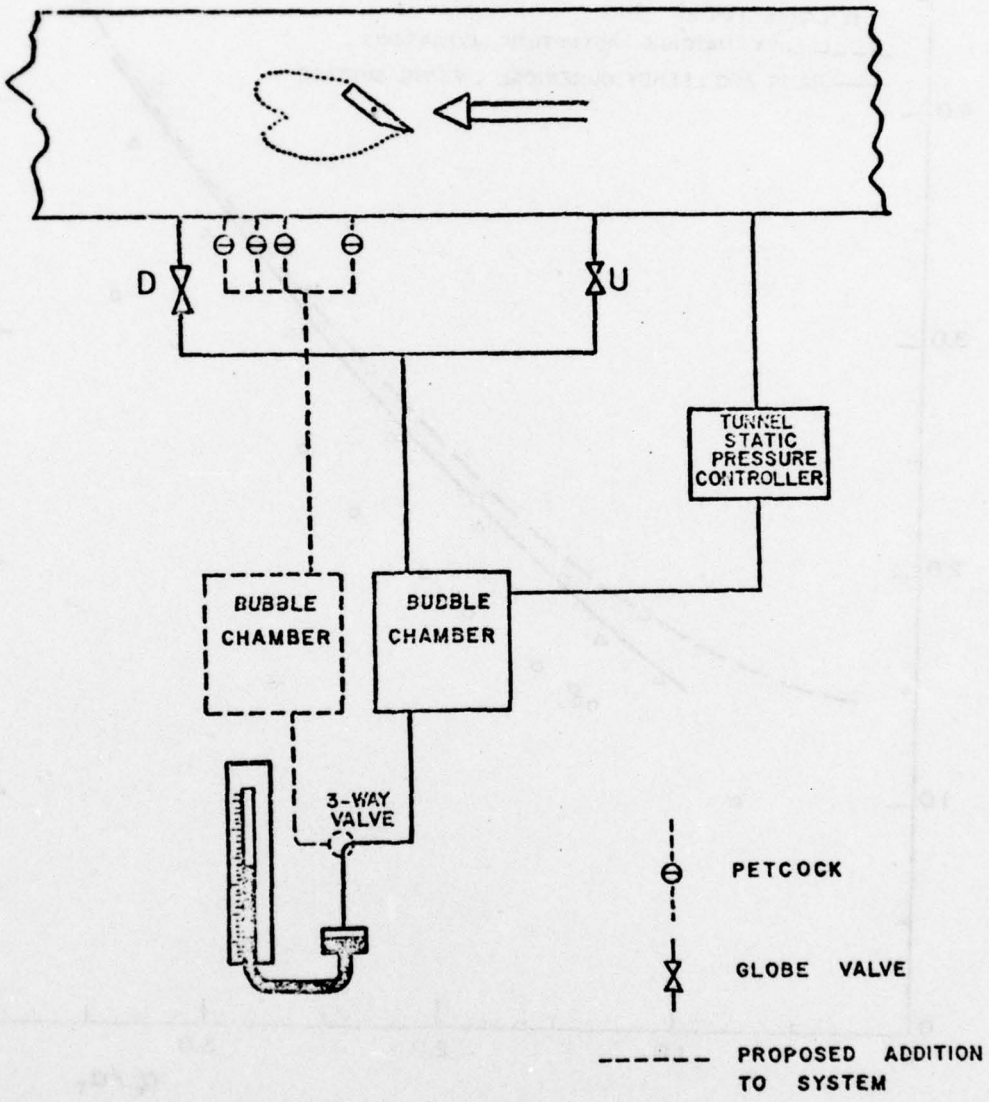

FIG.3 : STATIC PRESSURE MEASUREMENT

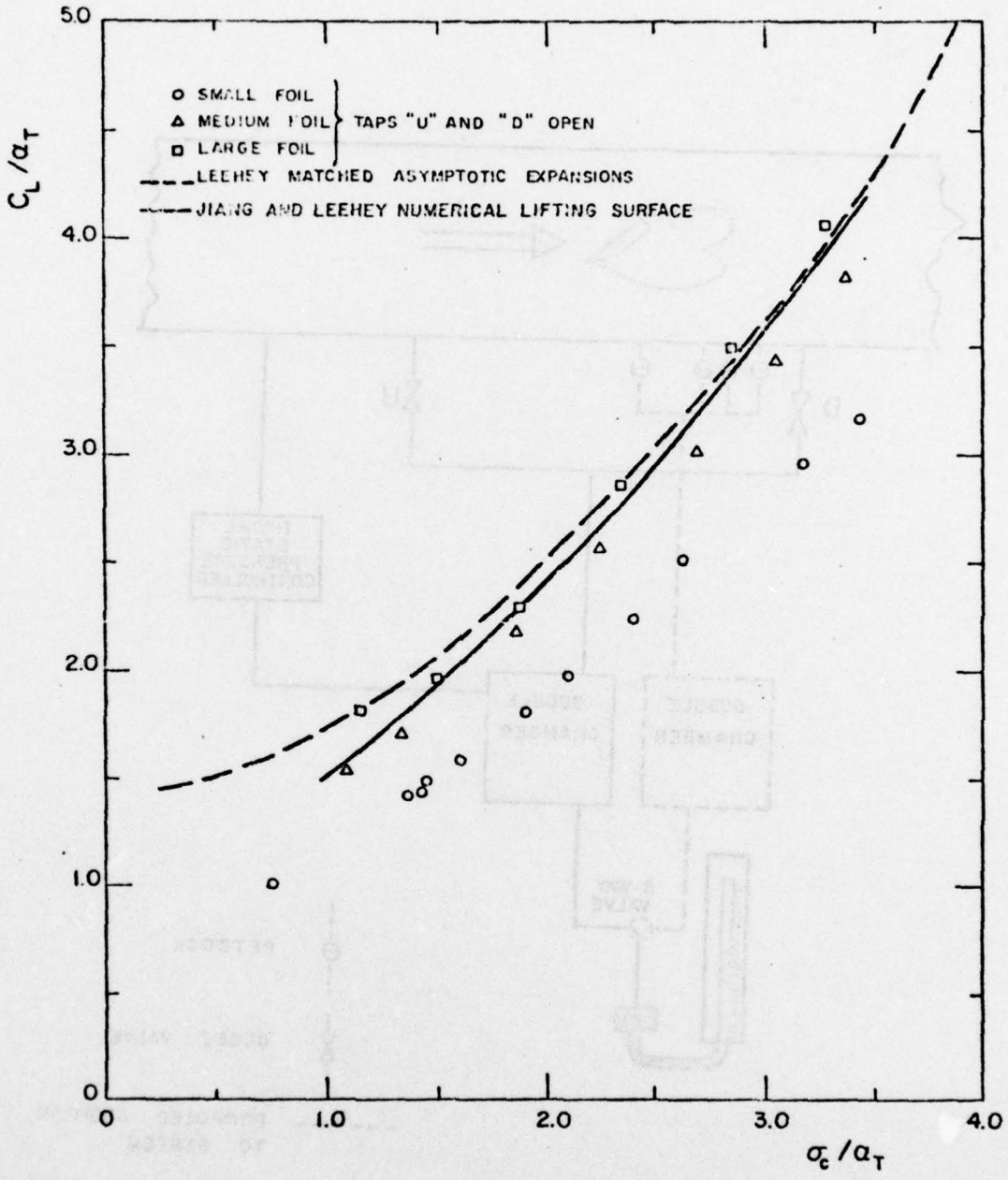

FIG. 4: C_L/α_T vs σ_c/α_T, $\alpha = 8.0°$

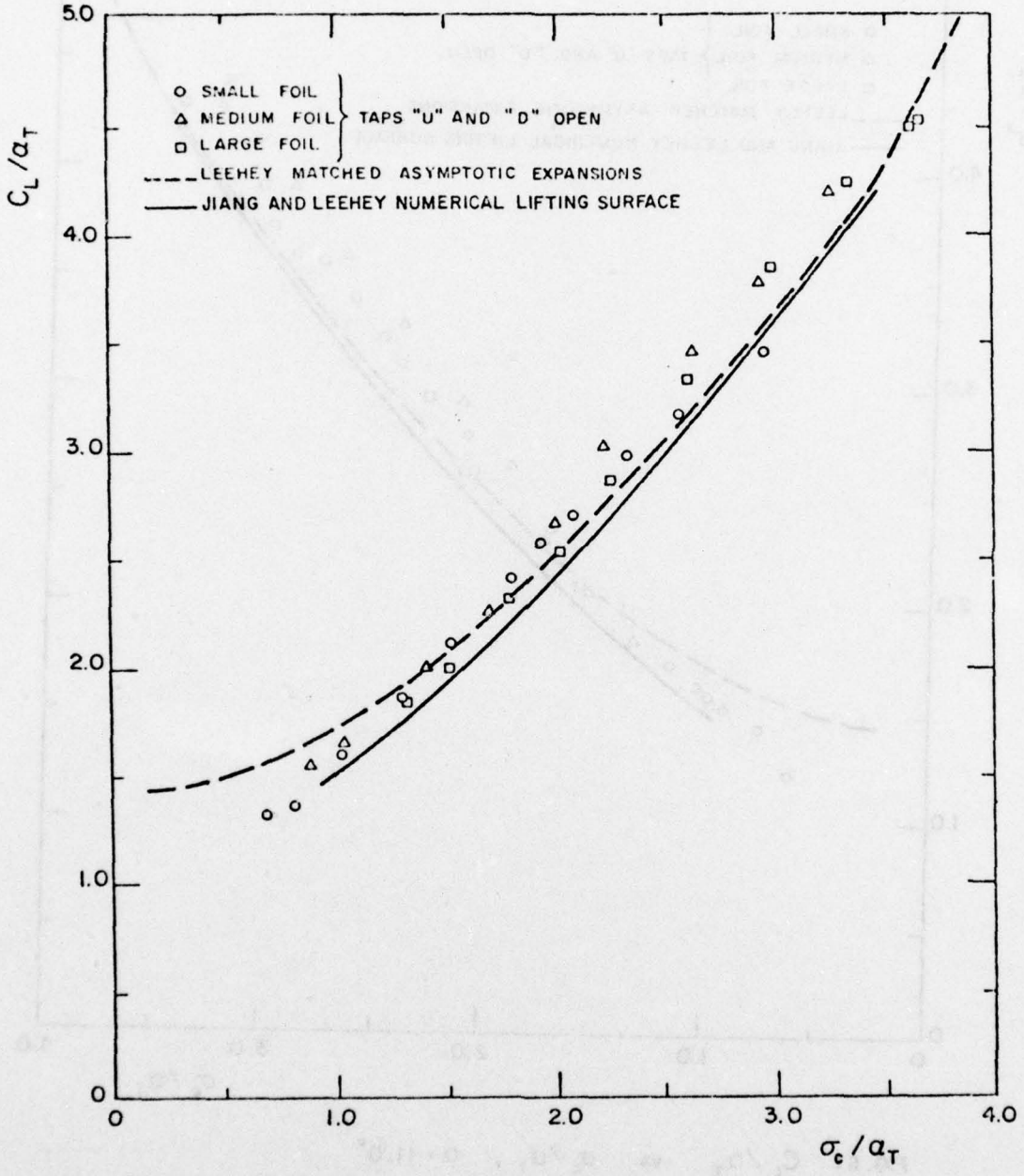

FIG. 5: C_L/a_T vs σ_c/a_T, $\alpha = 9.5°$

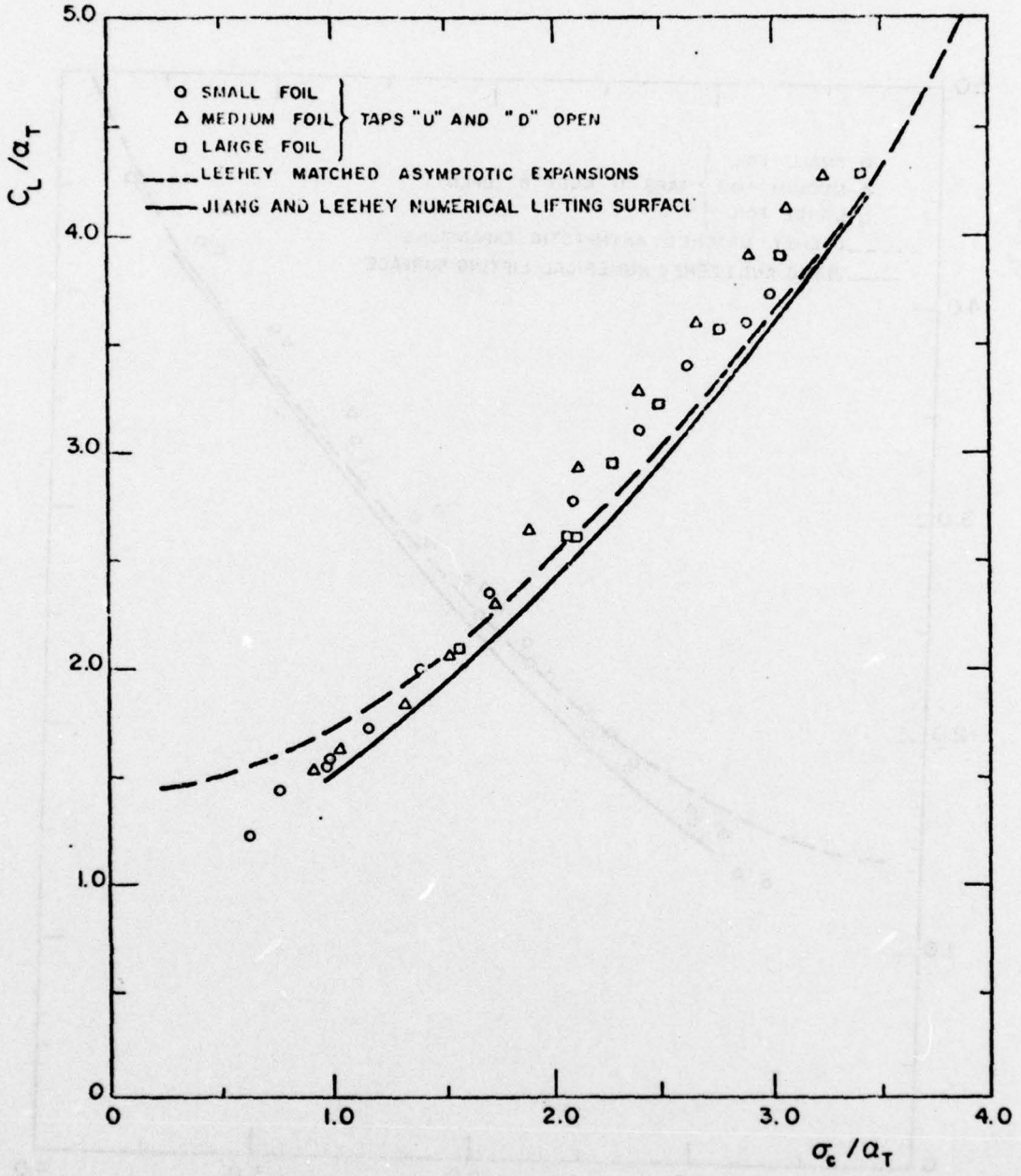

FIG. 6: C_L/α_T vs σ_c/α_T, $\alpha = 11.0^\circ$

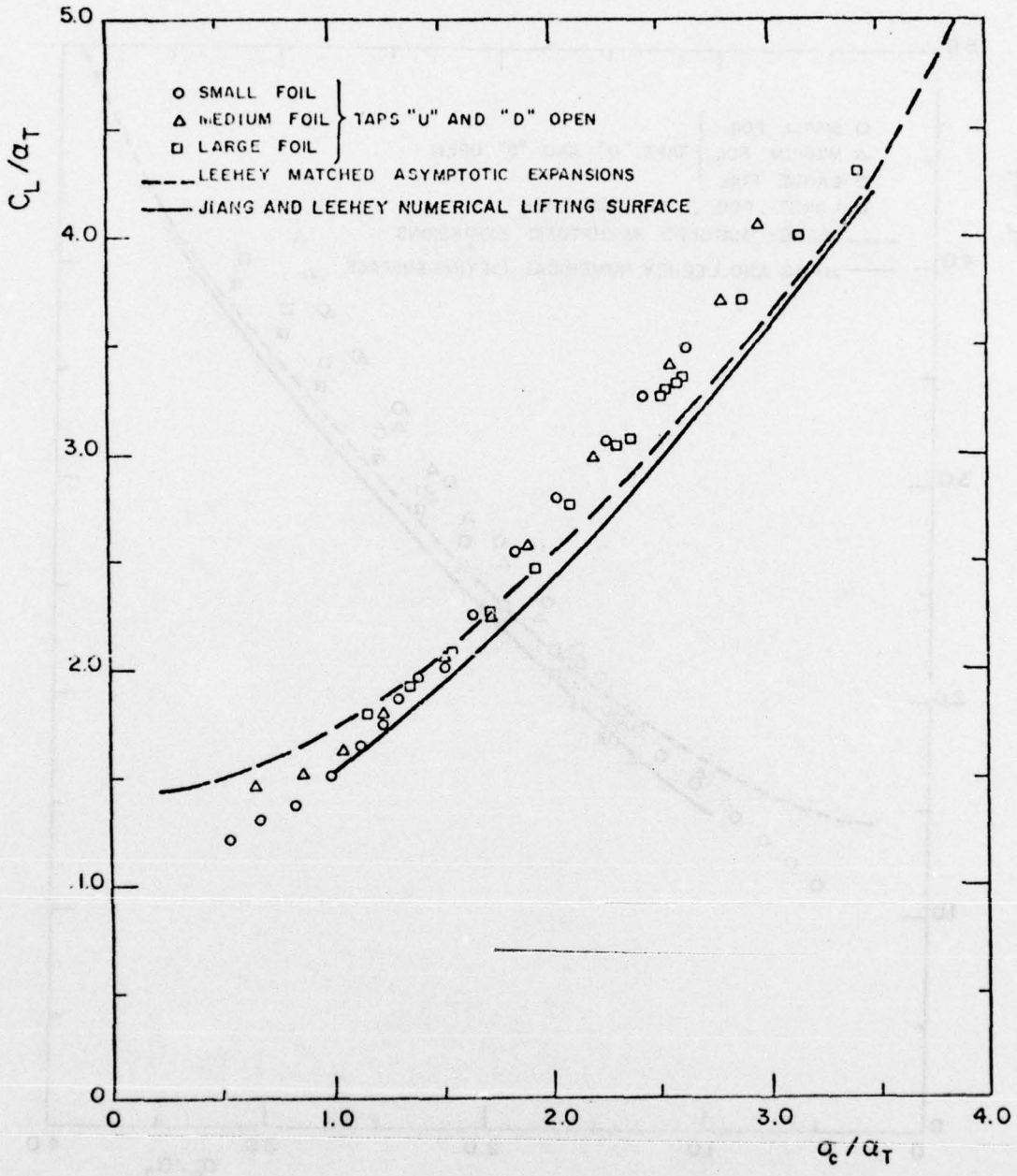

FIG. 7: C_L/a_T vs σ_c/a_T, $\alpha = 12.0°$

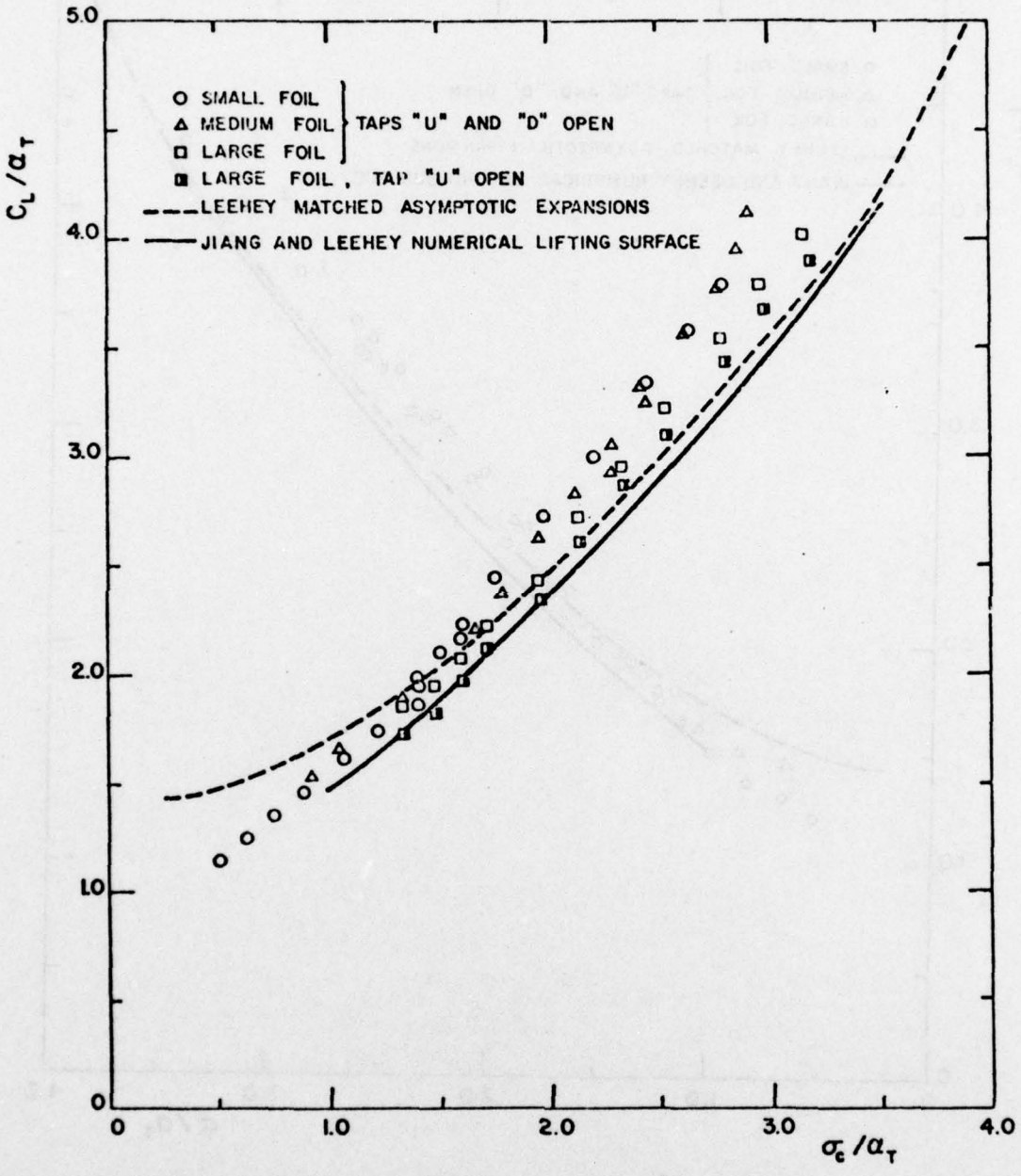

FIG. 8 : C_L/α_T vs σ_c/α_T, $\alpha = 14.0°$

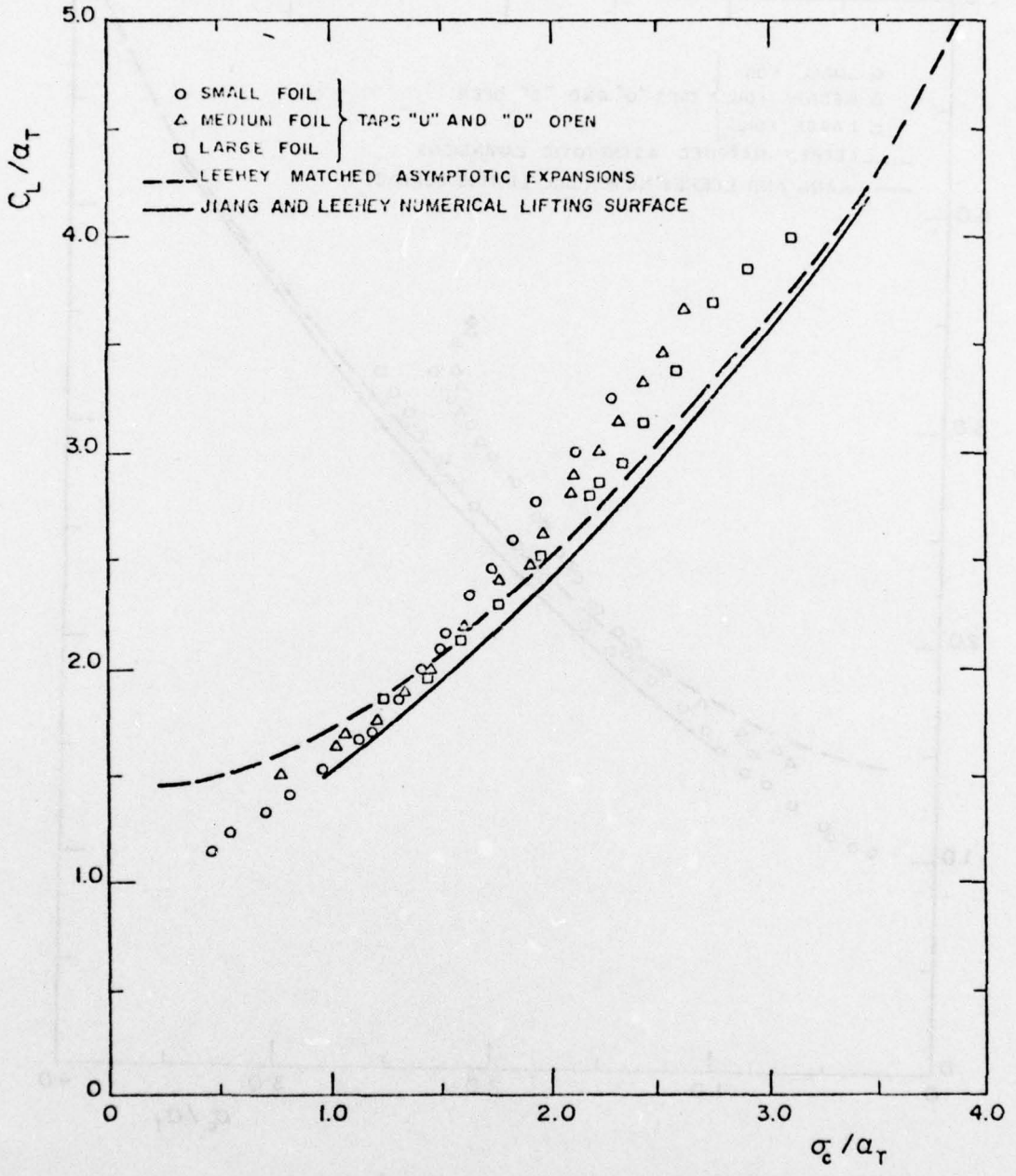

FIG. 9: C_L/α_T vs σ_c/α_T, $\alpha = 16.0°$

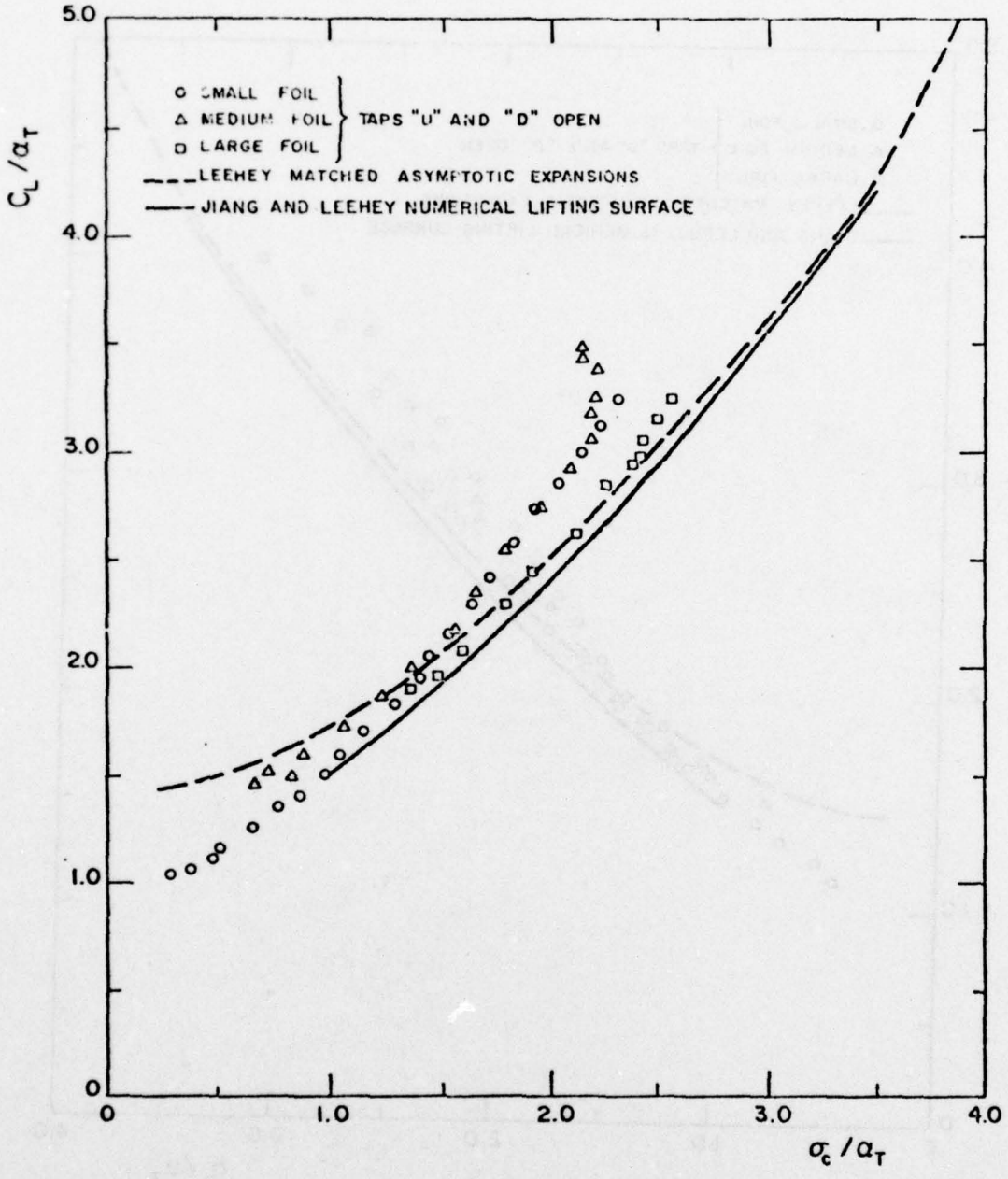

FIG. 10: C_L/α_T vs σ_c/α_T, $\alpha = 18.0°$

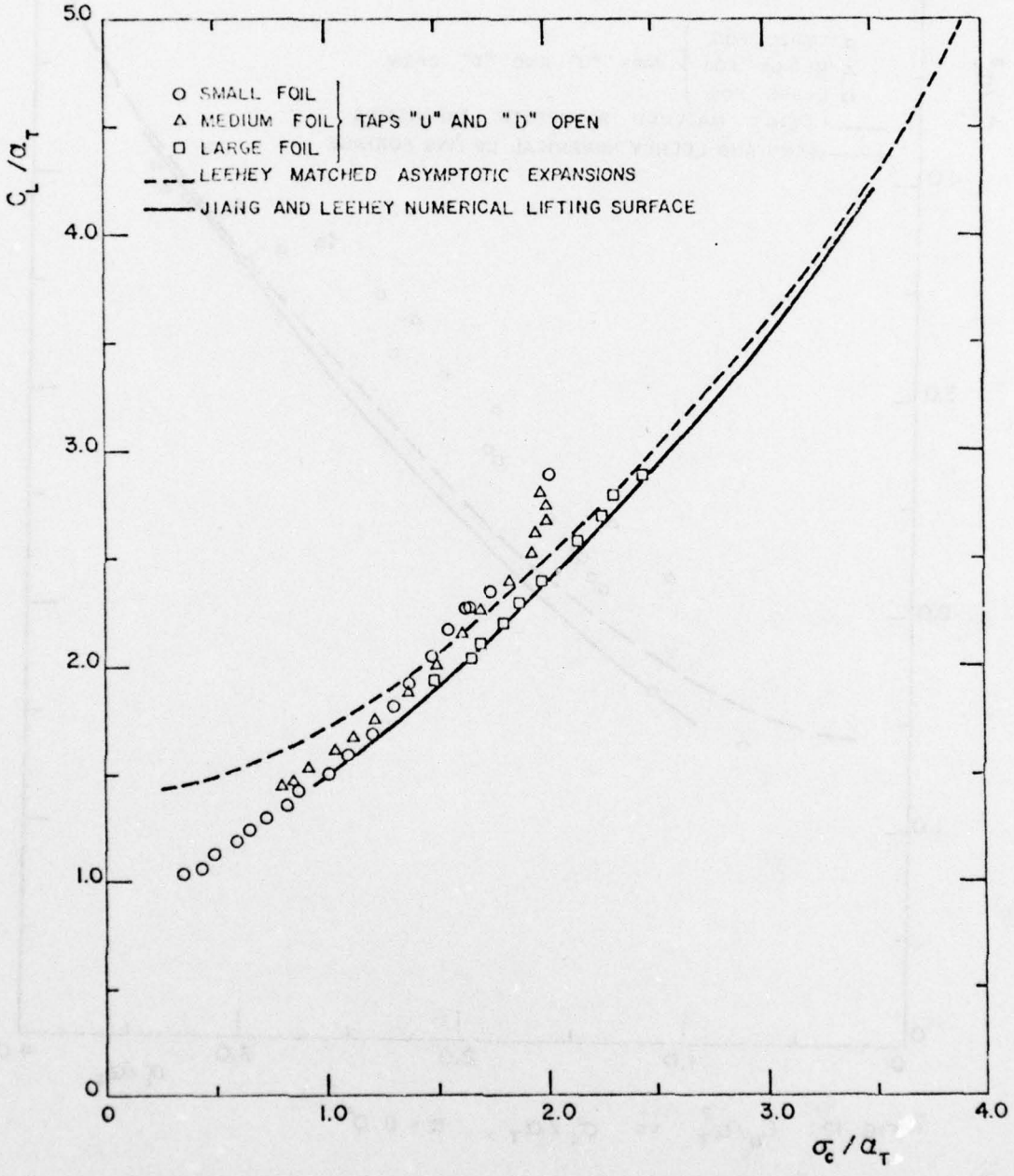

FIG. 11 : C_L/α_T vs σ_c/α_T , $\alpha = 21.0°$

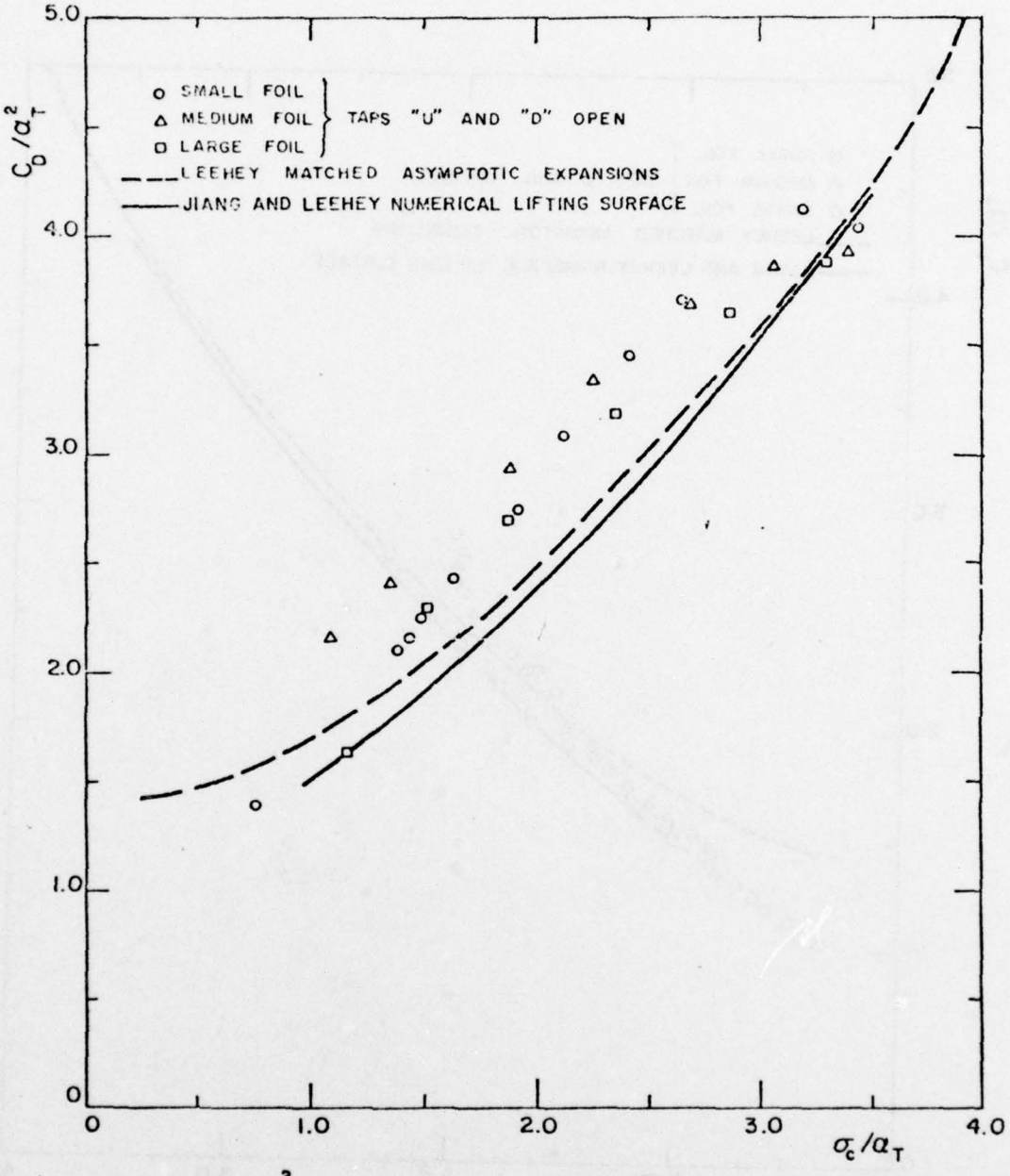

FIG. 12: C_D/a_T^2 vs σ_c/a_T, $\alpha = 8.0°$

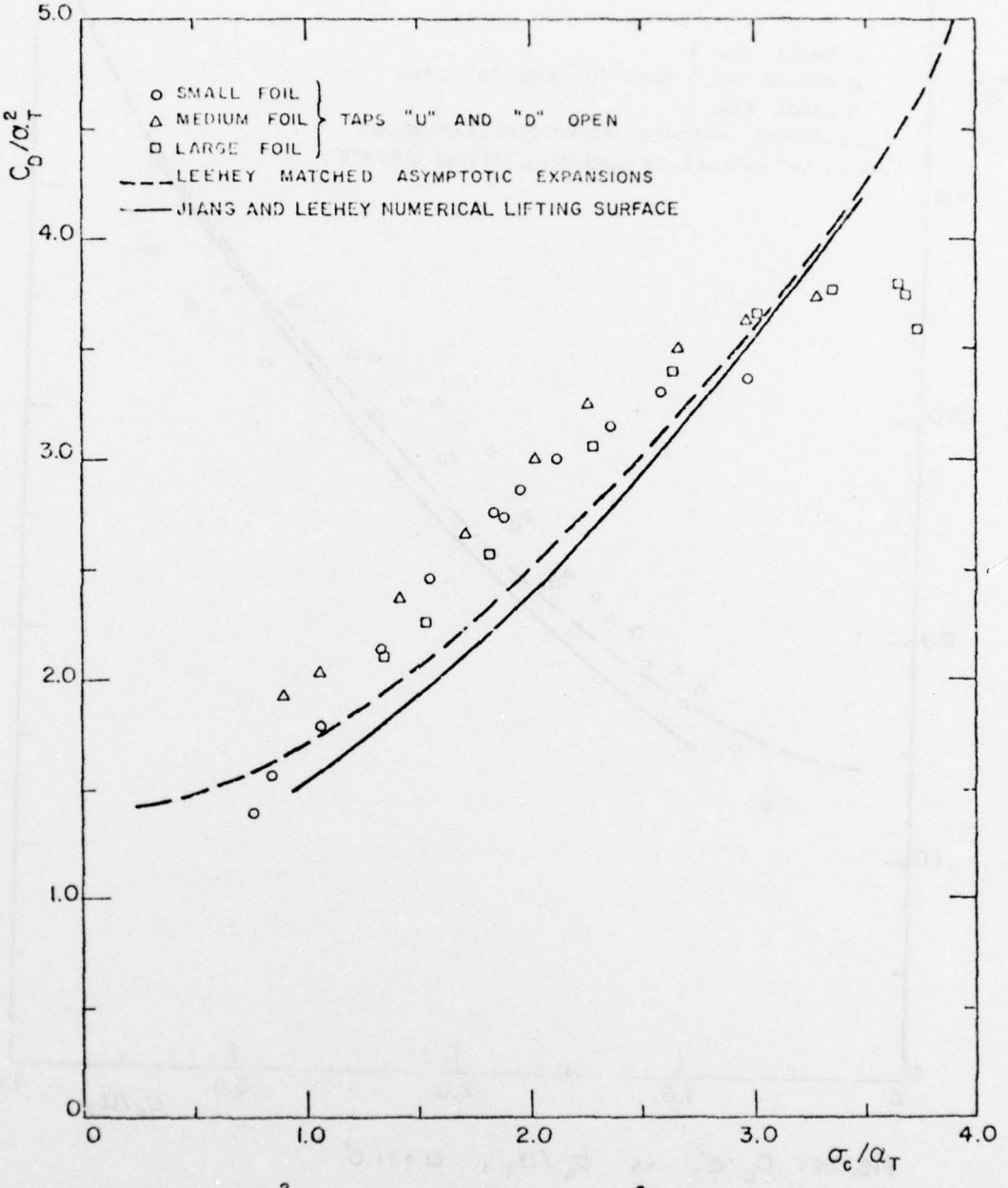

FIG. 13: C_D/a_T^2 vs σ_c/a_T, $a = 9.5°$

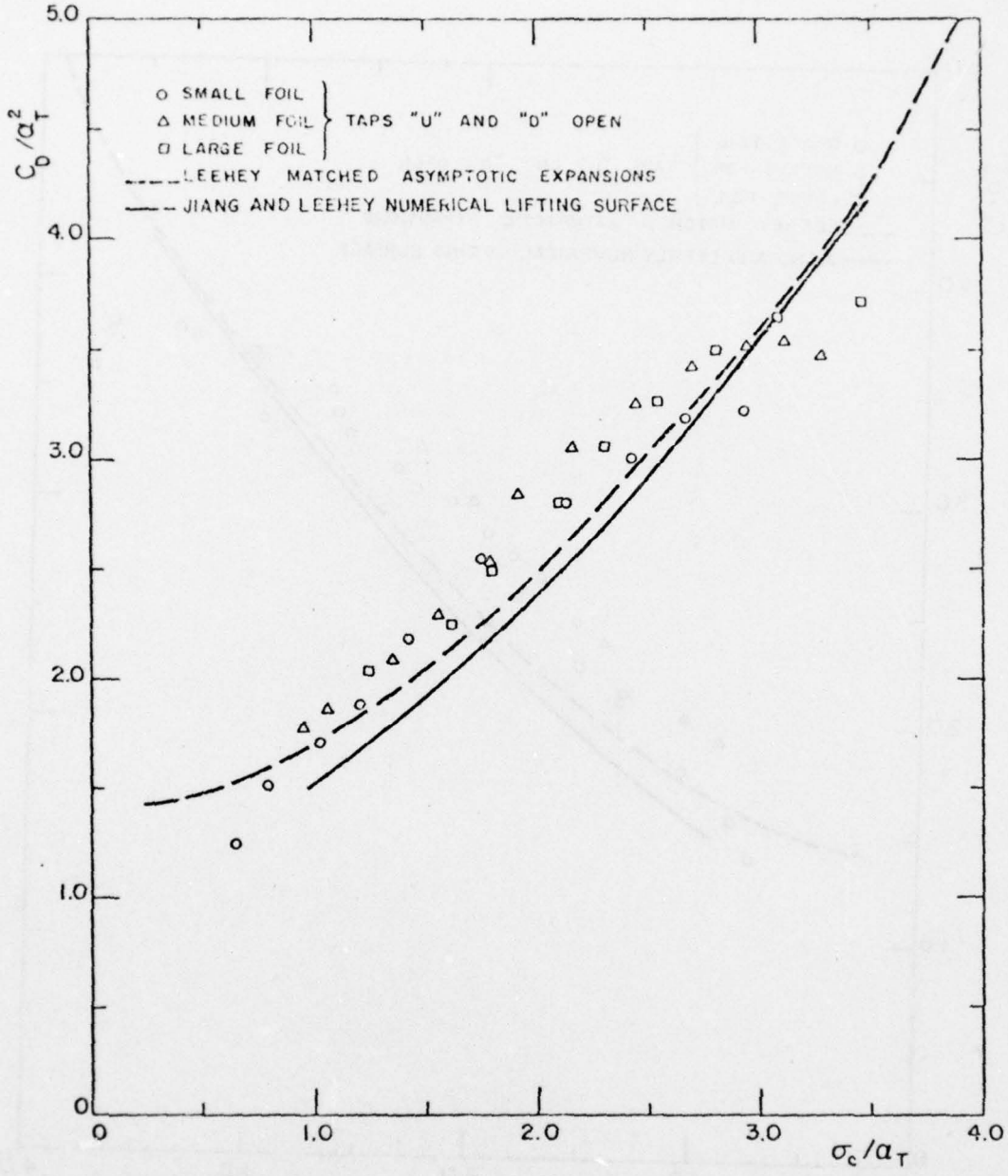

FIG. 14: C_D/a_T^2 vs σ_c/a_T, $\alpha = 11.0°$

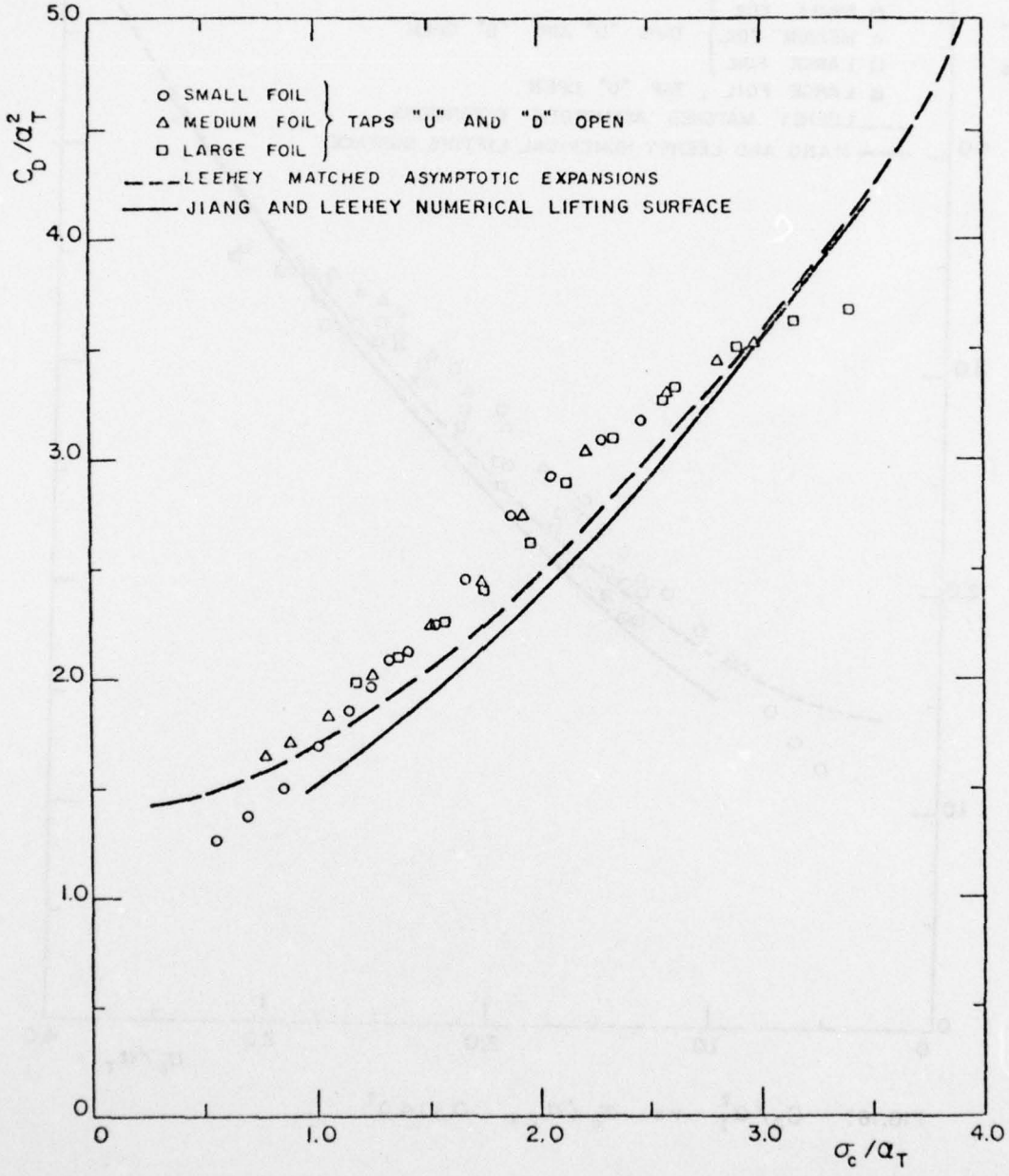

FIG. 15: C_D/a_T^2 vs σ_c/a_T, $\alpha = 12.0°$

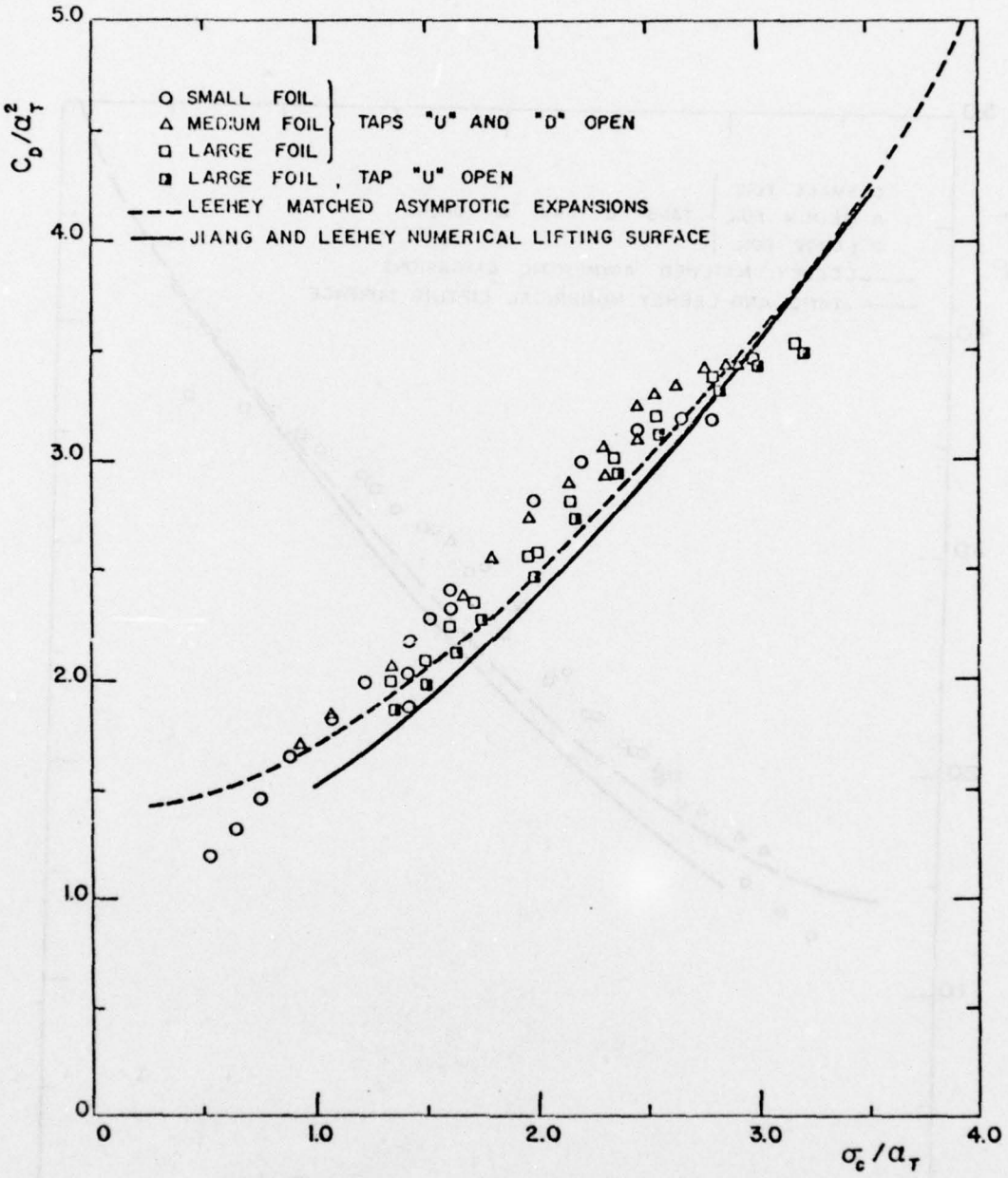

FIG. 16: C_D/α_T^2 vs σ_c/α_T, $\alpha = 14.0°$

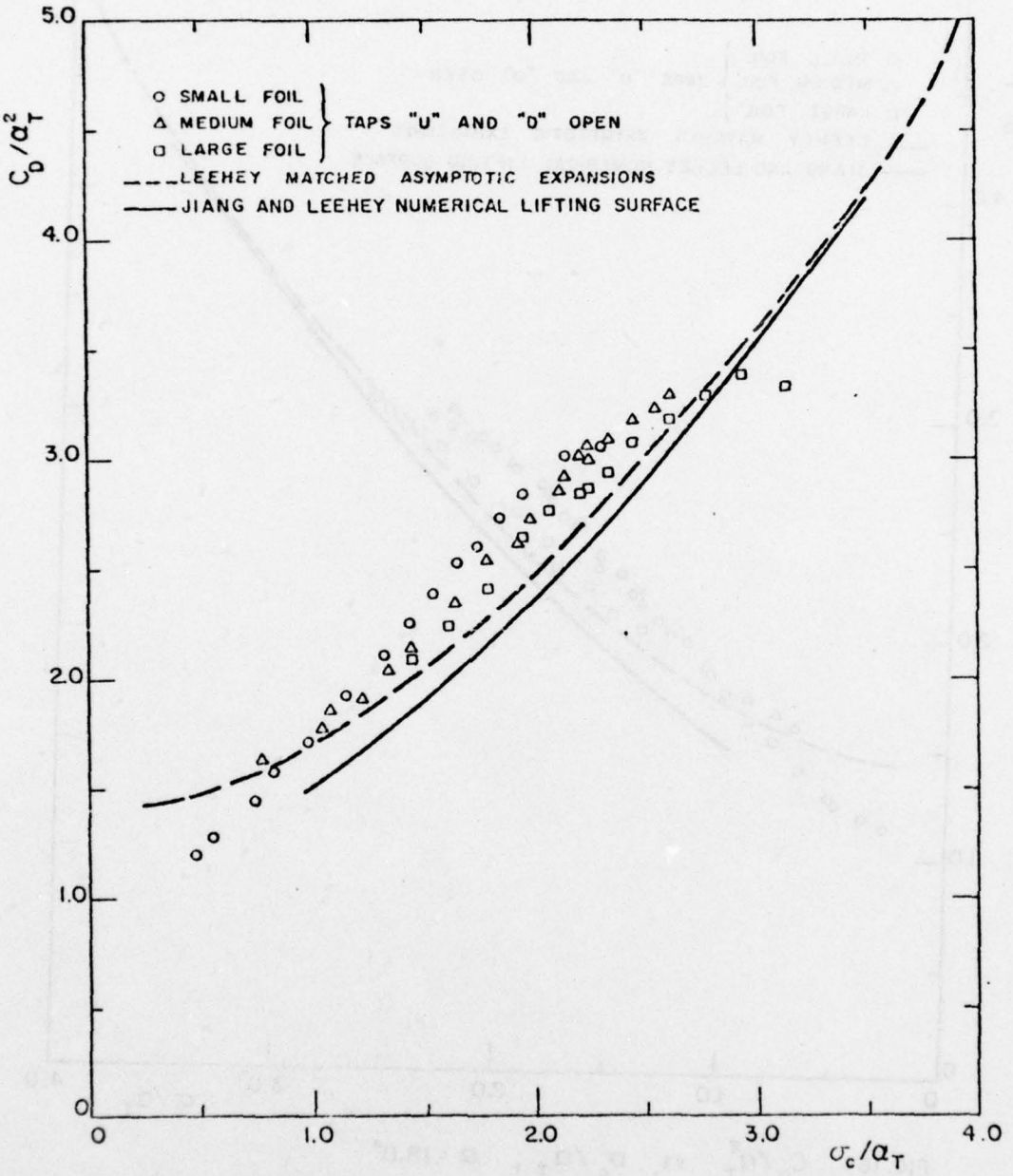

FIG. 17 : C_D/α_T^2 vs σ_c/α_T , $\alpha = 16.0°$

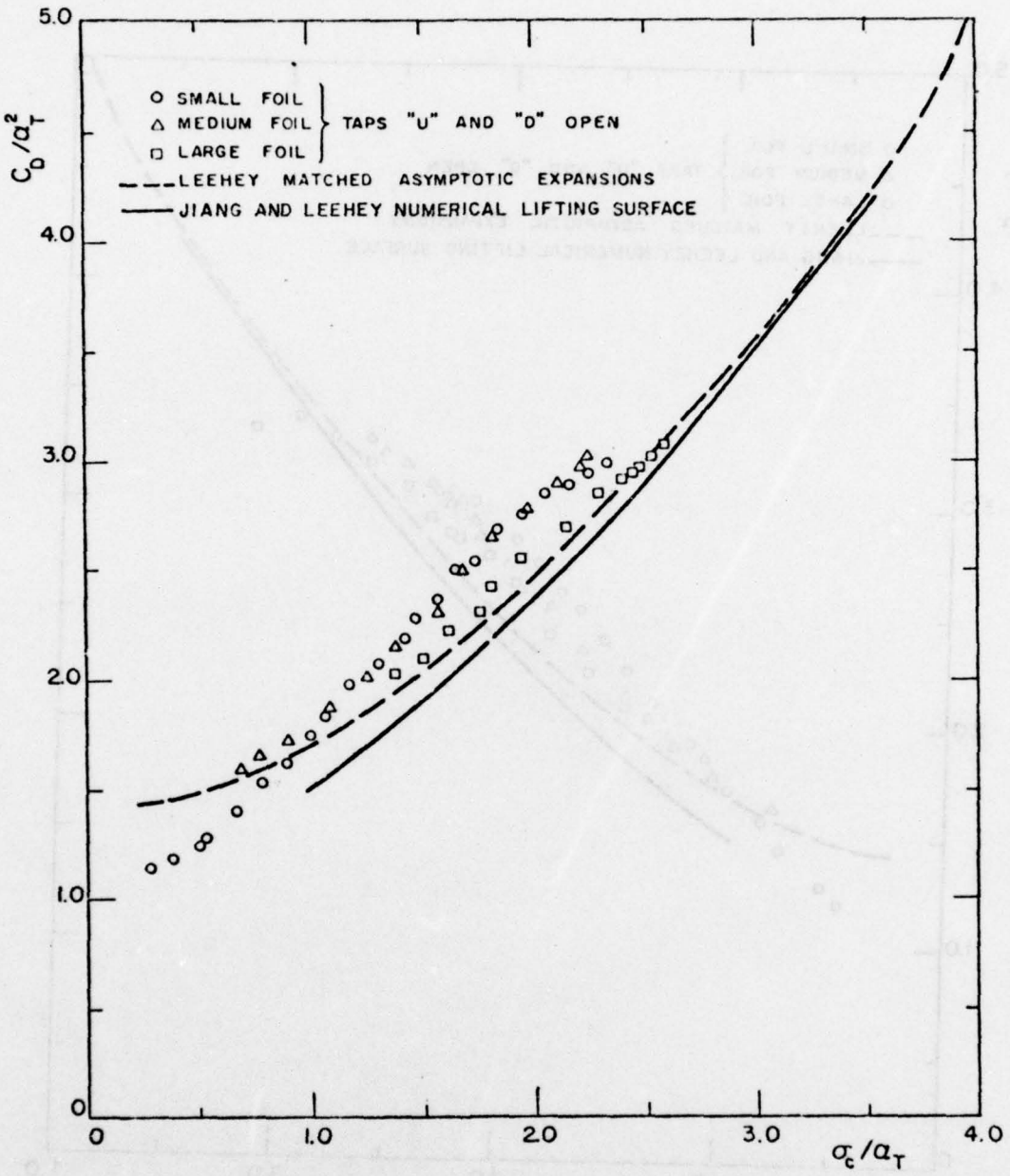

FIG. 18: C_D/a_T^2 vs σ_c/a_T, $\alpha = 18.0°$

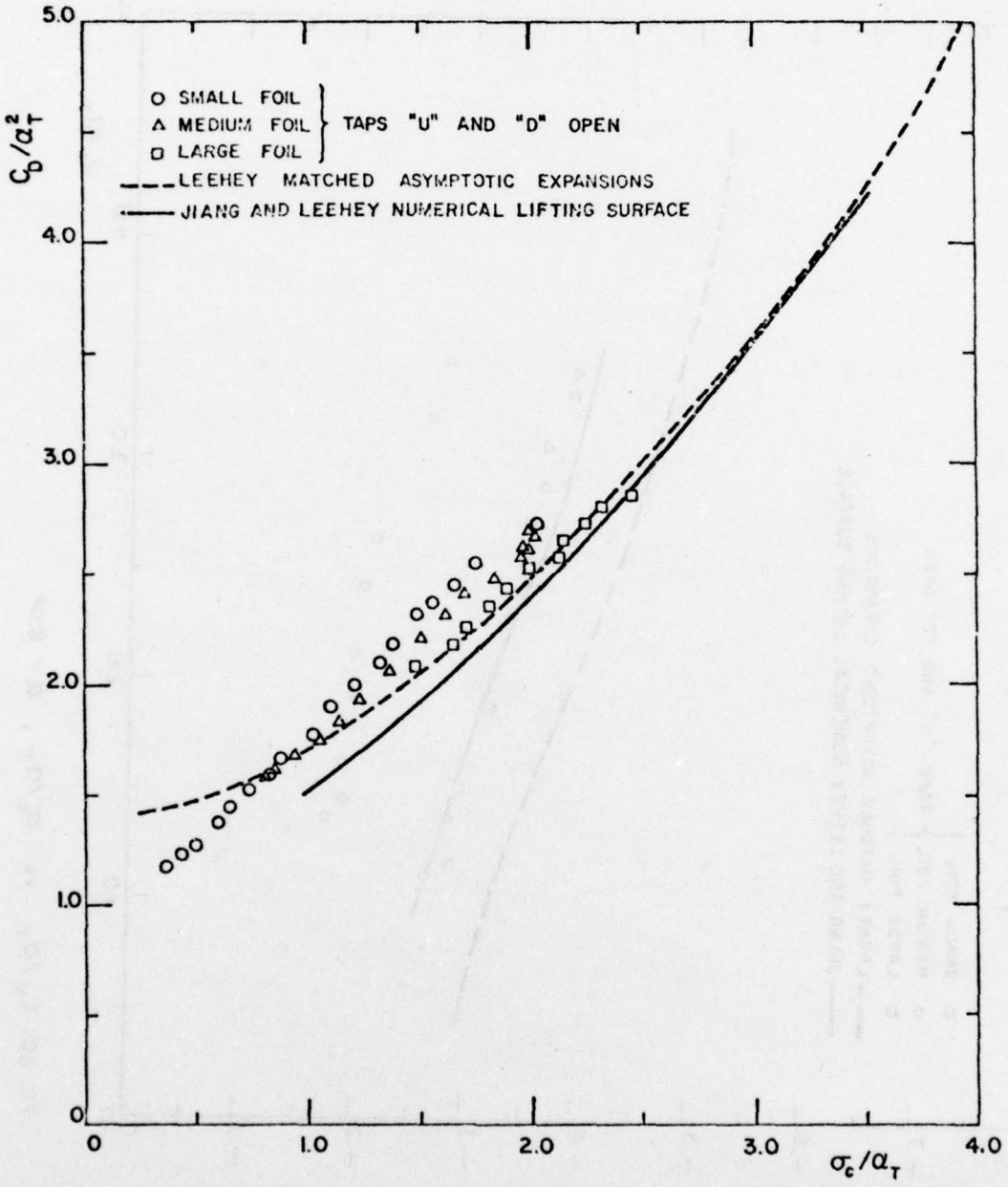

FIG. 19: C_D/α_T^2 vs σ_c/α_T, $\alpha = 21.0°$

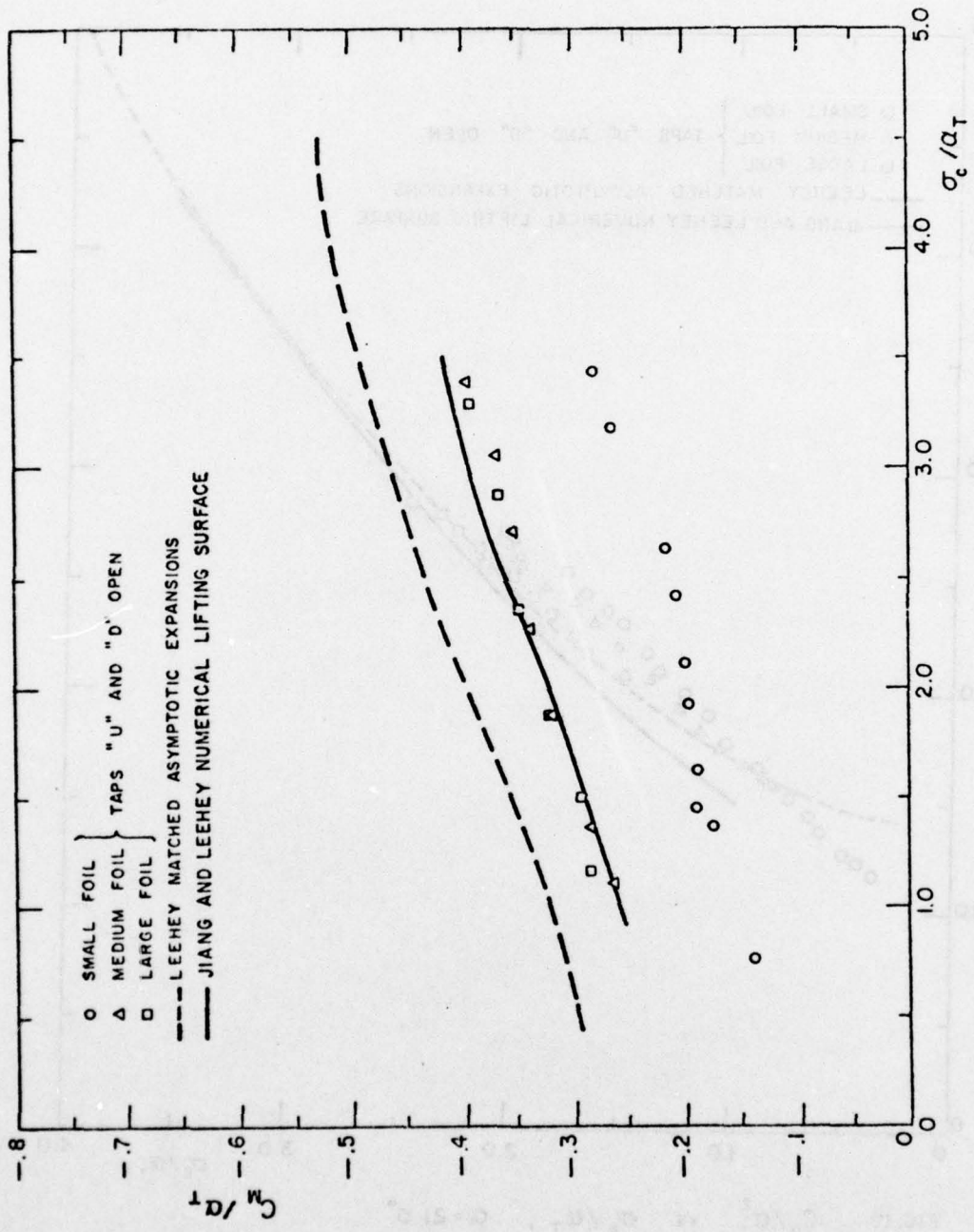

FIG. 20: C_M/α_T vs σ_c/α_T, $\alpha = 8.0°$

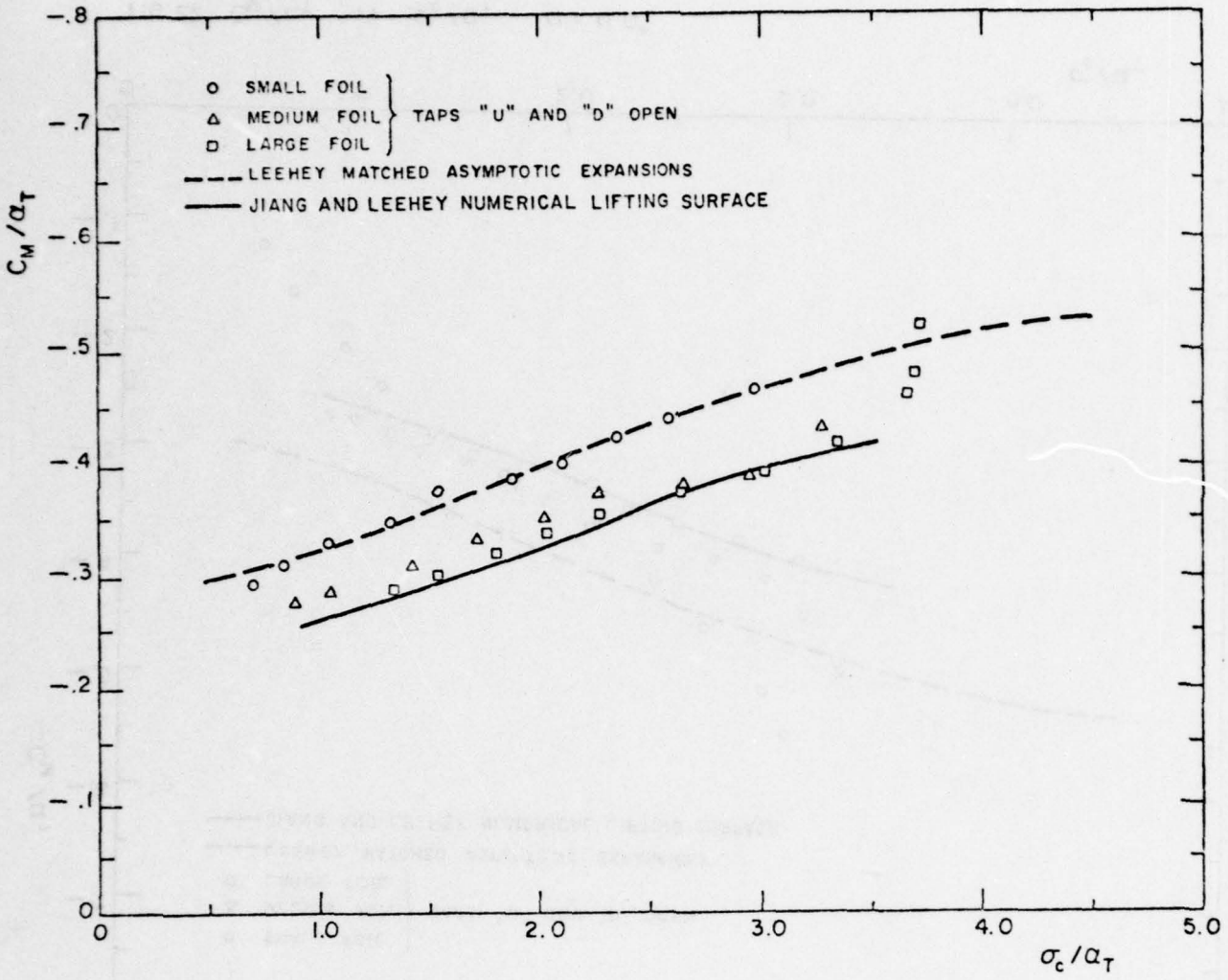

FIG. 21: C_M/a_T vs σ_c/a_T , $\alpha = 9.5°$

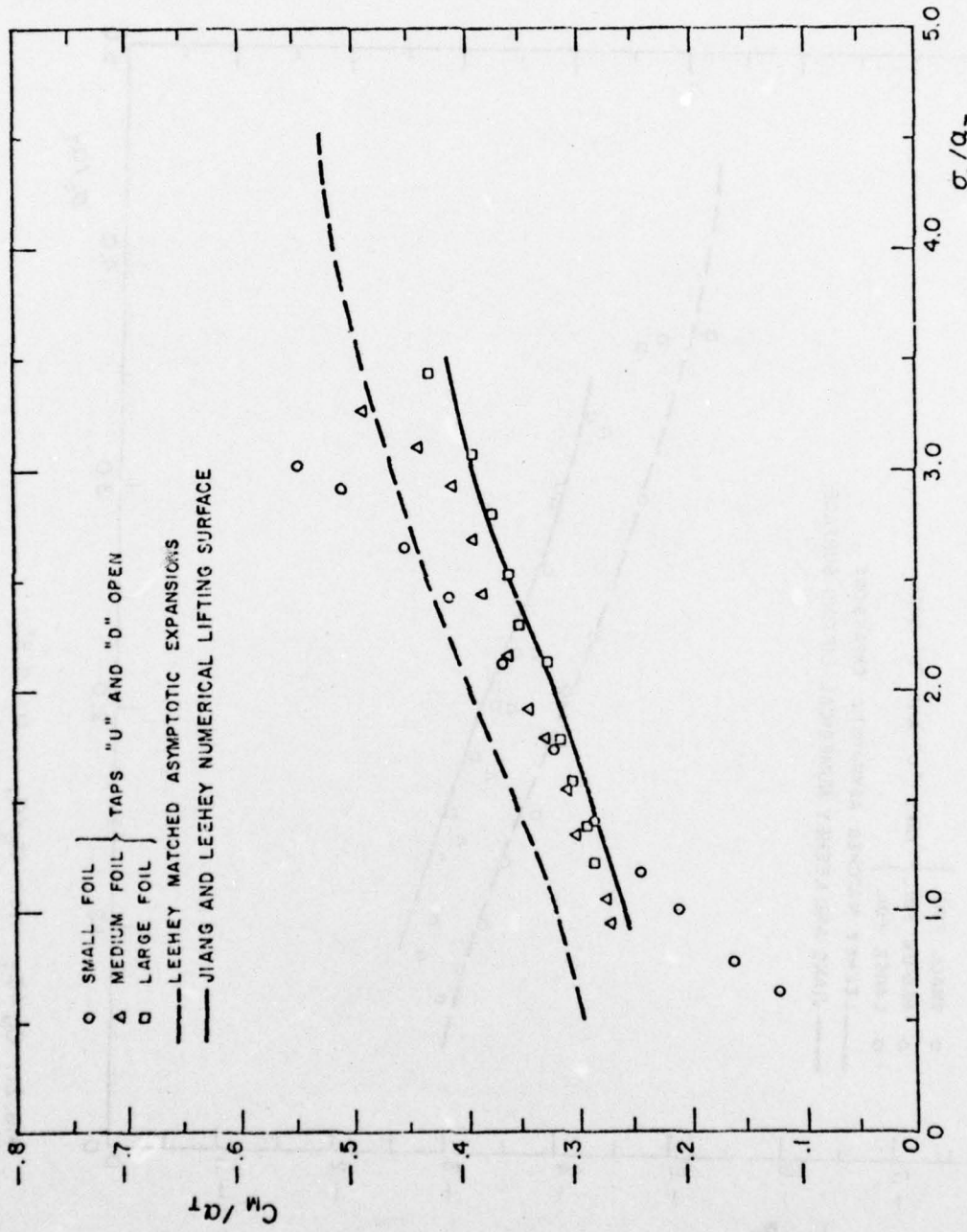

FIG.22: C_M/a_T vs σ_c/a_T , $\alpha = 11.0°$

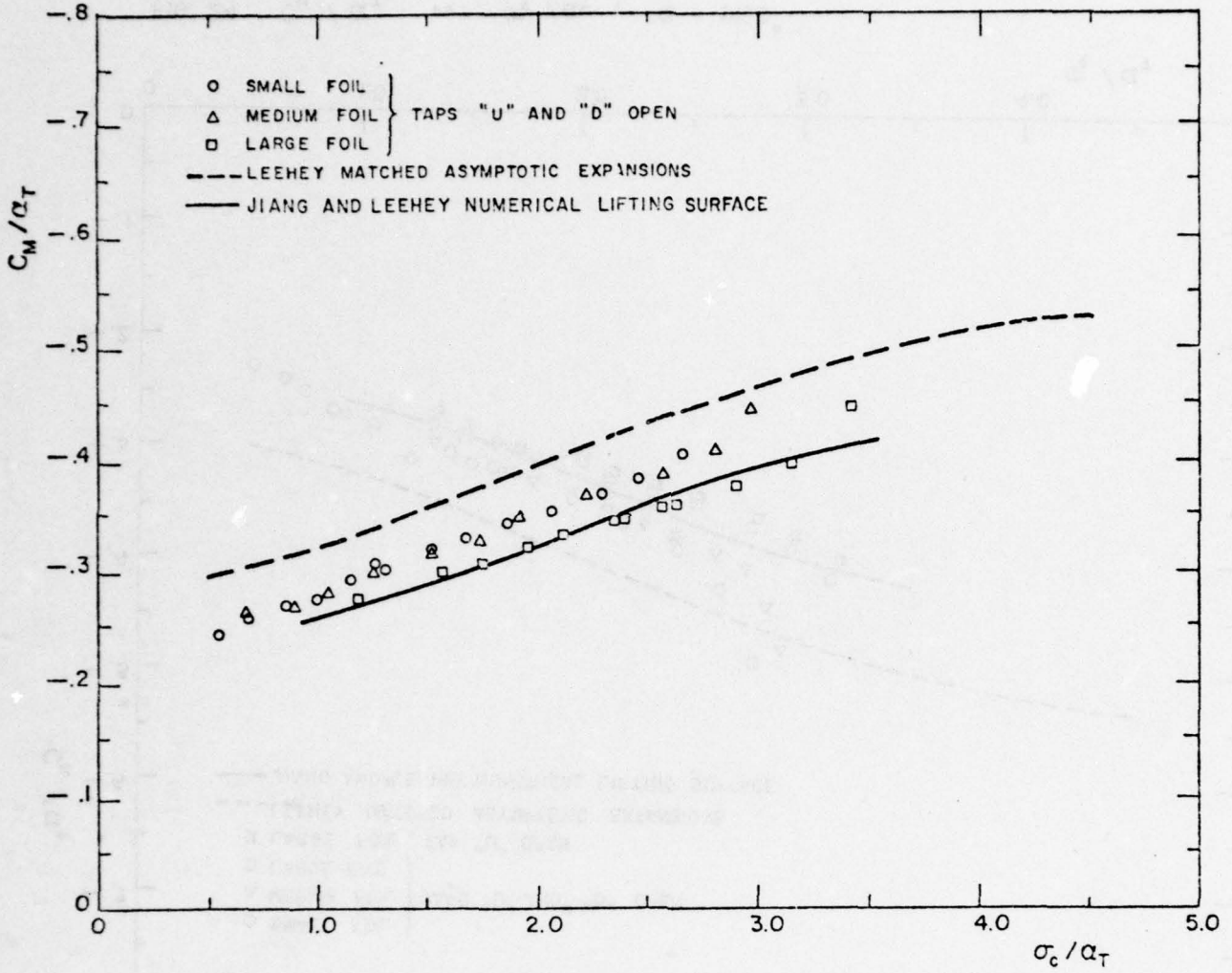

FIG. 23: C_M/α_T vs σ_c/α_T , $\alpha = 12.0°$

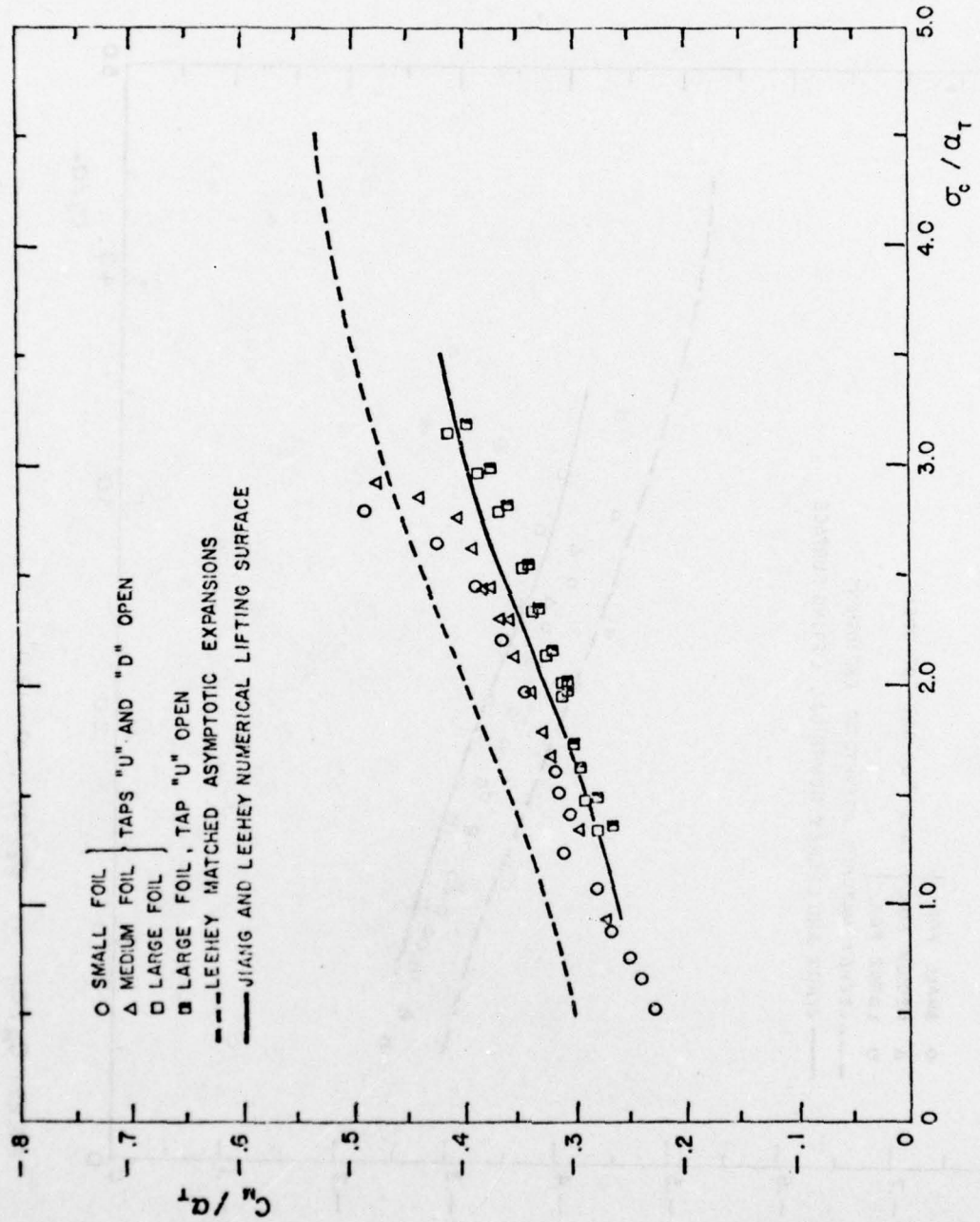

FIG. 24: C_M / α_T vs σ_c / α_T, $\alpha = 14.0°$

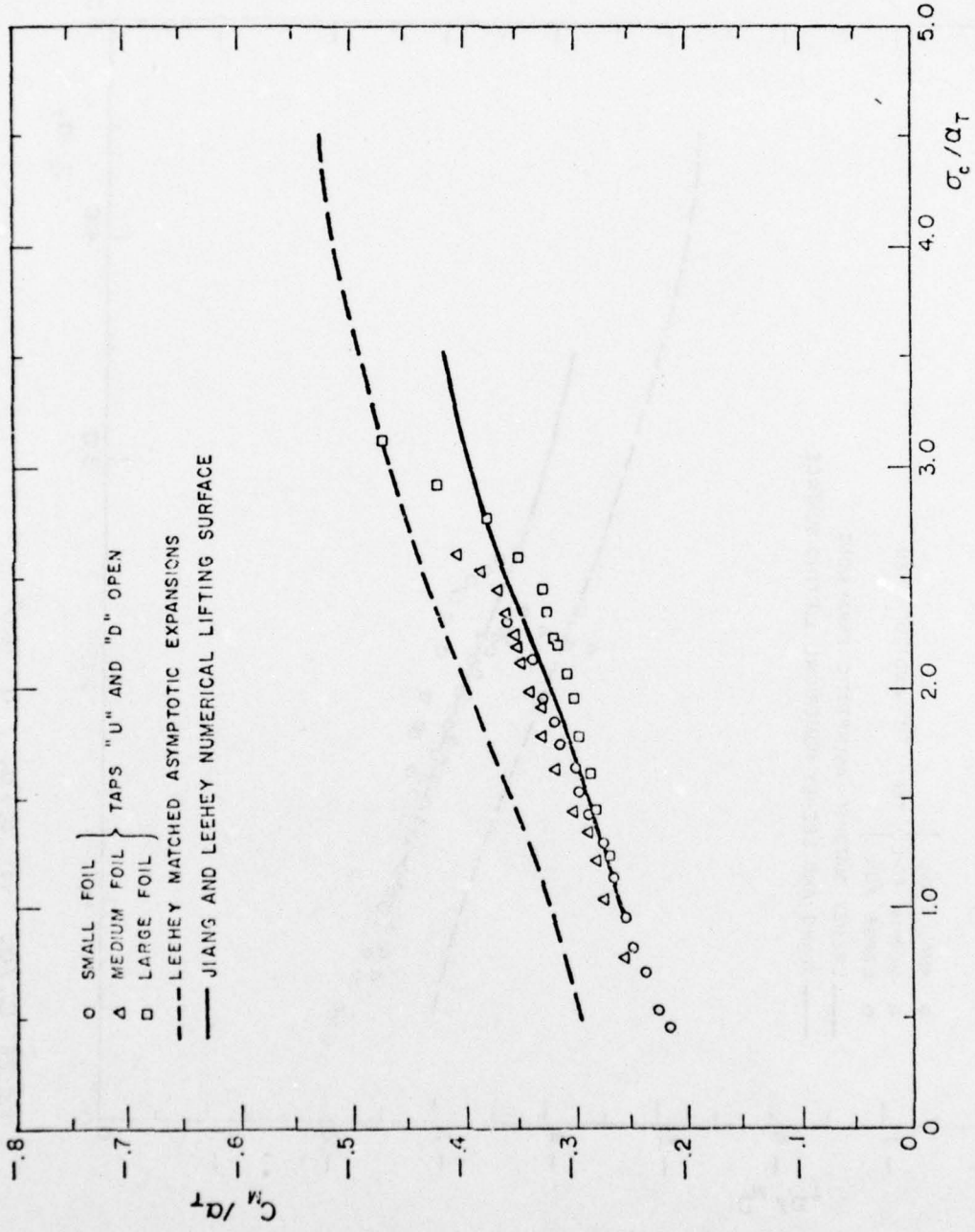

FIG. 25: C_M/a_T vs σ_c/a_T , $\alpha = 16.0°$

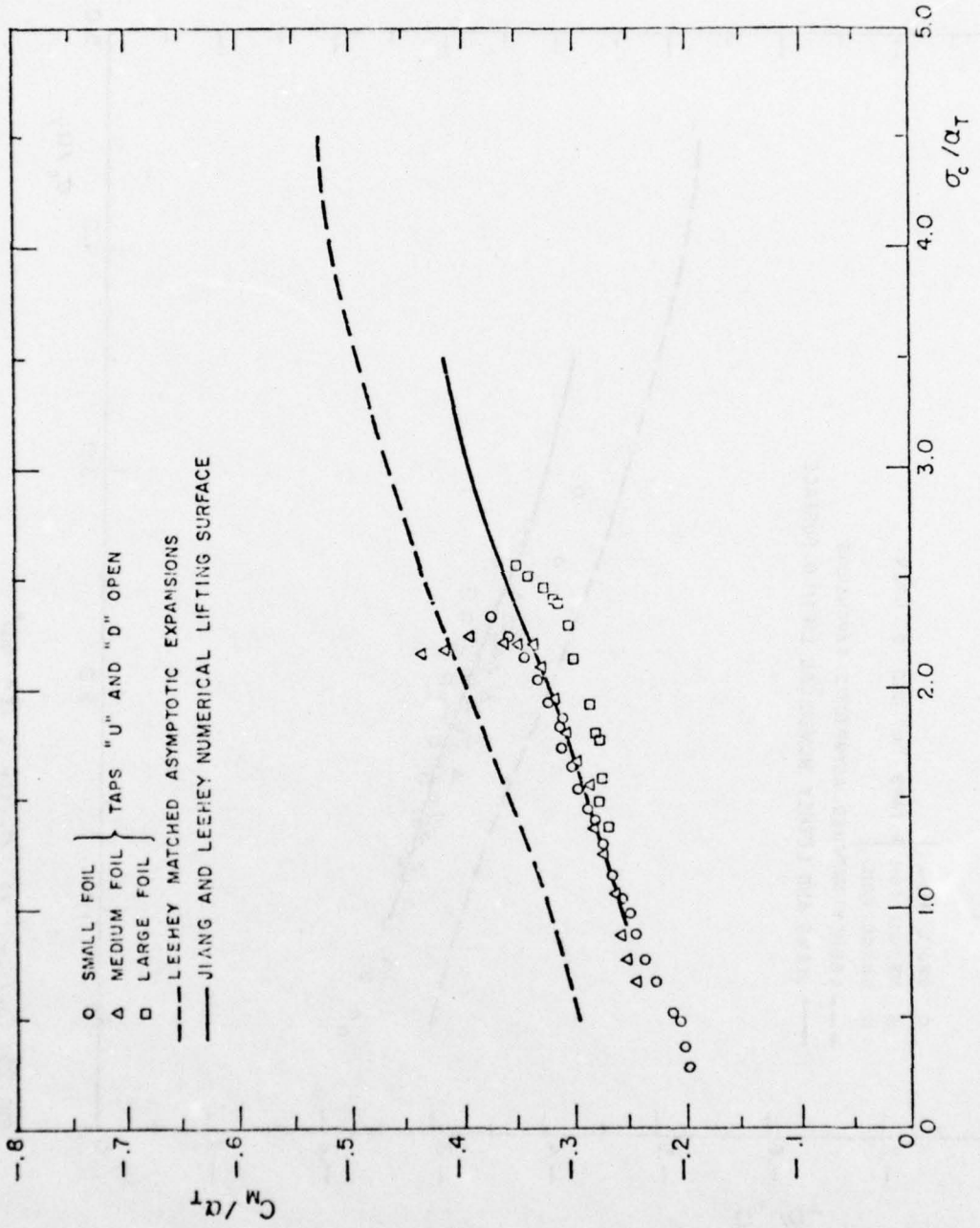

FIG. 26: C_{M_c}/α_T vs σ_c/α_T , $\alpha = 18.0°$

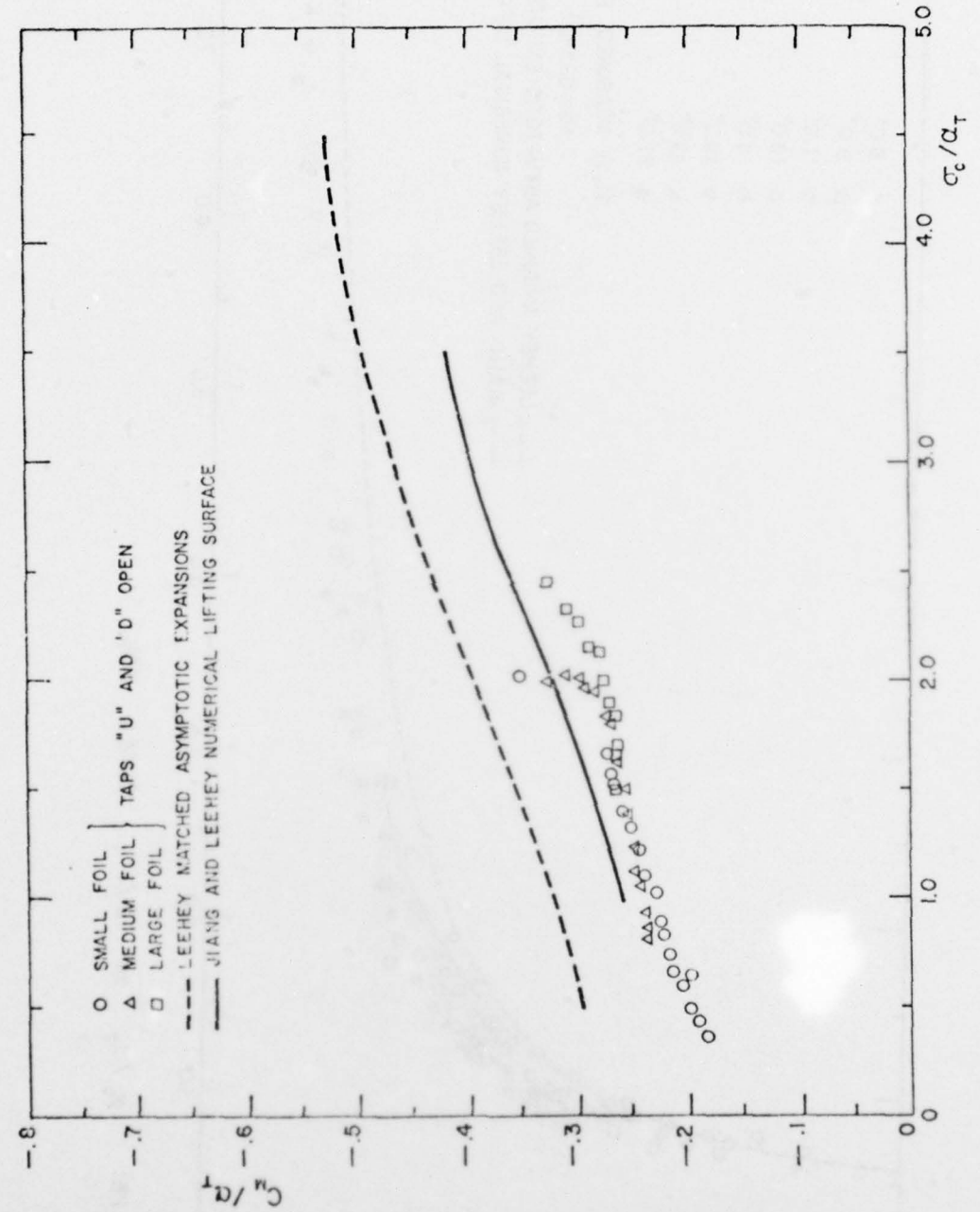

FIG.27: C_M/α_T vs σ_c/α_T , $\alpha = 21.0°$

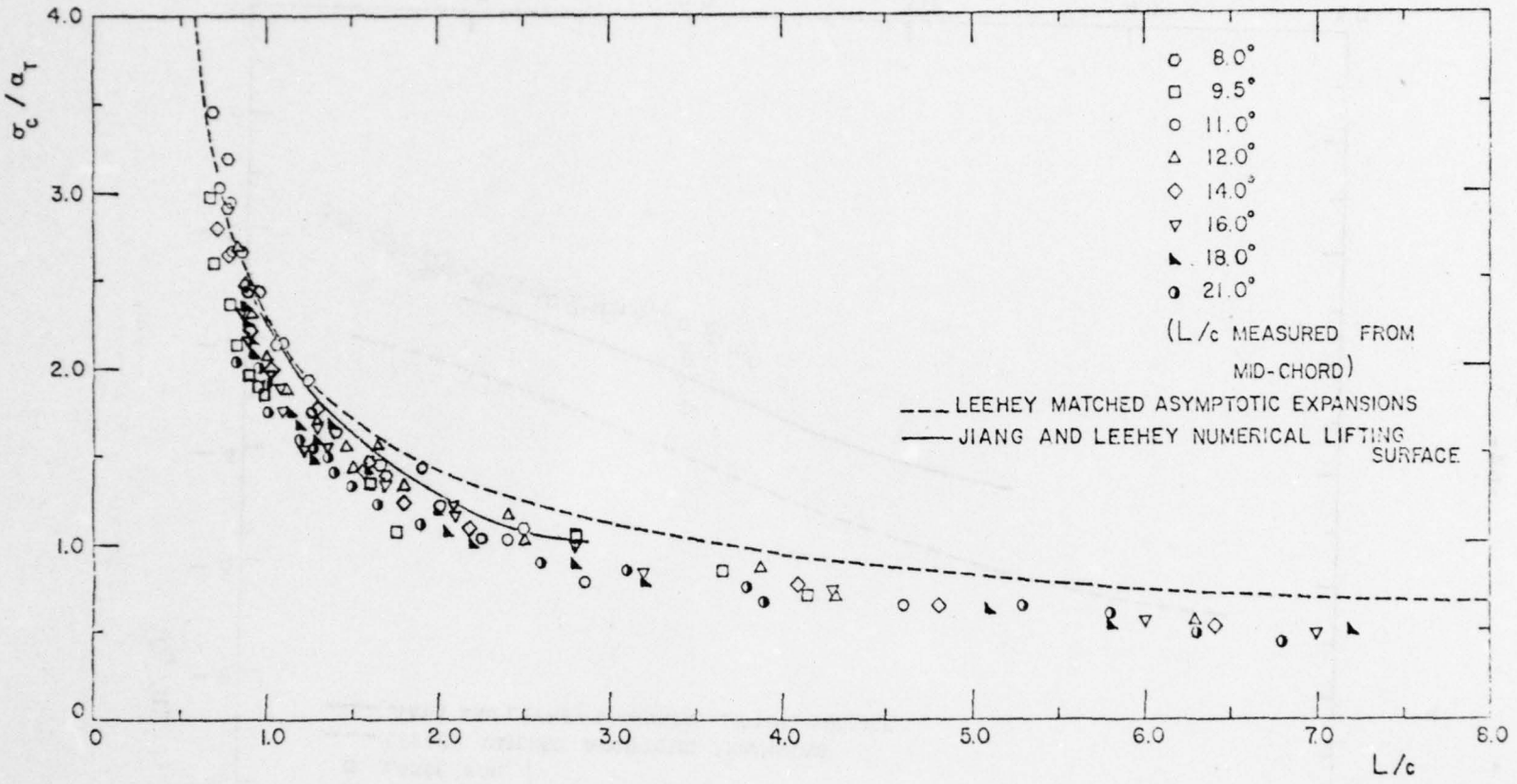

FIG. 28: σ_c / α_T vs L/c , SMALL FOIL

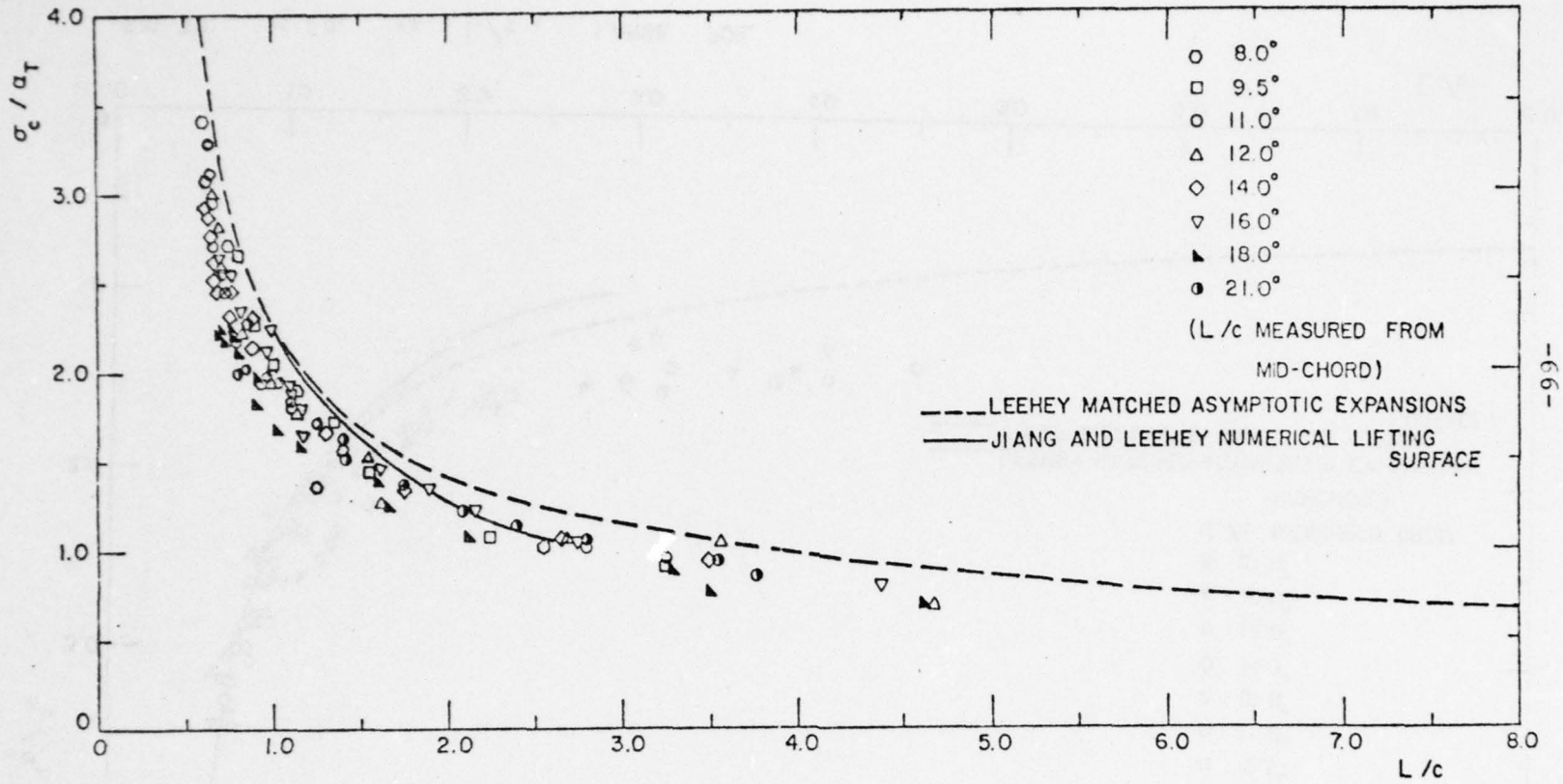

FIG. 29: σ_c / a_T vs L /c , MEDIUM FOIL

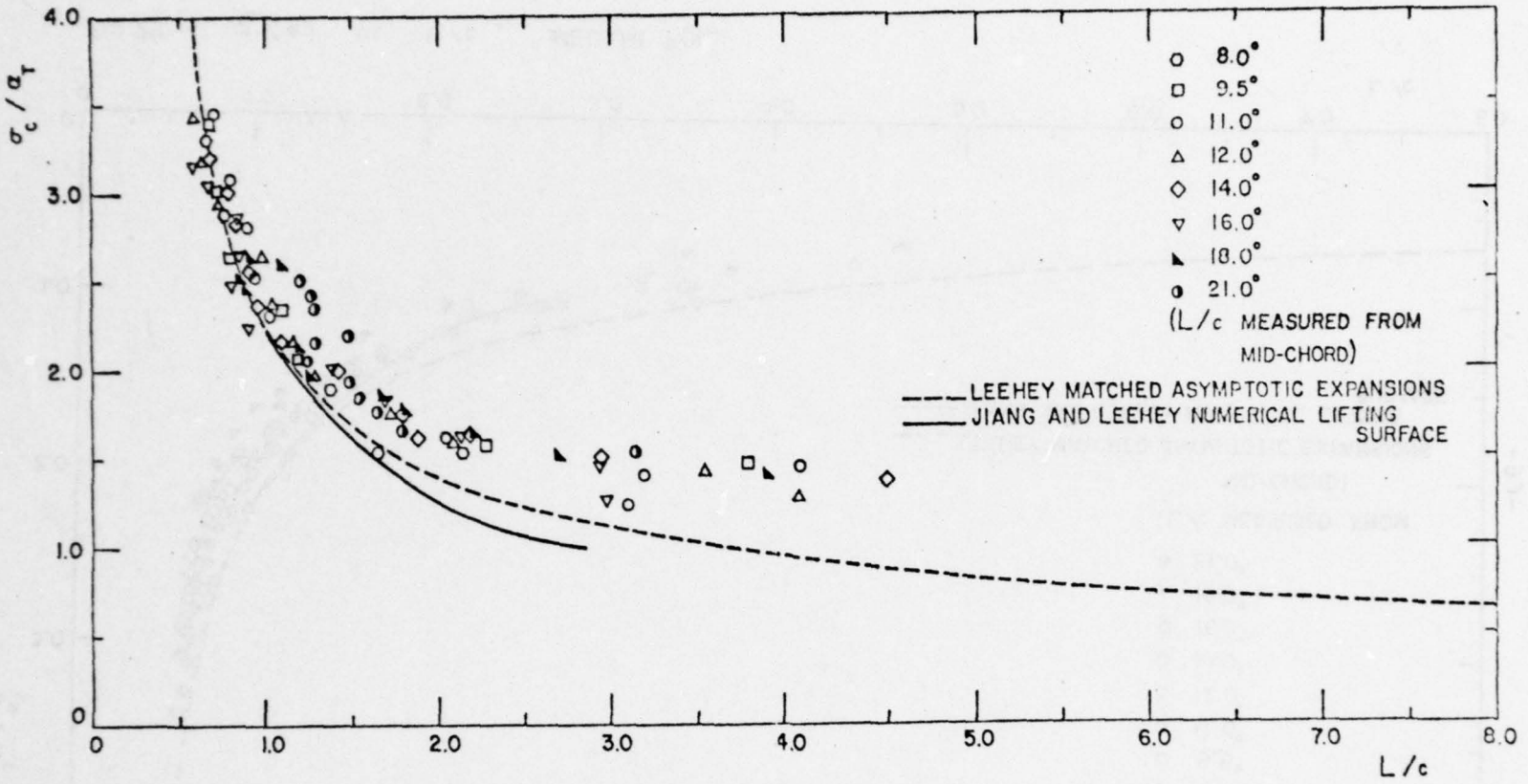

FIG. 30: σ_c / α_T vs L/c , LARGE FOIL

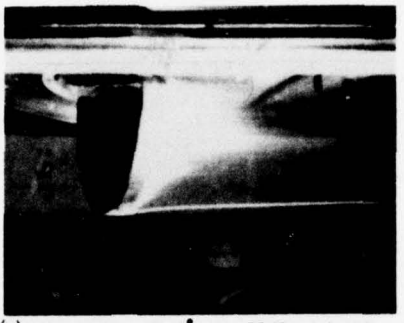

(a) SMALL FOIL: $\alpha = 12^{\circ}$, $\sigma_c = .3545$, $L/c = 1.3$

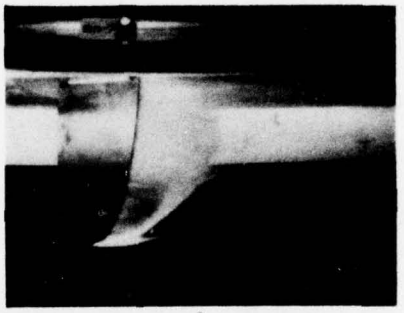

(b) MEDIUM FOIL: $\alpha = 12^{\circ}$, $\sigma_c = .3473$, $L/c = 1.55$

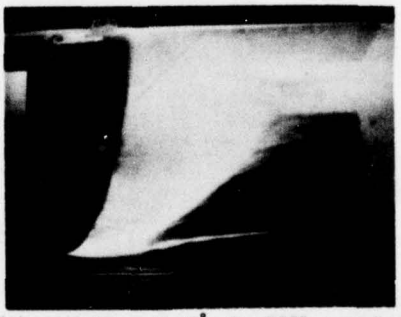

(c) LARGE FOIL: $\alpha = 12^{\circ}$, $\sigma_c = .3265$, $L/c = 2.1$

FIG. 31: COMPARISON OF CAVITY LENGTHS

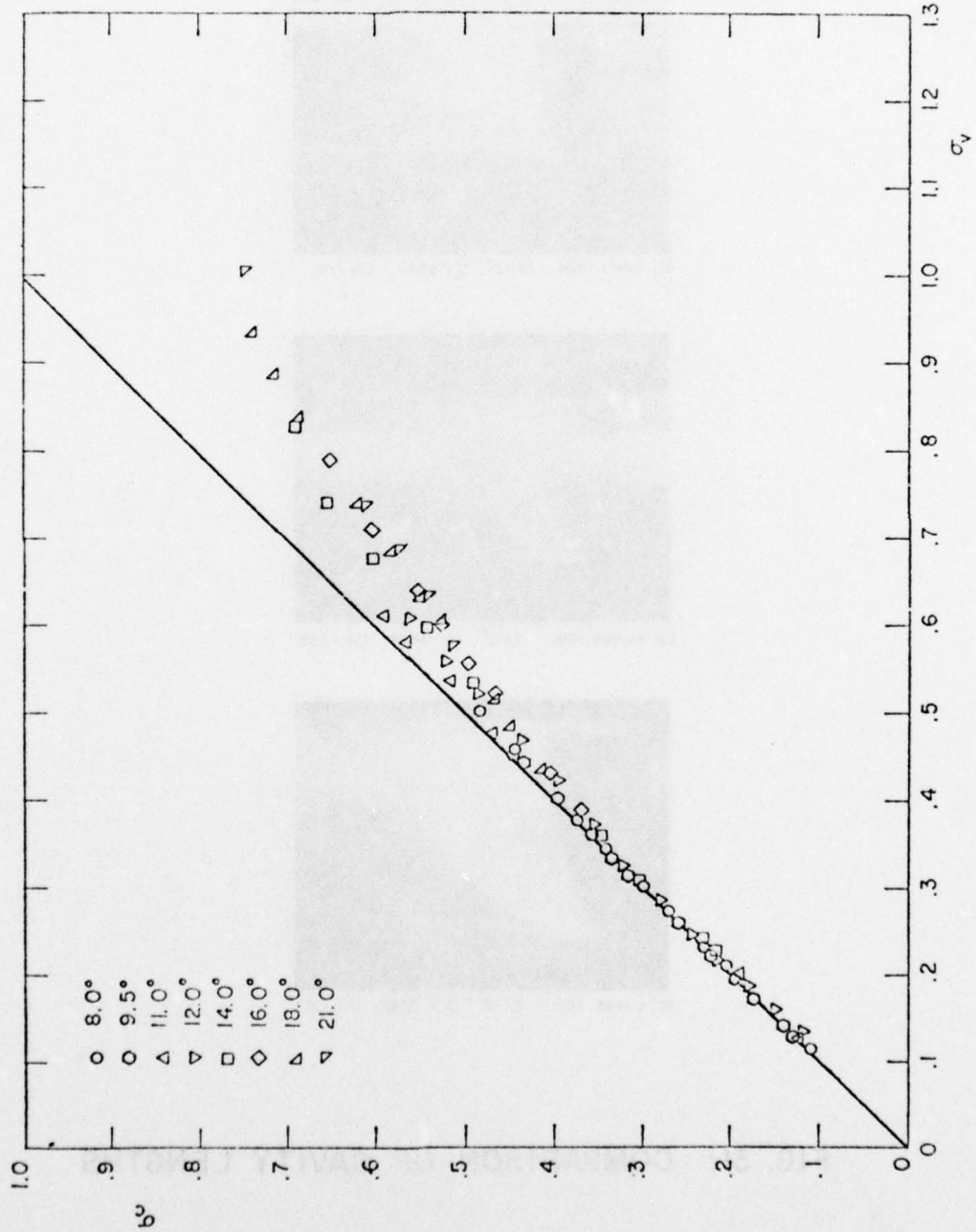

FIG. 32: σ_c vs σ_v , SMALL FOIL

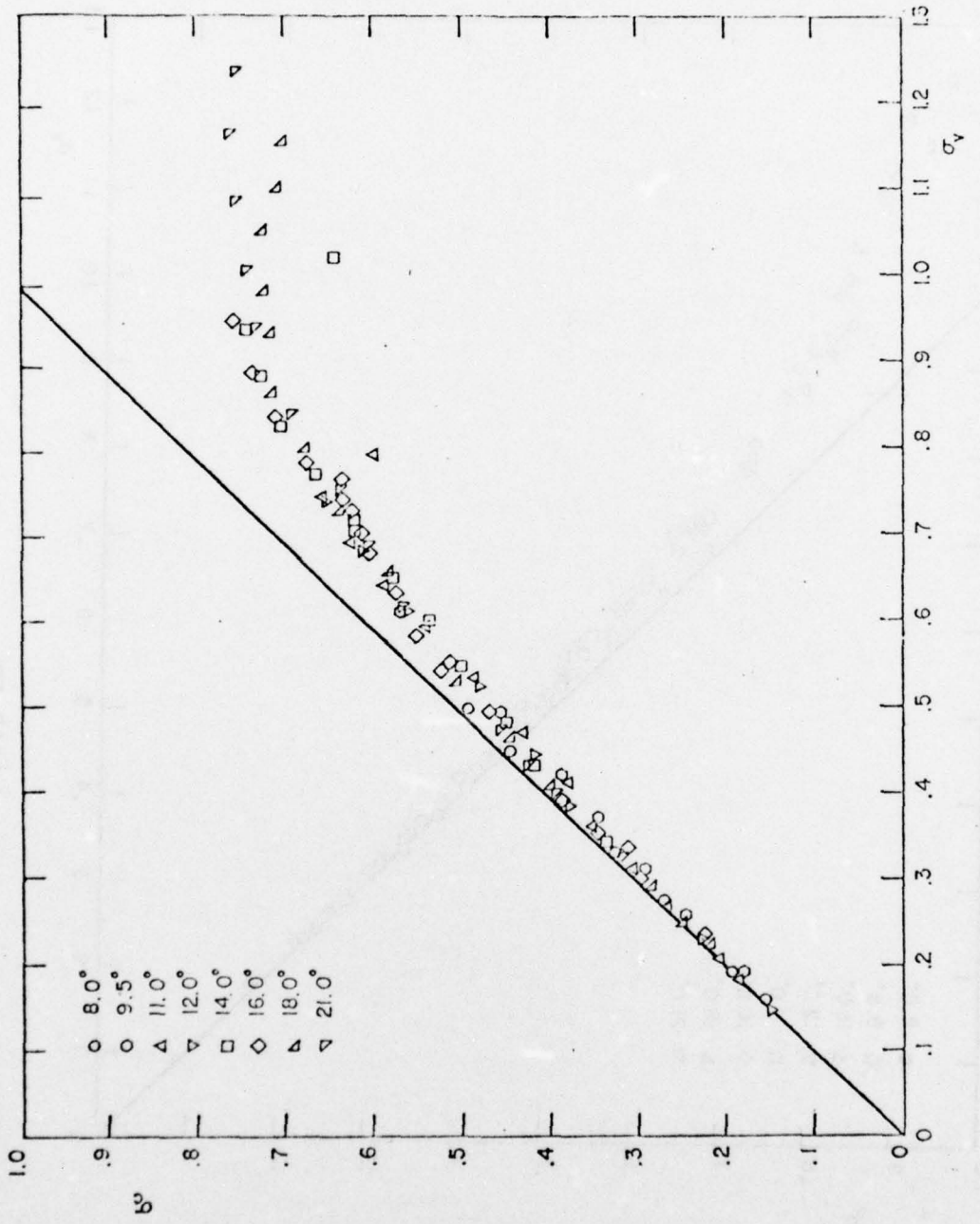

FIG. 33: σ_c vs σ_v , MEDIUM FOIL

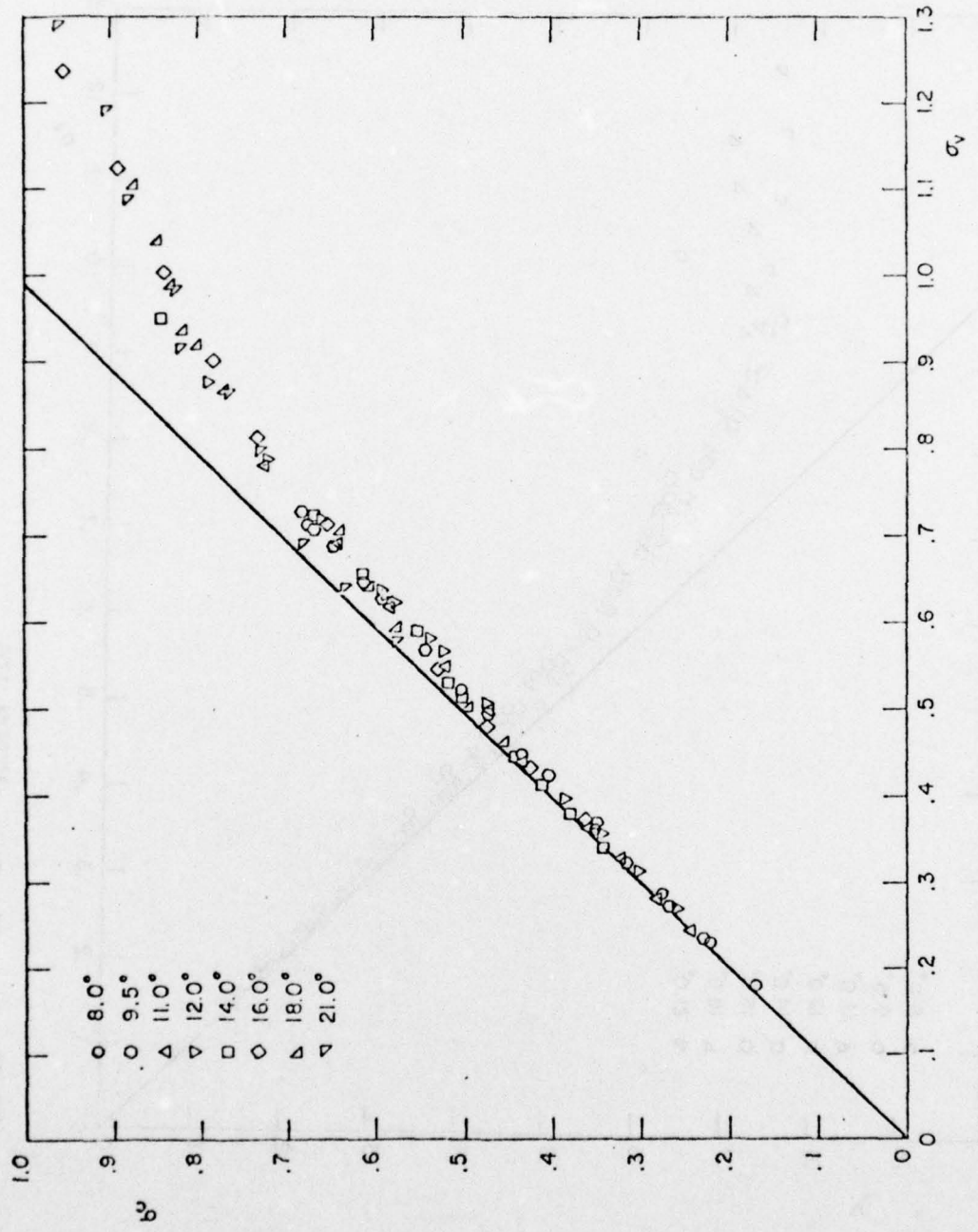

FIG. 34: σ_c vs σ_v , LARGE FOIL

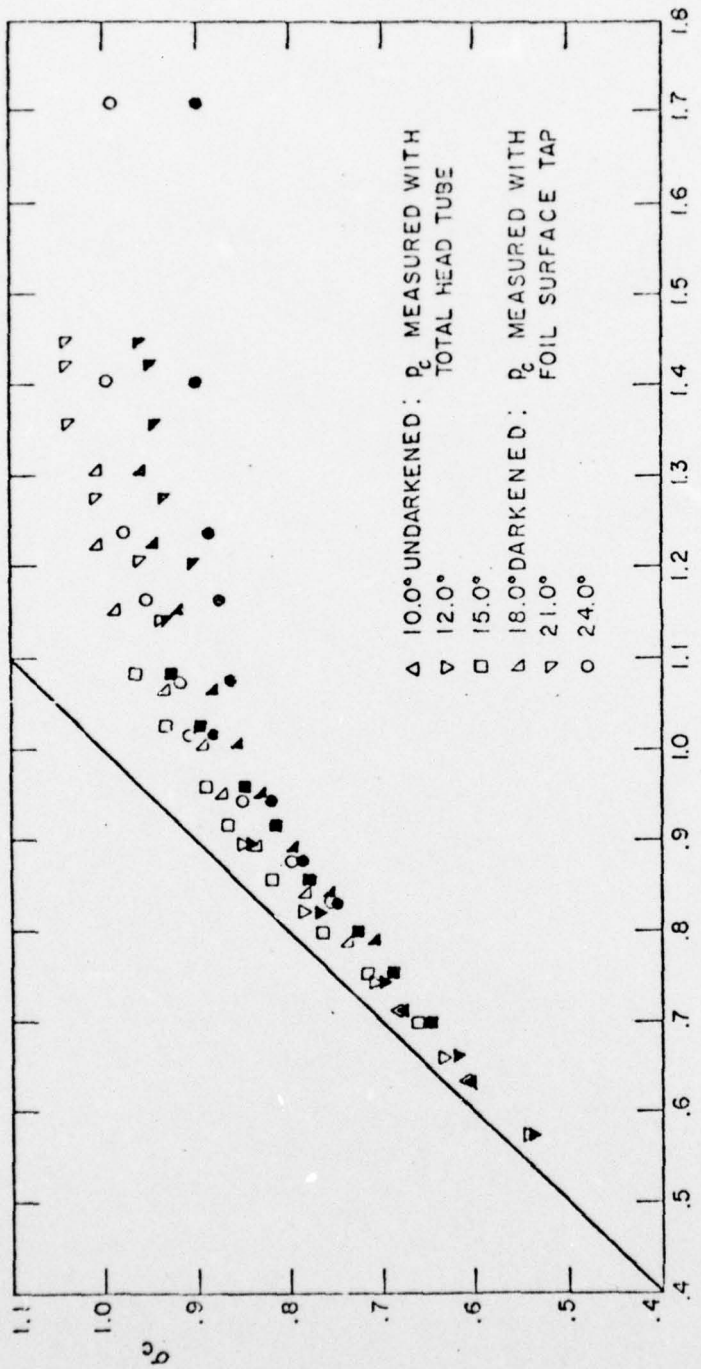

FIG.35: σ_c vs σ_v, LARGE FOIL: COMPARISON OF CAVITY PRESSURE MEASUREMENT TECHNIQUES

APPENDIX I

Standard Wind Tunnel Corrections for Effects of Images of Trailing Vortices

The experimental data shown in Figs. 4 through 30 are corrected for the apparent upwash due to the interference of the tunnel walls, in accordance with standard wind tunnel practice. The boundary condition of zero normal velocity at the tunnel walls is satisfied in the analytical treatment of the problem by introducing a doubly infinite system of image vortices; the interference due to the presence of the tunnel walls is then calculated to be the interference caused by the series of vortex images on the flow at the model. The net result is an additive correction to the induced drag and the angle of attack (to be perfectly correct, there is also a slight negative correction to the measured lift, but this is usually neglected). Upon application of the correction factor, the flow about the model is transformed to the flow which would be seen if the foil were in an infinite stream.

Since the hydrofoils tested in the square tunnel were only of half-span, a full-span model would require a duplex tunnel (that is, one whose ratio of height to width is 1/2). The ratio of model span to tunnel width for the small, medium, and large foils is 1/4, 1/2, and 3/4, respectively. Entering Fig. 6.34 of Pope and Harper [1], δ, the tunnel correction

factor for the influence of the images of the trailing vortex system was found to be 0.126 for the small, 0.104 for the medium, and 0.092 for the large foil. If the ratio of the foil area to tunnel cross-sectional area is S/S_o, then the change in angle of attack is

$$\Delta\alpha_i = \delta\frac{S}{S_o} C_L. \qquad \text{(radians)} \tag{I-1}$$

The maximum value for $\Delta\alpha_i$ encountered in the experiments was 1.47 degrees. When $\Delta\alpha_i$ is added to the measured geometrical angle of attack, α, the "true" angle of attack is obtained

$$\alpha_T = \alpha + \Delta\alpha_i. \tag{I-2}$$

(In addition to the above correction, the data reduction program accounted for the dynamometer shaft twist, which never exceeded 0.06 degree.) The change in induced drag is

$$\Delta C_{D_i} = \delta\frac{S}{S_o} C_L^2$$

$$= \Delta\alpha_i \, C_L \tag{I-3}$$

so that the total drag coefficient is

$$C_D = C_{D_{uncor}} + \Delta C_{D_i} \tag{I-4}$$

where $C_{D_{uncor}}$ is the uncorrected drag coefficient calculated from the raw experimental data.

APPENDIX II

Leehey's Matched Asymptotic Solution for Supercavitating Hydrofoils of Large Aspect Ratio

A synopsis of Leehey's theoretical results, as derived in references [9] and [11], is given.

Leehey's linearized steady-flow theory, which utilizes the method of matched asymptotic expansions, is valid to first order in angle of attack, and to second order in the reciprocal of the aspect ratio. Gravitational effects were neglected in the derivation. The analysis shows that the lift, drag, and moment coefficients, and non-dimensional cavity length (measured from midchord) are given by the following relationships:

$$C_L = \frac{\pi\alpha}{\sin\gamma(1+\sin\gamma)} \left\{1 - \frac{2\sin\gamma-1}{A(1+\sin\gamma)}\right\}, \qquad \text{(II-1)}$$

$$C_D = \alpha C_L = \frac{\pi\alpha^2}{\sin\gamma(1+\sin\gamma)} \left\{1 - \frac{2\sin\gamma-1}{A(1+\sin\gamma)}\right\}, \qquad \text{(II-2)}$$

$$C_M = \frac{-4\alpha}{\pi(1+\sin\gamma)^2} \left\{1 - \frac{1-2\sin\gamma+2\sin^2\gamma}{A\,\sin\gamma(1+\sin\gamma)}\right\}, \qquad \text{(II-3)}$$

and

$$L/c = \sec^2\gamma - 1/2 - \frac{8}{\pi\alpha A}\left[\frac{\alpha}{\sigma_c}\right]^2 C_{L_{2D}}, \qquad \text{(II-4)}$$

where $C_{L_{2D}}$, the two-dimensional lift coefficient may be expressed as

$$C_{L_{2D}} = \frac{\pi\alpha}{\sin\gamma(1+\sin\gamma)}, \qquad \text{(II-5)}$$

and where

$$\gamma \equiv \arctan\left(\frac{2\alpha}{\sigma_c}\right), \qquad \text{(II-6)}$$

and

$$\sigma_c \equiv \frac{p_\infty - p_c}{(1/2)\rho U^2}. \qquad \text{(II-7)}$$

Experiments performed by Leehey and Stellinger [9] showed that the above predictions for lift and drag coefficients and for cavity lengths were good; it was evident from the experimental results, however, that lifting surface corrections would be needed to improve the moment coefficient prediction.

APPENDIX III

Numerical Lifting Surface Theory for Supercavitating Hydrofoils of Finite Span

A brief description of the numerical lifting surface theory developed by Jiang and Leehey [12] for supercavitating hydrofoils of finite span will be given.

The steady flow theory is linearized for application to thin wings at small attack angles. Discrete sources and vortices are utilized in the representation of the physical model, and the coupled integral equations are reduced to a set of simultaneous algebraic equations. The cavity closure condition is applied stripwise on the cavity in an iterative process to obtain the desired cavitation number over the supercavitated planform.

This numerical theory should prove to be more accurate than the asymptotic theory of Leehey [11]; an implicit assumption in the latter theory is that the cavity length is less than the span, so that for small σ_c/α (i.e., long cavities), the numerical theory should indeed give better predictions. It should be noted, also, that for the $\sigma/\alpha_T = 1.0$ curves in Figs. 4, 5, 7, and 8 of reference [9], there is an ever-present difference between the experimental data and Leehey's asymptotic theoretical predictions for lift and drag coefficients. For long and short cavities, however, there is an even stronger disagreement between data

and Leehey's predictions for moment coefficient (Figs. 9 and 10 of reference [9]). The numerical lifting surface theory was developed in an attempt to overcome these difficulties.

The foil-cavity surface is collapsed to become a region in the (x-z) plane of the foil. The relationships for the jump in the tangential and normal components of the perturbation velocity upon crossing the foil surface and cavity projection surface are:

$$u(x,z,^{+}0) - u(x,z,^{-}0) = -\gamma(x,z), \qquad \text{(III-1)}$$

$$v(x,z,^{+}0) - v(x,z,^{-}0) = q(x,z), \qquad \text{(III-2)}$$

where γ and q are the vortex and source distributions, respectively. The boundary conditions are:

$$v(x,z,^{-}0) = \frac{dy(x,z,^{-}0)}{dx} \qquad \text{on the foil wetted surface} \qquad \text{(III-3)}$$

$$u = \sigma_c/2 \qquad \text{on the cavity boundary} \qquad \text{(III-4)}$$

$$\int_{x_\ell(z)}^{\ell(z)} q(\xi,\zeta)\,d\xi = 0 \qquad \text{cavity closure condition,} \qquad \text{(III-5)}$$

where $\ell(z)$ is the cavity length, measured from the leading edge as a function of spanwise position, and $x_\ell(z)$ is the

chordwise coordinate of the leading edge as a function of spanwise position.

The discrete vortex and source method is utilized in the formulation of a series of simultaneous equations. Upon subdividing the projected surface into small elements, a discrete bound vortex, a trailing vortex, and a source are located within each of these elements. The bound vortex is situated on the quarter-chord line of each element, and induced velocities are calculated for all elements at their midspan, three-quarter chord positions. The concentrated source is taken to be a constant distribution across each element at its three-quarter chord position. The boundary condition of fixed cavity pressure is imposed on each element at its midspan, quarter-chord position. Utilizing these boundary conditions, the following equations are obtained:

$$\frac{1}{4\pi}\sum_{i,j} a_{ijk\ell}\frac{\gamma_{ij}}{\alpha} - \frac{1}{2}\frac{q_{k\ell}}{\alpha} = -1, \qquad \begin{matrix} i = 1,\ldots,Ml \\ j = 1,\ldots,N \end{matrix} \qquad \text{(III-6)}$$

$$-\frac{\gamma_{k\ell}}{\alpha} + \frac{1}{2\pi}\sum_{i,j} b_{ijk\ell}\frac{q_{ij}}{\alpha} - \frac{\sigma_c}{\alpha} = 0, \qquad \begin{matrix} i = 1,\ldots,M \\ j = 1,\ldots,N \\ \gamma_{k\ell} = 0 \text{ for } k > Ml \end{matrix} \qquad \text{(III-7)}$$

$$\sum_{i} \frac{q_{ij}}{\alpha}\Delta s_{ij} = 0, \qquad j = 1,\ldots,N, \qquad \text{(III-8)}$$

where $a_{ijk\ell}$ and $b_{ijk\ell}$ are the v and u velocities at the (k,ℓ)

-th control point induced by the unit strength vortex and source at element (i,j). For the (i,j)-th element, Δs_{ij} is the element length, γ_{ij} the discrete vortex strength, and q_{ij} the discrete source strength. Ml and N are the number of elements on the foil along the chord and span, respectively. M is the number of elements along the chord in the cavity.

APPENDIX IV

Data Printout

For each foil at each angle of attack, a complete printout of the data is given. The data points are given in nondimensional form with no wall effect corrections applied, and then with corrections applied to account for the effects of the images of the trailing vortex system (Appendix I).

The format for the run numbers is Q-XXX-YY, where Q is the foil tested (S for small, M for medium, and L for large), XXX is α, the geometric angle of attack in degrees and YY is the run number for this foil at this attack angle.

EIPER INVES OF WALL EFFECTS ON SUPERCAVITATING HYDROFOILS OF FINITE SPAN

HYDROFOIL DATA IN NONDIMENSIONAL FORM (NO CORRECTIONS APPLIED)

RUN NO	ALPHA	CL	CDUNC	CM	L/D	D/L	RN*10**-6
S-8.0-01	8.00	0.4482	0.0799	0.0397	5.6080	0.1783	0.5841
S-8.0-02	8.00	0.4423	0.0810	0.0397	5.4617	0.1831	0.5830
S-8.0-03	8.00	0.4183	0.0816	0.0376	5.1285	0.1950	0.5809
S-8.0-04	8.00	0.3877	0.0770	0.0334	5.0355	0.1986	0.5805
S-8.0-05	8.00	0.3527	0.0732	0.0307	4.8201	0.2075	0.5775
S-8.0-06	8.00	0.3151	0.0680	0.0291	4.6346	0.2158	0.5762
S-8.0-07	8.00	0.2794	0.0607	0.0281	4.6005	0.2174	0.5767
S-8.0-08	8.00	0.2534	0.0540	0.0276	4.6970	0.2129	0.5752
S-8.0-09	8.00	0.2230	0.0479	0.0264	4.6599	0.2146	0.5738
S-8.0-10	8.00	0.1985	0.0413	0.0246	4.8094	0.2079	0.5750
S-8.0-11	8.00	0.1703	0.0347	0.0236	4.9038	0.2039	0.5762
S-8.0-12	8.00	0.1424	0.0273	0.0195	5.2115	0.1919	0.5843
S-8.0-13	8.00	0.2019	0.0424	0.0229	4.7601	0.2101	0.5405
S-8.0-14	8.00	0.2088	0.0445	0.0264	4.6952	0.2130	0.4822
S-8.0-15	8.00	0.1915	0.0375	0.0270	5.1078	0.1958	0.4832

LEGEND

ALPHA GEOMETRIC ANGLE OF ATTACK CORRECTED FOR SHAFT TWIST
CL LIFT COEFFICIENT, NONDIMENSIONALIZED ON UPSTREAM VELOCITY AND MODEL PLANFORM AREA
CDUNC CD(UNCORRECTED), THE UNCORRECTED DRAG COEFFICIENT AS COMPUTED FROM MEASURED DRAG, AND NONDIMENSIONALIZED ON UPSTREAM VELOCITY AND MODEL PLANFORM AREA
CM MOMENT COEFFICIENT, NONDIMENSIONALIZED ON UPSTREAM VELOCITY, MODEL PLANFORM AREA, AND MEAN CHORD
L/D LIFT-TO-DRAG RATIO = CL/CDUNC
D/L DRAG-TO-LIFT RATIO = CDUNC/CL
RN REYNOLDS NUMBER, BASED ON MEAN CHORD

EIPER INVES OF WALL EFFECTS ON SUPERCAVITATING HYDROFOILS OF FINITE SPAN

PRIOR DATA CORRECTED FOR EFFECTS OF IMAGES OF TRAILING VORTEX SYSTEM

RUN NO	ALPHAT	CL	CD	CM	(D/L)	SIGV/AT	SIGC/AT	CL/AT	CD/AT2	CM/AT	SIGV	SIGC	CAVLTH	COMMENTS/REMARKS
S-8.0-01	8.08	0.448	0.081	0.040	0.180	3.580	3.441	3.177	4.049	0.282	0.505	0.485	0.68	PC
S-8.0-02+	8.08	0.442	0.082	0.040	0.184	3.589	3.481	3.136	4.102	0.281	0.506	0.491	----	PC
S-8.0-03	8.08	0.418	0.082	0.038	0.196	3.269	3.192	2.968	4.133	0.267	0.461	0.450	0.78	PC
S-8.0-04+	8.07	0.388	0.077	0.033	0.200	2.953	2.909	2.752	3.904	0.237	0.416	0.410	0.78	PC
S-8.0-05	8.06	0.353	0.074	0.031	0.209	2.688	2.648	2.506	3.713	0.218	0.378	0.373	0.86	PC
S-8.0-06	8.06	0.315	0.068	0.029	0.217	2.455	2.422	2.241	3.454	0.207	0.345	0.341	0.96	PC
S-8.0-07	8.05	0.279	0.061	0.028	0.218	2.152	2.124	1.988	3.088	0.200	0.302	0.298	1.05	PC
S-8.0-08	8.05	0.253	0.054	0.028	0.214	1.943	1.921	1.805	2.746	0.197	0.273	0.270	1.25	PC
S-8.0-09	8.04	0.223	0.048	0.026	0.215	1.649	1.634	1.589	2.438	0.188	0.231	0.229	1.40	PC
S-8.0-10	8.04	0.198	0.041	0.025	0.209	1.395	1.385	1.415	2.104	0.176	0.196	0.194	1.70	
S-8.0-11+	8.03	0.170	0.035	0.024	0.204	1.115	1.085	1.215	1.772	0.168	0.156	0.152	2.50	
S-8.0-12	8.03	0.142	0.027	0.019	0.192	0.817	0.768	1.017	1.396	0.139	0.114	0.108	6.60	QUESTIONABLE
S-8.0-13	8.04	0.202	0.043	0.023	0.211	1.496	1.445	1.439	2.162	0.163	0.210	0.203	1.65	
S-8.0-14	8.04	0.209	0.045	0.026	0.214	1.525	1.471	1.489	2.267	0.188	0.214	0.206	1.60	
S-8.0-15	8.03	0.191	0.038	0.027	0.196	1.511	1.465	1.365	1.912	0.192	0.212	0.206	----	

UNLESS OTHERWISE INDICATED, ALL DATA ARE FOR:
1. SUPERCAVITATING FLOW.
2. BOTH STATIC PRESSURE TAPS OPEN.

LEGEND
+ ONLY UPSTREAM STATIC PRESSURE TAP UTILIZED
* ONLY DNSTREAM STATIC PRESSURE TAP UTILIZED
PC PARTIALLY CAVITATING
PC(TW) PARTIALLY CAVITATING (TAP WETTED)
FW FULLY WETTED
AT (ALPHAT) (TRUE) ANGLE OF ATTACK, CORRECTED FOR EFFECTS OF IMAGES OF TRAILING VORTICES
AT2 ALPHAT**2
SIGC CAVITATION NUMBER COMPUTED WITH MEASURED CAVITY PRESSURE
SIGV CAVITATION NUMBER COMPUTED WITH CALCULATED VAPOR PRESSURE
CD DRAG COEFFICIENT, CORRECTED FOR EFFECTS OF IMAGES OF TRAILING VORTICES
(D/L) CORRECTED DRAG-TO-LIFT RATIO = CD/CL
CAVLTH CAVITY LENGTH MEASURED FROM MIDCHORD AT CENTROID POSITION, NONDIMENSIONALIZED ON MEAN CHORD (OBTAINED FROM PHOTOGRAPHS)

EXPER INVES OF WALL EFFECTS ON SUPERCAVITATING HYDROFOILS OF FINITE SPAN

HYDROFOIL DATA IN NONDIMENSIONAL FORM (NO CORRECTIONS APPLIED)

RUN NO	ALPHA	CL	CDUNC	CM	L/D	D/L	RN*10**-6
S-9.5-01	9.50	0.5764	0.0933	0.0784	6.1771	0.1619	0.5605
S-9.5-02	9.50	0.5772	0.0926	0.0787	6.2314	0.1605	0.5601
S-9.5-03	9.50	0.5294	0.0915	0.0738	5.7864	0.1728	0.5588
S-9.5-04	9.50	0.5300	0.0900	0.0703	5.8864	0.1699	0.5563
S-9.5-05	9.50	0.4972	0.0872	0.0711	5.6989	0.1755	0.5552
S-9.5-06	9.50	0.4505	0.0833	0.0673	5.4053	0.1850	0.5550
S-9.5-07	9.50	0.4010	0.0757	0.0651	5.2950	0.1889	0.5540
S-9.5-08	9.50	0.3511	0.0680	0.0633	5.1601	0.1938	0.5533
S-9.5-09	9.50	0.3085	0.0588	0.0585	5.2514	0.1904	0.5524
S-9.5-10	9.50	0.2650	0.0492	0.0554	5.3855	0.1857	0.5524
S-9.5-11	9.50	0.2516	0.0464	0.0534	5.4162	0.1846	0.5540
S-9.5-12	9.50	0.2266	0.0429	0.0521	5.2813	0.1893	0.5559
S-9.5-13	9.50	0.2181	0.0381	0.0492	5.7288	0.1746	0.5564
S-9.5-14	9.50	0.4302	0.0790	0.0740	5.4440	0.1837	0.4612
S-9.5-15	9.50	0.4027	0.0763	0.0693	5.2777	0.1895	0.5193

LEGEND
- ALPHA GEOMETRIC ANGLE OF ATTACK CORRECTED FOR SHAFT TWIST
- CL LIFT COEFFICIENT, NONDIMENSIONALIZED ON UPSTREAM VELOCITY AND MODEL PLANFORM AREA
- CDUNC CD(UNCORRECTED), THE UNCORRECTED DRAG COEFFICIENT AS COMPUTED FROM MEASURED DRAG, AND NONDIMENSIONALIZED ON UPSTREAM VELOCITY AND MODEL PLANFORM AREA
- CM MOMENT COEFFICIENT, NONDIMENSIONALIZED ON UPSTREAM VELOCITY, MODEL PLANFORM AREA, AND MEAN CHORD
- L/D LIFT-TO-DRAG RATIO = CL/CDUNC
- D/L DRAG-TO-LIFT RATIO = CDUNC/CL
- RN REYNOLDS NUMBER, BASED ON MEAN CHORD

EIPER INVES OF WALL EFFECTS ON SUPERCAVITATING HYDROFOILS OF FINITE SPAN

PRIOR DATA CORRECTED FOR EFFECTS OF IMAGES OF TRAILING VORTEX SYSTEM

RUN NO	ALPHAT	CL	CD	CM	(D/L)	SIGV/AT	SIGC/AT	CL/AT	CD/AT2	CM/AT	SIGV	SIGC	CAVLTH	COMMENTS/REMARKS
S-9.5-01	9.61	0.576	0.094	0.078	0.164	3.038	2.974	3.438	3.357	0.468	0.509	0.499	0.68	
S-9.5-02+	9.61	0.577	0.094	0.079	0.162	3.016	2.956	3.443	3.333	0.469	0.506	0.496	----	
S-9.5-03	9.60	0.529	0.092	0.074	0.174	2.653	2.596	3.161	3.293	0.441	0.444	0.435	0.70	
S-9.5-04+	9.60	0.530	0.091	0.070	0.172	2.719	2.665	3.164	3.241	0.420	0.455	0.446	----	
S-9.5-05	9.59	0.497	0.088	0.071	0.177	2.413	2.363	2.970	3.142	0.425	0.404	0.396	0.80	
S-9.5-06	9.58	0.450	0.084	0.067	0.186	2.166	2.120	2.694	3.002	0.403	0.362	0.354	0.83	
S-9.5-07	9.57	0.401	0.076	0.065	0.190	1.901	1.880	2.400	2.731	0.390	0.318	0.314	0.95	
S-9.5-08	9.56	0.351	0.068	0.063	0.195	1.565	1.548	2.103	2.455	0.379	0.261	0.258	1.30	
S-9.5-09	9.56	0.309	0.059	0.059	0.191	1.340	1.327	1.850	2.123	0.351	0.224	0.221	1.60	
S-9.5-10	9.55	0.265	0.049	0.055	0.187	1.064	1.055	1.590	1.780	0.332	0.177	0.176	1.75	
S-9.5-11+	9.55	0.252	0.047	0.053	0.185	1.054	1.049	1.510	1.680	0.320	0.176	0.175	2.80	
S-9.5-12	9.54	0.227	0.043	0.052	0.190	0.842	0.840	1.360	1.553	0.313	0.140	0.140	3.65	
S-9.5-13	9.54	0.218	0.038	0.049	0.175	0.769	0.771	1.310	1.378	0.296	0.128	0.128	4.15	
S-9.5-14	9.58	0.430	0.080	0.074	0.185	2.020	1.963	2.573	2.848	0.443	0.338	0.328	0.90	
S-9.5-15	9.57	0.403	0.077	0.069	0.191	1.872	1.832	2.410	2.751	0.415	0.313	0.306	1.00	

UNLESS OTHERWISE INDICATED, ALL DATA ARE FOR:
1. SUPERCAVITATING FLOW.
2. BOTH STATIC PRESSURE TAPS OPEN.

LEGEND
+ ONLY UPSTREAM STATIC PRESSURE TAP UTILIZED
* ONLY DNSTREAM STATIC PRESSURE TAP UTILIZED
PC PARTIALLY CAVITATING
PC(TW) PARTIALLY CAVITATING (TAP WETTED)
FW FULLY WETTED
AT (ALPHAT) (TRUE) ANGLE OF ATTACK, CORRECTED FOR EFFECTS OF IMAGES OF TRAILING VORTICES
AT2 ALPHAT**2
SIGC CAVITATION NUMBER COMPUTED WITH MEASURED CAVITY PRESSURE
SIGV CAVITATION NUMBER COMPUTED WITH CALCULATED VAPOR PRESSURE
CD DRAG COEFFICIENT, CORRECTED FOR EFFECTS OF IMAGES OF TRAILING VORTICES
(D/L) CORRECTED DRAG-TO-LIFT RATIO = CD/CL
CAVLTH CAVITY LENGTH MEASURED FROM MIDCHORD AT CENTROID POSITION, NONDIMENSIONALIZED ON MEAN CHORD (OBTAINED FROM PHOTOGRAPHS)

EXPER INVES OF WALL EFFECTS ON SUPERCAVITATING HYDROFOILS OF FINITE SPAN

HYDROFOIL DATA IN NONDIMENSIONAL FORM (NO CORRECTIONS APPLIED)

RUN NO	ALPHA	CL	CDUNC	CM	L/D	D/L	RN*10**-6
S-11.-01	11.00	0.7207	0.1202	0.1069	5.9966	0.1668	0.5345
S-11.-02	11.00	0.7153	0.1199	0.1038	5.9682	0.1676	0.5349
S-11.-03	11.00	0.6979	0.1203	0.0991	5.7995	0.1724	0.5336
S-11.-04	11.00	0.6925	0.1200	0.0956	5.7705	0.1733	0.5339
S-11.-05	11.00	0.6584	0.1189	0.0885	5.5393	0.1805	0.5326
S-11.-06	11.00	0.6450	0.1177	0.0862	5.4797	0.1825	0.5330
S-11.-07	11.00	0.6008	0.1121	0.0807	5.3612	0.1865	0.5324
S-11.-08	11.00	0.5894	0.1122	0.0772	5.2543	0.1903	0.5319
S-11.-09	11.00	0.5229	0.1037	0.0715	5.0428	0.1983	0.5321
S-11.-10	11.00	0.5354	0.1045	0.0697	5.1255	0.1951	0.5319
S-11.-11	11.00	0.4531	0.0945	0.0629	4.7957	0.2085	0.5317
S-11.-12	11.00	0.4405	0.0919	0.0599	4.7954	0.2085	0.5317
S-11.-13	11.00	0.3786	0.0810	0.0554	4.6749	0.2139	0.5317
S-11.-14	11.00	0.3669	0.0786	0.0515	4.6672	0.2143	0.5310
S-11.-15	11.00	0.3327	0.0700	0.0472	4.7546	0.2103	0.5317
S-11.-16	11.00	0.3212	0.0684	0.0444	4.6928	0.2131	0.5308
S-11.-17	11.00	0.3040	0.0632	0.0413	4.8082	0.2080	0.5311
S-11.-18	11.00	0.2866	0.0588	0.0379	4.8745	0.2051	0.5317
S-11.-19	11.00	0.2952	0.0596	0.0361	4.9517	0.2019	0.5311
S-11.-20	11.00	0.2739	0.0560	0.0334	4.8879	0.2046	0.5317
S-11.-21	11.00	0.2594	0.0521	0.0303	4.9751	0.2010	0.5336
S-11.-22	11.00	0.2325	0.0457	0.0240	5.0920	0.1964	0.5404
S-11.-23	11.00	0.2289	0.0465	0.0208	4.9233	0.2031	0.5395

LEGEND
- ALPHA GEOMETRIC ANGLE OF ATTACK CORRECTED FOR SHAFT TWIST
- CL LIFT COEFFICIENT, NONDIMENSIONALIZED ON UPSTREAM VELOCITY AND MODEL PLANFORM AREA
- CDUNC CD(UNCORRECTED), THE UNCORRECTED DRAG COEFFICIENT AS COMPUTED FROM MEASURED DRAG, AND NONDIMENSIONALIZED ON UPSTREAM VELOCITY AND MODEL PLANFORM AREA
- CM MOMENT COEFFICIENT, NONDIMENSIONALIZED ON UPSTREAM VELOCITY, MODEL PLANFORM AREA, AND MEAN CHORD
- L/D LIFT-TO-DRAG RATIO = CL/CDUNC
- D/L DRAG-TO-LIFT RATIO = CDUNC/CL
- RN REYNOLDS NUMBER, BASED ON MEAN CHORD

ZIPER INVES OF WALL EFFECTS ON SUPERCAVITATING HYDROFOILS OF FINITE SPAN

PRIOR DATA CORRECTED FOR EFFECTS OF IMAGES OF TRAILING VORTEX SYSTEM

RUN NO	ALPHAT	CL	CD	CM	(D/L)	SIGV/AT	SIGC/AT	CL/AT	CD/AT2	CM/AT	SIGV	SIGC	CAVLTH	COMMENTS/REMARKS
S-11.-01	11.13	0.721	0.122	0.107	0.169	3.155	3.031	3.710	3.227	0.550	0.613	0.589	0.73	
S-11.-02+	11.13	0.715	0.121	0.104	0.170	3.148	3.027	3.682	3.219	0.534	0.612	0.588	----	
S-11.-03	11.13	0.698	0.122	0.099	0.175	3.020	2.921	3.594	3.231	0.510	0.586	0.567	0.78	
S-11.-04+	11.13	0.693	0.122	0.096	0.175	3.013	2.897	3.566	3.223	0.492	0.585	0.563	----	
S-11.-05	11.12	0.658	0.120	0.089	0.183	2.783	2.669	3.392	3.192	0.456	0.540	0.518	0.81	
S-11.-06+	11.12	0.645	0.119	0.086	0.185	2.776	2.666	3.324	3.161	0.444	0.539	0.517	----	
S-11.-07	11.11	0.601	0.113	0.081	0.188	2.476	2.429	3.099	3.011	0.416	0.480	0.471	0.88	
S-11.-08+	11.11	0.589	0.113	0.077	0.192	2.499	2.455	3.040	3.014	0.398	0.484	0.476	----	
S-11.-09+	11.10	0.523	0.105	0.071	0.200	2.170	2.129	2.700	2.788	0.369	0.420	0.412	1.08	
S-11.-10	11.10	0.535	0.105	0.070	0.197	2.169	2.131	2.764	2.808	0.360	0.420	0.413	----	
S-11.-11+	11.08	0.453	0.095	0.063	0.210	1.781	1.746	2.343	2.543	0.325	0.345	0.338	1.25	
S-11.-12	11.08	0.441	0.092	0.060	0.210	1.799	1.747	2.278	2.473	0.310	0.348	0.338	----	
S-11.-13+	11.07	0.379	0.081	0.055	0.215	1.450	1.421	1.960	2.182	0.287	0.280	0.274	1.90	
S-11.-14	11.07	0.367	0.079	0.051	0.215	1.430	1.404	1.900	2.119	0.266	0.276	0.271	----	
S-11.-15+	11.06	0.333	0.070	0.047	0.211	1.240	1.196	1.723	1.887	0.244	0.239	0.231	2.00	
S-11.-16	11.06	0.321	0.069	0.044	0.214	1.241	1.221	1.664	1.846	0.230	0.240	0.236	----	
S-11.-17+	11.06	0.304	0.064	0.041	0.209	1.031	1.014	1.576	1.706	0.214	0.199	0.196	2.40	
S-11.-18	11.05	0.287	0.059	0.038	0.206	1.047	1.033	1.486	1.587	0.196	0.202	0.199	----	
S-11.-19+	11.05	0.295	0.060	0.036	0.203	1.025	0.994	1.530	1.609	0.187	0.198	0.192	2.50	
S-11.-20	11.05	0.274	0.056	0.033	0.205	0.815	0.787	1.420	1.513	0.173	0.157	0.152	2.85	
S-11.-21+	11.05	0.259	0.052	0.030	0.202	0.806	0.802	1.345	1.408	0.157	0.155	0.155	----	
S-11.-22	11.04	0.232	0.046	0.024	0.197	0.664	0.643	1.206	1.234	0.125	0.128	0.124	4.60	
S-11.-23+	11.04	0.229	0.047	0.021	0.204	0.683	0.605	1.188	1.257	0.108	0.132	0.117	----	QUESTIONABLE

UNLESS OTHERWISE INDICATED, ALL DATA ARE FOR:
1. SUPERCAVITATING FLOW.
2. BOTH STATIC PRESSURE TAPS OPEN.

LEGEND
+ ONLY UPSTREAM STATIC PRESSURE TAP UTILIZED
* ONLY DNSTREAM STATIC PRESSURE TAP UTILIZED
PC PARTIALLY CAVITATING
PC(TW) PARTIALLY CAVITATING (TAP WETTED)
FW FULLY WETTED
AT (ALPHAT) (TRUE) ANGLE OF ATTACK, CORRECTED FOR EFFECTS OF IMAGES OF TRAILING VORTICES
AT2 ALPHAT**2
SIGC CAVITATION NUMBER COMPUTED WITH MEASURED CAVITY PRESSURE
SIGV CAVITATION NUMBER COMPUTED WITH CALCULATED VAPOR PRESSURE
CD DRAG COEFFICIENT, CORRECTED FOR EFFECTS OF IMAGES OF TRAILING VORTICES
(D/L) CORRECTED DRAG-TO-LIFT RATIO = CD/CL
CAVLTH CAVITY LENGTH MEASURED FROM MIDCHORD AT CENTROID POSITION, NONDIMENSIONALIZED ON MEAN CHORD (OBTAINED FROM PHOTOGRAPHS)

EXPER INVES OF WALL EFFECTS ON SUPERCAVITATING HYDROFOILS OF FINITE SPAN

HYDROFOIL DATA IN NONDIMENSIONAL FORM (NO CORRECTIONS APPLIED)

RUN NO	ALPHA	CL	CDUNC	CM	L/D	D/L	RN*10**-6
S-12.-01	12.00	0.7384	0.1441	0.0867	5.1258	0.1951	0.5241
S-12.-02	12.00	0.7438	0.1441	0.0851	5.1609	0.1938	0.5235
S-12.-03	12.00	0.6901	0.1408	0.0814	4.9024	0.2040	0.5245
S-12.-04	12.00	0.6470	0.1370	0.0783	4.7226	0.2117	0.5247
S-12.-05	12.00	0.5880	0.1292	0.0754	4.5508	0.2197	0.5245
S-12.-06	12.00	0.5371	0.1213	0.0732	4.4271	0.2259	0.5245
S-12.-07	12.00	0.4724	0.1081	0.0700	4.3708	0.2288	0.5250
S-12.-08	12.00	0.4218	0.0994	0.0674	4.2423	0.2357	0.5249
S-12.-09	12.00	0.3932	0.0919	0.0639	4.2778	0.2338	0.5239
S-12.-10	12.00	0.3473	0.0817	0.0618	4.2507	0.2353	0.5231
S-12.-11	12.00	0.3195	0.0741	0.0581	4.3094	0.2320	0.5247
S-12.-12	12.00	0.3069	0.0714	0.0579	4.2984	0.2326	0.5245
S-12.-13	12.00	0.2891	0.0659	0.0571	4.3890	0.2278	0.5250
S-12.-14	12.00	0.2745	0.0601	0.0546	4.5648	0.2191	0.5266
S-12.-15	12.00	0.2537	0.0556	0.0517	4.5655	0.2190	0.5303
S-12.-16	12.00	0.7091	0.1125	0.1358	6.3016	0.1587	0.5249
S-12.-17	12.00	0.3710	0.0865	0.0651	4.2886	0.2332	0.5235
S-12.-18	12.00	0.4152	0.0935	0.0693	4.4412	0.2252	0.4300
S-12.-19	12.00	0.4143	0.0904	0.0765	4.5842	0.2181	0.3116
S-12.-20	12.00	0.7299	0.1067	0.1196	6.8414	0.1462	0.3113

LEGEND
- ALPHA GEOMETRIC ANGLE OF ATTACK CORRECTED FOR SHAFT TWIST
- CL LIFT COEFFICIENT, NONDIMENSIONALIZED ON UPSTREAM VELOCITY AND MODEL PLANFORM AREA
- CDUNC CD(UNCORRECTED), THE UNCORRECTED DRAG COEFFICIENT AS COMPUTED FROM MEASURED DRAG, AND NONDIMENSIONALIZED ON UPSTREAM VELOCITY AND MODEL PLANFORM AREA
- CM MOMENT COEFFICIENT, NONDIMENSIONALIZED ON UPSTREAM VELOCITY, MODEL PLANFORM AREA, AND MEAN CHORD
- L/D LIFT-TO-DRAG RATIO = CL/CDUNC
- D/L DRAG-TO-LIFT RATIO = CDUNC/CL
- RN REYNOLDS NUMBER, BASED ON MEAN CHORD

EIPER INVES OF WALL EFFECTS ON SUPERCAVITATING HYDROFOILS OF FINITE SPAN

PRIOR DATA CORRECTED FOR EFFECTS OF IMAGES OF TRAILING VORTEX SYSTEM

RUN NO	ALPHAT	CL	CD	CM	(D/L)	SIGV/AT	SIGC/AT	CL/AT	CD/AT2	CM/AT	SIGV	SIGC	CAVLTH	COMMENTS/REMARKS
S-12.-01	12.13	0.738	0.146	0.087	0.197	2.894	2.661	3.487	3.250	0.409	0.613	0.564	0.82	
S-12.-02+	12.14	0.744	0.146	0.085	0.196	2.897	2.686	3.512	3.252	0.402	0.614	0.569	----	
S-12.-03	12.13	0.690	0.142	0.081	0.206	2.657	2.467	3.261	3.176	0.385	0.562	0.522	0.91	
S-12.-04	12.12	0.647	0.138	0.078	0.214	2.481	2.293	3.059	3.092	0.370	0.525	0.485	0.92	
S-12.-05	12.11	0.588	0.130	0.075	0.222	2.233	2.066	2.783	2.918	0.357	0.472	0.437	1.00	
S-12.-06	12.10	0.537	0.122	0.073	0.228	2.020	1.875	2.543	2.741	0.346	0.427	0.396	1.10	
S-12.-07	12.09	0.472	0.109	0.070	0.230	1.766	1.680	2.239	2.445	0.332	0.372	0.354	1.30	
S-12.-08	12.08	0.422	0.100	0.067	0.237	1.554	1.529	2.001	2.251	0.320	0.328	0.322	1.47	
S-12.-09	12.07	0.393	0.092	0.064	0.235	1.345	1.322	1.866	2.081	0.303	0.283	0.279	1.80	
S-12.-10	12.06	0.347	0.082	0.062	0.236	1.173	1.152	1.650	1.852	0.294	0.247	0.243	2.40	
S-12.-11	12.06	0.320	0.074	0.058	0.233	1.029	1.011	1.518	1.681	0.276	0.217	0.213	2.50	
S-12.-12+	12.06	0.307	0.072	0.058	0.234	1.028	1.012	1.458	1.619	0.275	0.216	0.213	----	
S-12.-13	12.05	0.289	0.066	0.057	0.229	0.889	0.855	1.374	1.495	0.272	0.187	0.180	3.87	
S-12.-14	12.05	0.274	0.060	0.055	0.220	0.767	0.697	1.305	1.365	0.260	0.161	0.147	4.30	
S-12.-15	12.05	0.254	0.056	0.052	0.220	0.621	0.555	1.207	1.262	0.246	0.131	0.117	6.30	
S-12.-16	12.13	0.709	0.114	0.136	0.161	-----	-----	3.349	2.546	0.642	-----	-----	----	FW
S-12.-17	12.07	0.371	0.087	0.065	0.234	1.310	1.266	1.761	1.960	0.309	0.276	0.267	----	
S-12.-18	12.08	0.415	0.094	0.069	0.226	1.478	1.417	1.970	2.117	0.329	0.312	0.299	1.50	
S-12.-19	12.08	0.414	0.091	0.077	0.219	2.207	1.549	1.966	2.047	0.363	0.465	0.327	1.65	VEL DROPPING
S-12.-20	12.13	0.730	0.108	0.120	0.148	-----	-----	3.447	2.417	0.565	-----	-----	----	FW

UNLESS OTHERWISE INDICATED, ALL DATA ARE FOR:
1. SUPERCAVITATING FLOW.
2. BOTH STATIC PRESSURE TAPS OPEN.

LEGEND
+ ONLY UPSTREAM STATIC PRESSURE TAP UTILIZED
* ONLY DNSTREAM STATIC PRESSURE TAP UTILIZED
PC PARTIALLY CAVITATING
PC(TW) PARTIALLY CAVITATING (TAP WETTED)
FW FULLY WETTED
AT (ALPHAT) (TRUE) ANGLE OF ATTACK, CORRECTED FOR EFFECTS OF IMAGES OF TRAILING VORTICES
AT2 ALPHAT**2
SIGC CAVITATION NUMBER COMPUTED WITH MEASURED CAVITY PRESSURE
SIGV CAVITATION NUMBER COMPUTED WITH CALCULATED VAPOR PRESSURE
CD DRAG COEFFICIENT, CORRECTED FOR EFFECTS OF IMAGES OF TRAILING VORTICES
(D/L) CORRECTED DRAG-TO-LIFT RATIO = CD/CL
CAVLTH CAVITY LENGTH MEASURED FROM MIDCHORD AT CENTROID POSITION, NONDIMENSIONALIZED ON MEAN CHORD
(OBTAINED FROM PHOTOGRAPHS)

EXPER INVES OF WALL EFFECTS ON SUPERCAVITATING HYDROFOILS OF FINITE SPAN

HYDROFOIL DATA IN NONDIMENSIONAL FORM (NO CORRECTIONS APPLIED)

RUN NO	ALPHA	CL	CDUNC	CM	L/D	D/L	RN*10**-6
S-14.-01	14.00	0.8556	0.1449	0.1588	5.9040	0.1694	0.3387
S-14.-02	14.00	0.8516	0.1500	0.1712	5.6766	0.1762	0.4538
S-14.-03	14.00	0.8450	0.1488	0.1773	5.6770	0.1761	0.5549
S-14.-04	14.00	0.9058	0.1505	0.1828	6.0197	0.1661	0.5521
S-14.-05	14.00	0.9410	0.1718	0.1577	5.4772	0.1826	0.5502
S-14.-06	14.00	0.9386	0.1925	0.1203	4.8767	0.2051	0.5497
S-14.-07	14.00	0.8869	0.1924	0.1044	4.6104	0.2169	0.5476
S-14.-08	14.00	0.8260	0.1895	0.0958	4.3580	0.2295	0.5459
S-14.-09	14.00	0.7420	0.1812	0.0896	4.0957	0.2442	0.5449
S-14.-10	14.00	0.6712	0.1703	0.0849	3.9411	0.2537	0.5451
S-14.-11	14.00	0.6030	0.1552	0.0809	3.8854	0.2574	0.5441
S-14.-12	14.00	0.5959	0.1556	0.0810	3.8308	0.2610	0.5436
S-14.-13	14.00	0.5471	0.1451	0.0780	3.7708	0.2652	0.5430
S-14.-14	14.00	0.4809	0.1311	0.0745	3.6691	0.2725	0.5428
S-14.-15	14.00	0.4274	0.1197	0.0696	3.5707	0.2801	0.5422
S-14.-16	14.00	0.3981	0.1097	0.0683	3.6296	0.2755	0.5422
S-14.-17	14.00	0.3616	0.0992	0.0650	3.6438	0.2744	0.5412
S-14.-18	14.00	0.3452	0.0927	0.0643	3.7244	0.2685	0.5409
S-14.-19	14.00	0.3324	0.0877	0.0611	3.7894	0.2639	0.5407
S-14.-20	14.00	0.3056	0.0789	0.0588	3.8725	0.2582	0.5420
S-14.-21	14.00	0.2834	0.0716	0.0558	3.9596	0.2526	0.5470
S-14.-22	14.00	0.5172	0.1373	0.0770	3.7664	0.2655	0.5405
S-14.-23	14.00	0.5296	0.1393	0.0778	3.8012	0.2631	0.4484
S-14.-24	14.00	0.4866	0.1216	0.0749	4.0017	0.2499	0.4036
S-14.-25	14.00	0.4554	0.1127	0.0753	4.0403	0.2475	0.3299

LEGEND
- ALPHA GEOMETRIC ANGLE OF ATTACK CORRECTED FOR SHAFT TWIST
- CL LIFT COEFFICIENT, NONDIMENSIONALIZED ON UPSTREAM VELOCITY AND MODEL PLANFORM AREA
- CDUNC CD(UNCORRECTED), THE UNCORRECTED DRAG COEFFICIENT AS COMPUTED FROM MEASURED DRAG, AND NONDIMENSIONALIZED ON UPSTREAM VELOCITY AND MODEL PLANFORM AREA
- CM MOMENT COEFFICIENT, NONDIMENSIONALIZED ON UPSTREAM VELOCITY, MODEL PLANFORM AREA, AND MEAN CHORD
- L/D LIFT-TO-DRAG RATIO = CL/CDUNC
- D/L DRAG-TO-LIFT RATIO = CDUNC/CL
- RN REYNOLDS NUMBER, BASED ON MEAN CHORD

EXPER INVES OF WALL EFFECTS ON SUPERCAVITATING HYDROFOILS OF FINITE SPAN

PRIOR DATA CORRECTED FOR EFFECTS OF IMAGES OF TRAILING VORTEX SYSTEM

RUN NO	ALPHAT	CL	CD	CM	(D/L)	SIGV/AT	SIGC/AT	CL/AT	CD/AT2	CM/AT	SIGV	SIGC	CAVLTH	COMMENTS/REMARKS
S-14.-01	14.16	0.856	0.147	0.159	0.172	-----	-----	3.463	2.412	0.643	-----	-----	----	FW
S-14.-02	14.16	0.852	0.152	0.171	0.179	-----	-----	3.447	2.495	0.693	-----	-----	----	FW
S-14.-03	14.16	0.845	0.151	0.177	0.179	-----	-----	3.420	2.476	0.718	-----	-----	----	FW
S-14.-04	14.17	0.906	0.153	0.183	0.169	-----	-----	3.663	2.504	0.739	-----	-----	----	PC(TW)
S-14.-05	14.17	0.941	0.175	0.158	0.186	-----	-----	3.804	2.854	0.637	-----	-----	----	PC(TW)
S-14.-06	14.17	0.939	0.195	0.120	0.208	3.361	2.792	3.795	3.192	0.486	0.831	0.690	0.72	
S-14.-07	14.16	0.887	0.195	0.104	0.220	3.022	2.640	3.588	3.190	0.422	0.747	0.653	0.78	
S-14.-08	14.15	0.826	0.192	0.096	0.232	2.753	2.451	3.345	3.143	0.388	0.680	0.605	0.88	
S-14.-09	14.14	0.742	0.183	0.090	0.246	2.442	2.205	3.008	3.005	0.363	0.603	0.544	0.91	
S-14.-10	14.12	0.671	0.172	0.085	0.256	2.184	1.981	2.723	2.827	0.344	0.538	0.488	1.03	
S-14.-11	14.11	0.603	0.156	0.081	0.259	1.933	1.764	2.449	2.578	0.328	0.476	0.434	1.30	
S-14.-12*	14.11	0.596	0.157	0.081	0.263	1.935	1.768	2.420	2.584	0.329	0.476	0.435	----	
S-14.-13	14.10	0.547	0.146	0.078	0.267	1.727	1.611	2.223	2.412	0.317	0.425	0.396	1.40	
S-14.-14	14.09	0.481	0.132	0.075	0.274	1.467	1.418	1.956	2.180	0.303	0.361	0.349	1.65	
S-14.-15	14.08	0.427	0.120	0.070	0.281	1.257	1.227	1.739	1.992	0.283	0.309	0.301	1.80	
S-14.-16	14.07	0.398	0.110	0.068	0.277	1.109	1.081	1.621	1.826	0.278	0.272	0.265	2.18	
S-14.-17	14.07	0.362	0.100	0.065	0.276	0.915	0.889	1.473	1.653	0.265	0.225	0.218	2.60	
S-14.-18*	14.06	0.345	0.093	0.064	0.270	0.914	0.890	1.406	1.545	0.262	0.224	0.219	----	
S-14.-19	14.06	0.332	0.088	0.061	0.265	0.781	0.760	1.355	1.463	0.249	0.192	0.186	4.10	
S-14.-20	14.06	0.306	0.079	0.059	0.259	0.660	0.642	1.246	1.316	0.240	0.162	0.158	4.80	
S-14.-21	14.05	0.283	0.072	0.056	0.253	0.534	0.518	1.155	1.194	0.228	0.131	0.127	6.40	
S-14.-22	14.09	0.517	0.138	0.077	0.267	1.591	1.512	2.102	2.283	0.313	0.391	0.372	----	
S-14.-23	14.10	0.530	0.140	0.078	0.265	1.713	1.602	2.153	2.316	0.316	0.421	0.394	1.40	
S-14.-24	14.09	0.487	0.122	0.075	0.251	1.494	1.420	1.979	2.024	0.305	0.367	0.349	1.55	
S-14.-25	14.08	0.455	0.113	0.075	0.249	1.526	1.422	1.853	1.877	0.306	0.375	0.349	1.50	

UNLESS OTHERWISE INDICATED, ALL DATA ARE FOR:
1. SUPERCAVITATING FLOW.
2. BOTH STATIC PRESSURE TAPS OPEN.

LEGEND
+ ONLY UPSTREAM STATIC PRESSURE TAP UTILIZED
* ONLY DNSTREAM STATIC PRESSURE TAP UTILIZED
PC PARTIALLY CAVITATING
PC(TW) PARTIALLY CAVITATING (TAP WETTED)
FW FULLY WETTED
AT (ALPHAT) (TRUE) ANGLE OF ATTACK, CORRECTED FOR EFFECTS OF IMAGES OF TRAILING VORTICES
AT2 ALPHAT**2
SIGC CAVITATION NUMBER COMPUTED WITH MEASURED CAVITY PRESSURE
SIGV CAVITATION NUMBER COMPUTED WITH CALCULATED VAPOR PRESSURE
CD DRAG COEFFICIENT, CORRECTED FOR EFFECTS OF IMAGES OF TRAILING VORTICES
(D/L) CORRECTED DRAG-TO-LIFT RATIO = CD/CL
CAVLTH CAVITY LENGTH MEASURED FROM MIDCHORD AT CENTROID POSITION, NONDIMENSIONALIZED ON MEAN CHORD (OBTAINED FROM PHOTOGRAPHS)

EXPER INVES OF WALL EFFECTS ON SUPERCAVITATING HYDROFOILS OF FINITE SPAN

HYDROFOIL DATA IN NONDIMENSIONAL FORM (NO CORRECTIONS APPLIED)

RUN NO	ALPHA	CL	CDUNC	CM	L/D	D/L	RN*10**-6
S-16.-01	16.00	0.9136	0.2404	0.1022	3.7995	0.2632	0.5235
S-16.-02	16.00	0.8478	0.2374	0.0958	3.5716	0.2800	0.5226
S-16.-03	16.00	0.8290	0.2333	0.0951	3.5528	0.2815	0.5228
S-16.-04	16.00	0.7796	0.2233	0.0927	3.4913	0.2864	0.5226
S-16.-05	16.00	0.7301	0.2151	0.0900	3.3947	0.2946	0.5224
S-16.-06	16.00	0.6902	0.2052	0.0881	3.3641	0.2973	0.5220
S-16.-07	16.00	0.6525	0.1982	0.0843	3.2914	0.3038	0.5224
S-16.-08	16.00	0.6049	0.1879	0.0840	3.2203	0.3105	0.5214
S-16.-09	16.00	0.5588	0.1774	0.0815	3.1493	0.3175	0.5216
S-16.-10	16.00	0.5191	0.1659	0.0776	3.1292	0.3196	0.5208
S-16.-11	16.00	0.5096	0.1628	0.0781	3.1306	0.3194	0.5210
S-16.-12	16.00	0.4693	0.1510	0.0746	3.1075	0.3218	0.5204
S-16.-13	16.00	0.4276	0.1351	0.0717	3.1656	0.3159	0.5206
S-16.-14	16.00	0.3918	0.1232	0.0699	3.1793	0.3145	0.5200
S-16.-15	16.00	0.3698	0.1133	0.0672	3.2642	0.3064	0.5192
S-16.-16	16.00	0.3396	0.1012	0.0643	3.3555	0.2980	0.5210
S-16.-17	16.00	0.3176	0.0943	0.0608	3.3658	0.2971	0.5239
S-16.-18	16.00	0.4771	0.1464	0.0773	3.2591	0.3068	0.4141
S-16.-19	16.00	0.5831	0.1654	0.0878	3.5261	0.2836	0.3444

LEGEND
- ALPHA GEOMETRIC ANGLE OF ATTACK CORRECTED FOR SHAFT TWIST
- CL LIFT COEFFICIENT, NONDIMENSIONALIZED ON UPSTREAM VELOCITY AND MODEL PLANFORM AREA
- CDUNC CD(UNCORRECTED), THE UNCORRECTED DRAG COEFFICIENT AS COMPUTED FROM MEASURED DRAG, AND NONDIMENSIONALIZED ON UPSTREAM VELOCITY AND MODEL PLANFORM AREA
- CM MOMENT COEFFICIENT, NONDIMENSIONALIZED ON UPSTREAM VELOCITY, MODEL PLANFORM AREA, AND MEAN CHORD
- L/D LIFT-TO-DRAG RATIO = CL/CDUNC
- D/L DRAG-TO-LIFT RATIO = CDUNC/CL
- RN REYNOLDS NUMBER, BASED ON MEAN CHORD

EIPER INVES OF WALL EFFECTS ON SUPERCAVITATING HYDROFOILS OF FINITE SPAN

PRIOR DATA CORRECTED FOR EFFECTS OF IMAGES OF TRAILING VORTEX SYSTEM

RUN NO	ALPHAT	CL	CD	CM	(D/L)	SIGV/AT	SIGC/AT	CL/AT	CD/AT2	CM/AT	SIGV	SIGC	CAVLTH	COMMENTS/REMARKS
S-16.-01	16.17	0.914	0.243	0.102	0.266	2.813	2.309	3.238	3.053	0.362	0.794	0.651	0.88	
S-16.-02	16.15	0.848	0.240	0.096	0.283	2.528	2.147	3.007	3.015	0.340	0.713	0.605	0.90	
S-16.-03+	16.15	0.829	0.235	0.095	0.284	2.509	2.161	2.941	2.964	0.337	0.707	0.609	----	
S-16.-04	16.14	0.780	0.225	0.093	0.289	2.279	1.962	2.767	2.837	0.329	0.642	0.553	1.02	
S-16.-05	16.13	0.730	0.217	0.090	0.297	2.140	1.872	2.593	2.734	0.320	0.603	0.527	1.09	
S-16.-06	16.13	0.690	0.207	0.088	0.299	1.988	1.751	2.452	2.609	0.313	0.559	0.493	1.10	
S-16.-07	16.12	0.652	0.200	0.084	0.306	1.869	1.655	2.319	2.522	0.300	0.523	0.466	1.30	
S-16.-08	16.11	0.605	0.189	0.084	0.312	1.695	1.538	2.151	2.391	0.299	0.476	0.432	1.35	
S-16.-09	16.10	0.559	0.178	0.081	0.319	1.536	1.393	1.988	2.259	0.290	0.432	0.406	1.58	
S-16.-10	16.09	0.519	0.167	0.078	0.321	1.384	1.323	1.848	2.113	0.276	0.389	0.372	1.70	
S-16.-11+	16.09	0.510	0.164	0.078	0.321	1.382	1.322	1.814	2.074	0.278	0.388	0.371	----	
S-16.-12	16.09	0.469	0.152	0.075	0.323	1.196	1.153	1.672	1.925	0.266	0.336	0.324	2.10	
S-16.-13	16.08	0.428	0.136	0.072	0.317	1.005	0.980	1.524	1.723	0.256	0.282	0.275	2.80	
S-16.-14	16.07	0.392	0.124	0.070	0.316	0.849	0.825	1.397	1.572	0.249	0.238	0.231	3.20	
S-16.-15	16.07	0.370	0.114	0.067	0.308	0.740	0.717	1.319	1.446	0.240	0.208	0.201	4.30	
S-16.-16	16.06	0.340	0.102	0.064	0.299	0.577	0.555	1.211	1.292	0.230	0.162	0.156	6.00	
S-16.-17	16.06	0.318	0.095	0.061	0.298	0.507	0.487	1.133	1.205	0.217	0.142	0.136	7.00	
S-16.-18	16.09	0.477	0.147	0.077	0.308	1.230	1.200	1.699	1.866	0.275	0.345	0.337	2.10	
S-16.-19	16.11	0.583	0.166	0.088	0.285	1.594	1.518	2.074	2.106	0.312	0.448	0.427	1.22	

UNLESS OTHERWISE INDICATED, ALL DATA ARE FOR:
1. SUPERCAVITATING FLOW.
2. BOTH STATIC PRESSURE TAPS OPEN.

LEGEND
+ ONLY UPSTREAM STATIC PRESSURE TAP UTILIZED
* ONLY DNSTREAM STATIC PRESSURE TAP UTILIZED
PC PARTIALLY CAVITATING
PC(TW) PARTIALLY CAVITATING (TAP WETTED)
FW FULLY WETTED
AT (ALPHAT) (TRUE) ANGLE OF ATTACK, CORRECTED FOR EFFECTS OF IMAGES OF TRAILING VORTICES
AT2 ALPHAT**2
SIGC CAVITATION NUMBER COMPUTED WITH MEASURED CAVITY PRESSURE
SIGV CAVITATION NUMBER COMPUTED WITH CALCULATED VAPOR PRESSURE
CD DRAG COEFFICIENT, CORRECTED FOR EFFECTS OF IMAGES OF TRAILING VORTICES
(D/L) CORRECTED DRAG-TO-LIFT RATIO = CD/CL
CAVLTH CAVITY LENGTH MEASURED FROM MIDCHORD AT CENTROID POSITION, NONDIMENSIONALIZED ON MEAN CHORD (OBTAINED FROM PHOTOGRAPHS)

AD-A045 769 MASSACHUSETTS INST OF TECH CAMBRIDGE DEPT OF OCEAN E--ETC F/G 20/4
AN EXPERIMENTAL INVESTIGATION OF WALL EFFECTS ON SUPERCAVITATIN--ETC(U)
JUL 77 M R MAIXNER N00014-76-C-0358
UNCLASSIFIED 83481-3 NL

2 OF 2
AD
AO45769

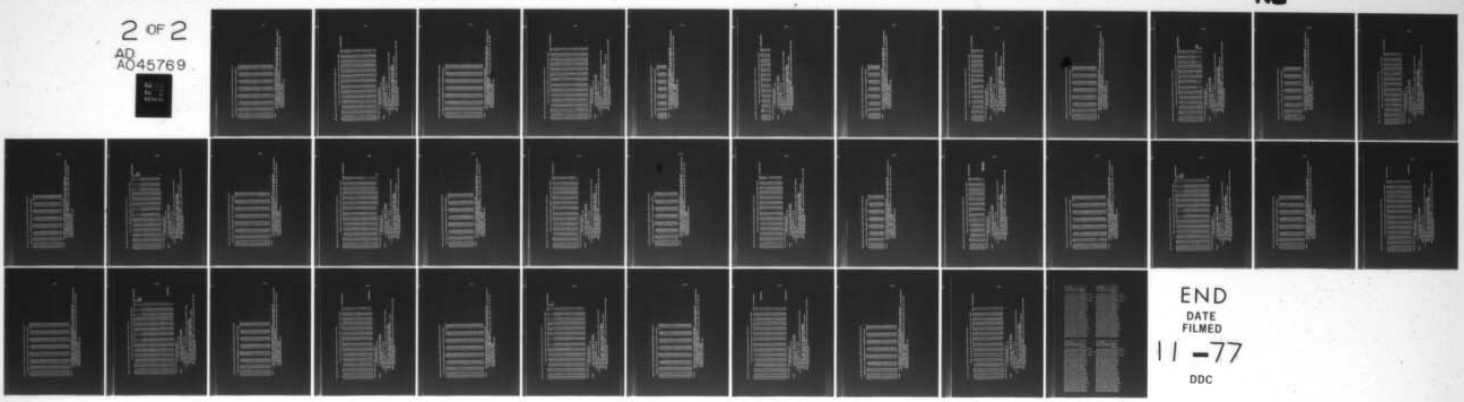

END
DATE
FILMED
11 -77
DDC

EXPER INVES OF WALL EFFECTS ON SUPERCAVITATING HYDROFOILS OF FINITE SPAN

HYDROFOIL DATA IN NONDIMENSIONAL FORM (NO CORRECTIONS APPLIED)

RUN NO	ALPHA	CL	CDUNC	CM	L/D	D/L	RN*10**-6
S-18.-01	18.00	1.0300	0.2966	0.1190	3.4724	0.2880	0.5694
S-18.-02	18.00	1.0156	0.2948	0.1190	3.4451	0.2903	0.5692
S-18.-03	18.00	0.9887	0.2928	0.1136	3.3770	0.2961	0.5692
S-18.-04	18.00	0.9507	0.2877	0.1093	3.3041	0.3027	0.5692
S-18.-05	18.00	0.9061	0.2842	0.1059	3.1883	0.3137	0.5678
S-18.-06	18.00	0.8653	0.2757	0.1024	3.1386	0.3186	0.5674
S-18.-07	18.00	0.8186	0.2672	0.0997	3.0635	0.3264	0.5678
S-18.-08	18.00	0.7671	0.2528	0.0983	3.0348	0.3295	0.5672
S-18.-09	18.00	0.7280	0.2487	0.0958	2.9273	0.3416	0.5661
S-18.-10	18.00	0.7161	0.2442	0.0952	2.9325	0.3410	0.5663
S-18.-11	18.00	0.6831	0.2358	0.0939	2.8976	0.3451	0.5658
S-18.-12	18.00	0.6508	0.2276	0.0916	2.8593	0.3497	0.5648
S-18.-13	18.00	0.6135	0.2175	0.0892	2.8204	0.3546	0.5643
S-18.-14	18.00	0.5759	0.2065	0.0878	2.7885	0.3586	0.5639
S-18.-15	18.00	0.5387	0.1965	0.0846	2.7410	0.3648	0.5632
S-18.-16	18.00	0.5013	0.1826	0.0815	2.7451	0.3643	0.5624
S-18.-17	18.00	0.4907	0.1778	0.0812	2.7594	0.3624	0.5619
S-18.-18	18.00	0.4786	0.1733	0.0793	2.7616	0.3621	0.5621
S-18.-19	18.00	0.4452	0.1601	0.0776	2.7798	0.3597	0.5612
S-18.-20	18.00	0.4233	0.1509	0.0745	2.8047	0.3565	0.5600
S-18.-21	18.00	0.4124	0.1492	0.0742	2.7651	0.3616	0.5595
S-18.-22	18.00	0.3972	0.1394	0.0724	2.8487	0.3510	0.5591
S-18.-23	18.00	0.3638	0.1273	0.0672	2.8582	0.3499	0.5604
S-18.-24	18.00	0.3521	0.1229	0.0660	2.8654	0.3490	0.5604
S-18.-25	18.00	0.3365	0.1170	0.0634	2.8751	0.3478	0.5636
S-18.-26	18.00	0.3280	0.1131	0.0621	2.9003	0.3448	0.5608
S-18.-27	18.00	0.6699	0.2333	0.0945	2.8712	0.3483	0.4422
S-18.-28	18.00	0.7569	0.2493	0.0983	3.0357	0.3294	0.3894

LEGEND

ALPHA GEOMETRIC ANGLE OF ATTACK CORRECTED FOR SHAFT TWIST
CL LIFT COEFFICIENT, NONDIMENSIONALIZED ON UPSTREAM VELOCITY AND MODEL PLANFORM AREA
CDUNC CD(UNCORRECTED), THE UNCORRECTED DRAG COEFFICIENT AS COMPUTED FROM MEASURED DRAG, AND NONDIMENSIONALIZED ON UPSTREAM VELOCITY AND MODEL PLANFORM AREA
CM MOMENT COEFFICIENT, NONDIMENSIONALIZED ON UPSTREAM VELOCITY, MODEL PLANFORM AREA, AND MEAN CHORD
L/D LIFT-TO-DRAG RATIO = CL/CDUNC
D/L DRAG-TO-LIFT RATIO = CDUNC/CL
RN REYNOLDS NUMBER, BASED ON MEAN CHORD

EXPER INVES OF WALL EFFECTS ON SUPERCAVITATING HYDROFOILS OF FINITE SPAN

PRIOR DATA CORRECTED FOR EFFECTS OF IMAGES OF TRAILING VORTEX SYSTEM

RUN NO	ALPHAT	CL	CD	CH	(D/L)	SIGV/AT	SIGC/AT	CL/AT	CD/AT2	CH/AT	SIGV	SIGC	CAVLTH	COMMENTS/REMARKS
S-18.-01	18.19	1.030	0.300	0.119	0.291	2.963	2.335	3.205	2.977	0.375	0.940	0.741	0.88	
S-18.-02+	18.19	1.016	0.298	0.119	0.293	2.964	2.360	3.200	2.959	0.375	0.941	0.749	----	
S-18.-03	18.18	0.989	0.296	0.114	0.299	2.814	2.246	3.116	2.939	0.358	0.893	0.713	0.89	
S-18.-04	18.17	0.951	0.291	0.109	0.306	2.654	2.167	2.997	2.888	0.345	0.842	0.687	0.91	
S-18.-05	18.17	0.906	0.287	0.106	0.317	2.494	2.053	2.858	2.853	0.334	0.791	0.651	0.92	
S-18.-06	18.16	0.865	0.278	0.102	0.321	2.347	1.952	2.730	2.769	0.323	0.744	0.619	0.95	
S-18.-07	18.15	0.819	0.269	0.100	0.329	2.183	1.835	2.584	2.684	0.315	0.691	0.581	0.97	
S-18.-08	18.14	0.767	0.255	0.098	0.332	2.013	1.736	2.423	2.540	0.311	0.637	0.550	1.15	
S-18.-09	18.13	0.728	0.250	0.096	0.344	1.916	1.662	2.300	2.500	0.303	0.606	0.526	1.20	
S-18.-10+	18.13	0.716	0.246	0.095	0.343	1.914	1.673	2.263	2.455	0.301	0.606	0.529	----	
S-18.-11	18.12	0.683	0.237	0.094	0.347	1.765	1.561	2.160	2.371	0.297	0.558	0.494	1.30	
S-18.-12	18.12	0.651	0.229	0.092	0.352	1.642	1.473	2.058	2.289	0.290	0.519	0.466	1.35	
S-18.-13	18.11	0.614	0.219	0.089	0.356	1.527	1.418	1.941	2.189	0.282	0.483	0.448	1.60	
S-18.-14	18.11	0.576	0.208	0.088	0.360	1.376	1.303	1.823	2.079	0.278	0.435	0.412	1.80	
S-18.-15	18.10	0.539	0.197	0.085	0.367	1.230	1.178	1.705	1.979	0.268	0.391	0.372	2.00	
S-18.-16	18.09	0.501	0.183	0.082	0.366	1.099	1.064	1.588	1.839	0.258	0.347	0.336	2.05	
S-18.-17+	18.09	0.491	0.179	0.081	0.364	1.088	1.066	1.554	1.791	0.257	0.343	0.337	----	
S-18.-18	18.09	0.479	0.174	0.079	0.364	1.015	0.995	1.516	1.746	0.251	0.320	0.314	2.20	
S-18.-19	18.08	0.445	0.161	0.078	0.361	0.899	0.880	1.411	1.614	0.246	0.284	0.278	2.80	
S-18.-20	18.08	0.423	0.151	0.075	0.358	0.794	0.777	1.342	1.522	0.236	0.250	0.245	3.20	
S-18.-21+	18.08	0.412	0.150	0.074	0.363	0.782	0.766	1.307	1.504	0.235	0.247	0.242	----	
S-18.-22	18.07	0.397	0.140	0.072	0.352	0.674	0.660	1.259	1.406	0.229	0.213	0.208	5.10	
S-18.-23	18.07	0.364	0.128	0.067	0.351	0.527	0.515	1.154	1.285	0.213	0.166	0.162	5.80	
S-18.-24	18.06	0.352	0.123	0.066	0.350	0.502	0.491	1.117	1.240	0.209	0.158	0.155	7.20	
S-18.-25	18.06	0.336	0.117	0.063	0.349	0.389	0.380	1.067	1.181	0.201	0.123	0.120	----	
S-18.-26	18.06	0.328	0.113	0.062	0.346	0.296	0.289	1.041	1.142	0.197	0.093	0.091	----	
S-18.-27	18.12	0.670	0.235	0.094	0.350	1.785	1.661	2.118	2.347	0.299	0.564	0.525	1.37	
S-18.-28	18.14	0.757	0.251	0.098	0.332	2.027	1.871	2.391	2.506	0.311	0.642	0.592	0.98	

UNLESS OTHERWISE INDICATED, ALL DATA ARE FOR:
1. SUPERCAVITATING FLOW.
2. BOTH STATIC PRESSURE TAPS OPEN.

LEGEND
+ ONLY UPSTREAM STATIC PRESSURE TAP UTILIZED
* ONLY DNSTREAM STATIC PRESSURE TAP UTILIZED
PC PARTIALLY CAVITATING
PC(TW) PARTIALLY CAVITATING (TAP WETTED)
FW FULLY WETTED
AT (ALPHAT) (TRUE) ANGLE OF ATTACK, CORRECTED FOR EFFECTS OF IMAGES OF TRAILING VORTICES
AT2 ALPHAT**2
SIGC CAVITATION NUMBER COMPUTED WITH MEASURED CAVITY PRESSURE
SIGV CAVITATION NUMBER COMPUTED WITH CALCULATED VAPOR PRESSURE
CD DRAG COEFFICIENT, CORRECTED FOR EFFECTS OF IMAGES OF TRAILING VORTICES
(D/L) CORRECTED DRAG-TO-LIFT RATIO = CD/CL
CAVLTH CAVITY LENGTH MEASURED FROM MIDCHORD AT CENTROID POSITION, NONDIMENSIONALIZED ON MEAN CHORD (OBTAINED FROM PHOTOGRAPHS)

RIPER INVES OF WALL EFFECTS ON SUPERCAVITATING HYDROFOILS OF FINITE SPAN

HYDROFOIL DATA IN NONDIMENSIONAL FORM (NO CORRECTIONS APPLIED)

RUN NO	ALPHA	CL	CDUNC	CM	L/D	D/L	RN*10**-6
S-21.-01	21.00	1.0712	0.3710	0.1304	2.8873	0.3463	0.5788
S-21.-02	21.00	1.0663	0.3698	0.1293	2.8837	0.3468	0.5781
S-21.-03	21.00	1.0438	0.3670	0.1237	2.8438	0.3516	0.5779
S-21.-04	21.00	1.0195	0.3657	0.1180	2.7878	0.3587	0.5761
S-21.-05	21.00	0.9828	0.3596	0.1110	2.7329	0.3659	0.5755
S-21.-06	21.00	0.9386	0.3520	0.1066	2.6668	0.3750	0.5750
S-21.-07	21.00	0.8975	0.3456	0.1023	2.5970	0.3851	0.5746
S-21.-08	21.00	0.8661	0.3429	0.1026	2.5253	0.3960	0.5736
S-21.-09	21.00	0.8776	0.3431	0.1022	2.5581	0.3909	0.5723
S-21.-10	21.00	0.8412	0.3332	0.1003	2.5246	0.3961	0.5716
S-21.-11	21.00	0.8423	0.3337	0.1003	2.5241	0.3962	0.5712
S-21.-12	21.00	0.8064	0.3232	0.0995	2.4947	0.4008	0.5703
S-21.-13	21.00	0.7603	0.3134	0.0969	2.4259	0.4122	0.5701
S-21.-14	21.00	0.7127	0.2975	0.0949	2.3960	0.4174	0.5705
S-21.-15	21.00	0.7029	0.2968	0.0943	2.3686	0.4222	0.5697
S-21.-16	21.00	0.6718	0.2848	0.0928	2.3626	0.4233	0.5697
S-21.-17	21.00	0.6226	0.2709	0.0911	2.2978	0.4352	0.5691
S-21.-18	21.00	0.5892	0.2570	0.0880	2.2925	0.4362	0.5682
S-21.-19	21.00	0.5581	0.2416	0.0844	2.3101	0.4329	0.5680
S-21.-20	21.00	0.5274	0.2263	0.0826	2.3311	0.4290	0.5676
S-21.-21	21.00	0.5047	0.2148	0.0819	2.3489	0.4257	0.5673
S-21.-22	21.00	0.4774	0.2048	0.0800	2.3310	0.4290	0.5671
S-21.-23	21.00	0.4732	0.2001	0.0981	2.3652	0.4228	0.5661
S-21.-24	21.00	0.4596	0.1963	0.0787	2.3410	0.4272	0.5659
S-21.-25	21.00	0.4391	0.1850	0.0755	2.3726	0.4215	0.5663
S-21.-26	21.00	0.4152	0.1733	0.0725	2.3964	0.4173	0.5663
S-21.-27	21.00	0.3943	0.1673	0.0693	2.3562	0.4244	0.5671
S-21.-28	21.00	0.3857	0.1601	0.0673	2.4096	0.4150	0.5674
S-21.-29	21.00	0.4303	0.1769	0.0723	2.4323	0.4111	0.4328
S-21.-30	21.00	0.6763	0.2761	0.0990	2.4494	0.4083	0.3837

LEGEND
ALPHA GEOMETRIC ANGLE OF ATTACK CORRECTED FOR SHAFT TWIST
CL LIFT COEFFICIENT, NONDIMENSIONALIZED ON UPSTREAM VELOCITY AND MODEL PLANFORM AREA
CDUNC CD(UNCORRECTED), THE UNCORRECTED DRAG COEFFICIENT AS COMPUTED FROM MEASURED DRAG, AND NONDIMENSIONALIZED ON UPSTREAM VELOCITY AND MODEL PLANFORM AREA
CM MOMENT COEFFICIENT, NONDIMENSIONALIZED ON UPSTREAM VELOCITY, MODEL PLANFORM AREA, AND MEAN CHORD
L/D LIFT-TO-DRAG RATIO = CL/CDUNC
D/L DRAG-TO-LIFT RATIO = CDUNC/CL
RN REYNOLDS NUMBER, BASED ON MEAN CHORD

EXPER IMVES OF WALL EFFECTS ON SUPERCAVITATING HYDROFOILS OF FINITE SPAN

PRIOR DATA CORRECTED FOR EFFECTS OF IMAGES OF TRAILING VORTEI SYSTEM

RUN NO	ALPHAT	CL	CD	CM	(D/L)	SIGV/AT	SIGC/AT	CL/AT	CD/AT2	CM/AT	SIGV	SIGC	CAVLTH	COMMENTS/REMARKS
S-21.-01	21.20	1.071	0.375	0.130	0.350	3.141	2.031	2.896	2.738	0.353	1.162	0.751	0.83	
S-21.-02+	21.19	1.066	0.373	0.129	0.350	3.149	2.056	2.883	2.728	0.350	1.165	0.760	----	
S-21.-03+	21.19	1.044	0.370	0.124	0.355	2.993	2.028	2.822	2.708	0.334	1.107	0.750	0.80	
S-21.-04+	21.19	1.020	0.369	0.118	0.362	2.844	2.032	2.757	2.699	0.319	1.052	0.751	0.85	
S-21.-05+	21.18	0.983	0.363	0.111	0.369	2.671	1.987	2.659	2.654	0.300	0.987	0.734	0.95	
S-21.-06+	21.17	0.939	0.355	0.107	0.378	2.478	1.892	2.540	2.598	0.288	0.916	0.699	0.98	
S-21.-07+	21.16	0.897	0.348	0.102	0.388	2.282	1.795	2.430	2.552	0.277	0.843	0.663	1.00	
S-21.-08+	21.16	0.866	0.345	0.103	0.399	2.149	1.742	2.345	2.532	0.278	0.794	0.643	1.02	
S-21.-09	21.16	0.878	0.345	0.102	0.394	2.158	1.760	2.376	2.533	0.277	0.797	0.650	1.10	
S-21.-10	21.15	0.841	0.335	0.100	0.399	2.022	1.674	2.279	2.461	0.272	0.747	0.618	1.16	
S-21.-11	21.15	0.842	0.336	0.100	0.399	2.014	1.666	2.282	2.465	0.272	0.744	0.615	1.18	
S-21.-12	21.15	0.806	0.325	0.099	0.403	1.879	1.571	2.185	2.388	0.270	0.693	0.580	1.19	
S-21.-13	21.14	0.760	0.315	0.097	0.415	1.728	1.492	2.061	2.316	0.263	0.638	0.550	1.35	
S-21.-14	21.13	0.713	0.299	0.095	0.420	1.574	1.399	1.933	2.199	0.257	0.580	0.516	1.40	
S-21.-15+	21.13	0.703	0.298	0.094	0.424	1.577	1.424	1.906	2.194	0.256	0.582	0.525	----	
S-21.-16	21.12	0.672	0.286	0.093	0.425	1.445	1.322	1.822	2.103	0.252	0.533	0.488	1.50	
S-21.-17	21.11	0.623	0.272	0.091	0.437	1.295	1.214	1.689	2.004	0.247	0.477	0.447	1.65	
S-21.-18	21.11	0.589	0.258	0.088	0.438	1.166	1.106	1.599	1.902	0.239	0.430	0.407	1.90	
S-21.-19	21.10	0.558	0.243	0.084	0.435	1.064	1.025	1.515	1.788	0.229	0.392	0.378	2.25	
S-21.-20	21.10	0.527	0.227	0.083	0.431	0.911	0.884	1.433	1.675	0.224	0.336	0.325	2.60	
S-21.-21	21.09	0.505	0.216	0.082	0.427	0.850	0.834	1.371	1.591	0.222	0.313	0.307	3.10	
S-21.-22	21.09	0.477	0.206	0.080	0.430	0.758	0.742	1.297	1.517	0.217	0.279	0.273	3.00	
S-21.-23+	21.09	0.473	0.201	0.098	0.424	0.760	0.745	1.286	1.482	0.267	0.280	0.274	----	
S-21.-24	21.08	0.460	0.197	0.079	0.429	0.677	0.663	1.249	1.455	0.214	0.249	0.244	3.90	
S-21.-25	21.08	0.439	0.186	0.076	0.423	0.614	0.600	1.193	1.372	0.205	0.226	0.221	5.80	
S-21.-26	21.08	0.415	0.174	0.073	0.419	0.510	0.497	1.129	1.285	0.197	0.188	0.183	6.40	
S-21.-27	21.07	0.394	0.168	0.069	0.426	0.446	0.435	1.072	1.241	0.188	0.164	0.160	6.80	
S-21.-28	21.07	0.386	0.161	0.067	0.416	0.383	0.373	1.049	1.187	0.183	0.141	0.137	----	
S-21.-29	21.08	0.430	0.177	0.072	0.412	0.657	0.640	1.170	1.311	0.196	0.242	0.236	5.30	
S-21.-30	21.12	0.676	0.278	0.099	0.410	1.503	1.529	1.834	2.042	0.268	0.554	0.564	1.25	

UNLESS OTHERWISE INDICATED, ALL DATA ARE FOR:
1. SUPERCAVITATING FLOW.
2. BOTH STATIC PRESSURE TAPS OPEN.

LEGEND
+ ONLY UPSTREAM STATIC PRESSURE TAP UTILIZED
* ONLY DNSTREAM STATIC PRESSURE TAP UTILIZED
PC PARTIALLY CAVITATING
PC(TW) PARTIALLY CAVITATING (TAP WETTED)
FW FULLY WETTED
AT (ALPHAT) (TRUE) ANGLE OF ATTACK, CORRECTED FOR EFFECTS OF IMAGES OF TRAILING VORTICES
AT2 ALPHAT**2
SIGC CAVITATION NUMBER COMPUTED WITH MEASURED CAVITY PRESSURE
SIGV CAVITATION NUMBER COMPUTED WITH CALCULATED VAPOR PRESSURE
CD DRAG COEFFICIENT, CORRECTED FOR EFFECTS OF IMAGES OF TRAILING VORTICES
(D/L) CORRECTED DRAG-TO-LIFT RATIO = CD/CL
CAVLTH CAVITY LENGTH MEASURED FROM MIDCHORD AT CENTROID POSITION, NONDIMENSIONALIZED ON MEAN CHORD (OBTAINED FROM PHOTOGRAPHS)

EXPER INVES OF WALL EFFECTS ON SUPERCAVITATING HYDROFOILS OF FINITE SPAN

HYDROFOIL DATA IN NONDIMENSIONAL FORM (NO CORRECTIONS APPLIED)

RUN NO	ALPHA	CL	CDUNC	CM	L/D	D/L	RN*10**-6
R-8.0-01	8.01	0.5557	0.0801	0.0580	6.9393	0.1341	1.0184
R-8.0-02	8.01	0.4981	0.0787	0.0537	6.3279	0.1580	1.0114
R-8.0-03	8.01	0.4352	0.0749	0.0515	5.8117	0.1721	1.0046
R-8.0-04	8.01	0.3691	0.0676	0.0487	5.4563	0.1833	1.0025
R-8.0-05	8.01	0.3107	0.0590	0.0459	5.2656	0.1899	1.0015
R-8.0-06	8.00	0.2421	0.0482	0.0405	5.0234	0.1991	1.0036
R-8.0-07	8.00	0.2160	0.0432	0.0373	4.9968	0.2001	1.0076

LEGEND
- ALPHA GEOMETRIC ANGLE OF ATTACK CORRECTED FOR SHAFT TWIST
- CL LIFT COEFFICIENT, NONDIMENSIONALIZED ON UPSTREAM VELOCITY AND MODEL PLANFORM AREA
- CDUNC CD(UNCORRECTED), THE UNCORRECTED DRAG COEFFICIENT AS COMPUTED FROM MEASURED DRAG, AND NONDIMENSIONALIZED ON UPSTREAM VELOCITY AND MODEL PLANFORM AREA
- CM MOMENT COEFFICIENT, NONDIMENSIONALIZED ON UPSTREAM VELOCITY, MODEL PLANFORM AREA, AND MEAN CHORD
- L/D LIFT-TO-DRAG RATIO = CL/CDUNC
- D/L DRAG-TO-LIFT RATIO = CDUNC/CL
- RN REYNOLDS NUMBER, BASED ON MEAN CHORD

EIPER INVES OF WALL EFFECTS ON SUPERCAVITATING HYDROFOILS OF FINITE SPAN

PRIOR DATA CORRECTED FOR EFFECTS OF IMAGES OF TRAILING VORTEX SYSTEM

RUN NO	ALPHAT	CL	CD	CM	(D/L)	SIGV/AT	SIGC/AT	CL/AT	CD/AT2	CM/AT	SIGV	SIGC	CAVLTH	COMMENTS/REMARKS
M-8.0-01	8.34	0.556	0.083	0.058	0.150	3.443	3.397	3.819	3.933	0.398	0.501	0.498	0.60	
M-8.0-02	8.30	0.498	0.081	0.054	0.163	3.109	3.070	3.438	3.872	0.371	0.451	0.445	0.62	
M-8.0-03	8.27	0.435	0.077	0.051	0.177	2.735	2.703	3.017	3.694	0.357	0.395	0.390	0.75	
M-8.0-04	8.23	0.369	0.069	0.049	0.187	2.298	2.274	2.571	3.351	0.339	0.330	0.326	0.85	
M-8.0-05	8.19	0.311	0.060	0.046	0.193	1.903	1.886	2.173	2.936	0.321	0.272	0.270	1.14	
M-8.0-06	8.15	0.242	0.049	0.041	0.202	1.386	1.351	1.702	2.413	0.285	0.197	0.192	1.75	
M-8.0-07	8.13	0.216	0.044	0.037	0.202	1.130	1.102	1.522	2.169	0.263	0.160	0.156	2.55	

UNLESS OTHERWISE INDICATED, ALL DATA ARE FOR:
1. SUPERCAVITATING FLOW.
2. BOTH STATIC PRESSURE TAPS OPEN.

LEGEND
+ ONLY UPSTREAM STATIC PRESSURE TAP UTILIZED
* ONLY DNSTREAM STATIC PRESSURE TAP UTILIZED
PC PARTIALLY CAVITATING
PC(TW) PARTIALLY CAVITATING (TAP WETTED)
FW FULLY WETTED
AT (ALPHAT) (TRUE) ANGLE OF ATTACK, CORRECTED FOR EFFECTS OF IMAGES OF TRAILING VORTICES
AT2 ALPHAT**2
SIGC CAVITATION NUMBER COMPUTED WITH MEASURED CAVITY PRESSURE
SIGV CAVITATION NUMBER COMPUTED WITH CALCULATED VAPOR PRESSURE
CD DRAG COEFFICIENT, CORRECTED FOR EFFECTS OF IMAGES OF TRAILING VORTICES
(D/L) CORRECTED DRAG-TO-LIFT RATIO = CD/CL
CAVLTH CAVITY LENGTH MEASURED FROM MIDCHORD AT CENTROID POSITION, NONDIMENSIONALIZED ON MEAN CHORD (OBTAINED FROM PHOTOGRAPHS)

EIPER INVES OF WALL EFFECTS ON SUPERCAVITATING HYDROFOILS OF FINITE SPAN

HYDROFOIL DATA IN NONDIMENSIONAL FORM (NO CORRECTIONS APPLIED)

RUN NO	ALPHA	CL	CDUNC	CM	L/D	D/L	RN*10**-6
M-9.5-01	9.51	0.7274	0.1066	0.0756	6.8254	0.1465	0.9686
M-9.5-02	9.51	0.6523	0.1037	0.0674	6.2927	0.1589	0.9676
M-9.5-03	9.51	0.5934	0.0997	0.0659	5.9497	0.1681	0.9666
M-9.5-04	9.51	0.5175	0.0924	0.0641	5.5980	0.1786	0.9672
M-9.5-05	9.51	0.4537	0.0849	0.0605	5.3469	0.1870	0.9652
M-9.5-06	9.51	0.3847	0.0748	0.0568	5.1402	0.1945	0.9629
M-9.5-07	9.51	0.3355	0.0666	0.0529	5.0376	0.1985	0.9629
M-9.5-08	9.51	0.2760	0.0567	0.0487	4.8715	0.2053	0.9652
M-9.5-09	9.51	0.2603	0.0534	0.0470	4.8715	0.2053	0.9659

LEGEND
- ALPHA GEOMETRIC ANGLE OF ATTACK CORRECTED FOR SHAFT TWIST
- CL LIFT COEFFICIENT, NONDIMENSIONALIZED ON UPSTREAM VELOCITY AND MODEL PLANFORM AREA
- CDUNC CD(UNCORRECTED), THE UNCORRECTED DRAG COEFFICIENT AS COMPUTED FROM MEASURED DRAG, AND NONDIMENSIONALIZED ON UPSTREAM VELOCITY AND MODEL PLANFORM AREA
- CM MOMENT COEFFICIENT, NONDIMENSIONALIZED ON UPSTREAM VELOCITY, MODEL PLANFORM AREA, AND MEAN CHORD
- L/D LIFT-TO-DRAG RATIO = CL/CDUNC
- D/L DRAG-TO-LIFT RATIO = CDUNC/CL
- RN REYNOLDS NUMBER, BASED ON MEAN CHORD

RIPER INVES OF WALL EFFECTS ON SUPERCAVITATING HYDROFOILS OF FINITE SPAN

PRIOR DATA CORRECTED FOR EFFECTS OF IMAGES OF TRAILING VORTEX SYSTEM

RUN NO	ALPHAT	CL	CD	CM	(D/L)	SIGV/AT	SIGC/AT	CL/AT	CD/AT2	CM/AT	SIGV	SIGC	CAVLTH	COMMENTS/REMARKS
M-9.5-01	9.94	0.727	0.112	0.076	0.154	3.529	3.285	4.192	3.722	0.436	0.612	0.570	0.63	
M-9.5-02	9.90	0.652	0.108	0.067	0.166	3.187	2.950	3.777	3.623	0.390	0.551	0.510	0.65	
M-9.5-03	9.86	0.593	0.103	0.066	0.174	2.883	2.653	3.448	3.491	0.383	0.496	0.457	0.80	
M-9.5-04	9.82	0.518	0.095	0.064	0.184	2.478	2.256	3.021	3.245	0.374	0.425	0.387	0.89	
M-9.5-05	9.78	0.454	0.087	0.060	0.192	2.194	2.025	2.659	2.988	0.354	0.374	0.346	1.00	
M-9.5-06	9.74	0.385	0.076	0.057	0.199	1.839	1.723	2.264	2.645	0.334	0.312	0.293	1.35	
M-9.5-07	9.71	0.336	0.068	0.053	0.202	1.536	1.430	1.981	2.362	0.312	0.260	0.242	1.55	
M-9.5-08	9.67	0.276	0.057	0.049	0.208	1.158	1.061	1.635	2.017	0.289	0.195	0.179	2.25	
M-9.5-09	9.66	0.260	0.054	0.047	0.208	0.987	0.901	1.544	1.904	0.279	0.166	0.152	3.25	

UNLESS OTHERWISE INDICATED, ALL DATA ARE FOR:
1. SUPERCAVITATING FLOW.
2. BOTH STATIC PRESSURE TAPS OPEN.

LEGEND
- * ONLY UPSTREAM STATIC PRESSURE TAP UTILIZED
- * ONLY DNSTREAM STATIC PRESSURE TAP UTILIZED
- PC PARTIALLY CAVITATING
- PC(TW) PARTIALLY CAVITATING (TAP WETTED)
- FW FULLY WETTED
- AT (ALPHAT) (TRUE) ANGLE OF ATTACK, CORRECTED FOR EFFECTS OF IMAGES OF TRAILING VORTICES
- AT2 ALPHAT**2
- SIGC CAVITATION NUMBER COMPUTED WITH MEASURED CAVITY PRESSURE
- SIGV CAVITATION NUMBER COMPUTED WITH CALCULATED VAPOR PRESSURE
- CD DRAG COEFFICIENT, CORRECTED FOR EFFECTS OF IMAGES OF TRAILING VORTICES
- (D/L) CORRECTED DRAG-TO-LIFT RATIO = CD/CL
- CAVLTH CAVITY LENGTH MEASURED FROM MIDCHORD AT CENTROID POSITION, NONDIMENSIONALIZED ON MEAN CHORD (OBTAINED FROM PHOTOGRAPHS)

EXPER INVES OF WALL EFFECTS ON SUPERCAVITATING HYDROFOILS OF FINITE SPAN

HYDROFOIL DATA IN NONDIMENSIONAL FORM (NO CORRECTIONS APPLIED)

RUN NO	ALPHA	CL	CDUNC	CM	L/D	D/L	RN*10**-6
A-11.-01	11.02	0.7944	0.1136	0.1445	6.9940	0.1430	1.0697
A-11.-02	11.01	0.8370	0.1231	0.1226	6.7986	0.1471	1.0669
A-11.-03	11.01	0.8608	0.1329	0.0991	6.4774	0.1544	1.0666
A-11.-04	11.01	0.8276	0.1354	0.0890	6.1132	0.1636	1.0621
A-11.-05	11.01	0.7774	0.1346	0.0829	5.7740	0.1732	1.0589
A-11.-06	11.01	0.7173	0.1311	0.0788	5.4696	0.1828	1.0558
A-11.-07	11.01	0.6523	0.1247	0.0767	5.2306	0.1912	1.0533
A-11.-08	11.01	0.5769	0.1163	0.0723	4.9594	0.2016	1.0523
A-11.-09	11.01	0.5161	0.1078	0.0680	4.7879	0.2089	1.0498
A-11.-10	11.01	0.4519	0.0961	0.0657	4.7021	0.2127	1.0491
A-11.-11	11.01	0.4034	0.0867	0.0613	4.6518	0.2150	1.0474
A-11.-12	11.01	0.3553	0.0785	0.0591	4.5253	0.2210	1.0453
A-11.-13	11.01	0.3150	0.0699	0.0544	4.5030	0.2221	1.0453
A-11.-14	11.01	0.2985	0.0666	0.0532	4.4819	0.2231	1.0463
A-11.-15	11.02	0.7703	0.1082	0.1510	7.1192	0.1405	1.0453
A-11.-16	11.02	0.7496	0.1095	0.1484	6.8474	0.1460	1.0456
A-11.-17	11.02	0.7221	0.1094	0.1376	6.5985	0.1516	1.0438
A-11.-18	11.01	0.7176	0.1099	0.1344	6.5280	0.1532	0.7589
A-11.-19	11.00	0.7038	0.1061	0.1384	6.6360	0.1507	0.5599

LEGEND
- ALPHA GEOMETRIC ANGLE OF ATTACK CORRECTED FOR SHAFT TWIST
- CL LIFT COEFFICIENT, NONDIMENSIONALIZED ON UPSTREAM VELOCITY AND MODEL PLANFORM AREA
- CDUNC CD(UNCORRECTED), THE UNCORRECTED DRAG COEFFICIENT AS COMPUTED FROM MEASURED DRAG, AND NONDIMENSIONALIZED ON UPSTREAM VELOCITY AND MODEL PLANFORM AREA
- CM MOMENT COEFFICIENT, NONDIMENSIONALIZED ON UPSTREAM VELOCITY, MODEL PLANFORM AREA, AND MEAN CHORD
- L/D LIFT-TO-DRAG RATIO = CL/CDUNC
- D/L DRAG-TO-LIFT RATIO = CDUNC/CL
- RN REYNOLDS NUMBER, BASED ON MEAN CHORD

EXPER INVES OF WALL EFFECTS ON SUPERCAVITATING HYDROFOILS OF FINITE SPAN

PRIOR DATA CORRECTED FOR EFFECTS OF IMAGES OF TRAILING VORTEX SYSTEM

RUN NO	ALPHAT	CL	CD	CM	(D/L)	SIGV/AT	SIGC/AT	CL/AT	CD/AT2	CM/AT	SIGV	SIGC	CAVLTH	COMMENTS/REMARKS
M-11.-01	11.49	0.794	0.120	0.145	0.151	4.217	1.276	3.961	2.987	0.721	0.846	0.256	0.66	PC
M-11.-02	11.51	0.837	0.130	0.123	0.156	3.954	2.991	4.166	3.230	0.610	0.795	0.601	0.65	
M-11.-03	11.52	0.861	0.141	0.099	0.163	3.694	3.281	4.280	3.475	0.493	0.743	0.660	0.63	
M-11.-04	11.50	0.828	0.143	0.089	0.172	3.452	3.113	4.122	3.535	0.443	0.693	0.625	0.64	
M-11.-05	11.47	0.777	0.141	0.083	0.181	3.219	2.935	3.882	3.514	0.414	0.644	0.588	0.66	
M-11.-06	11.44	0.717	0.137	0.079	0.190	2.963	2.700	3.594	3.426	0.395	0.591	0.539	0.66	
M-11.-07	11.40	0.652	0.129	0.077	0.198	2.681	2.439	3.279	3.263	0.386	0.533	0.485	0.72	
M-11.-08	11.35	0.577	0.120	0.072	0.208	2.371	2.169	2.912	3.051	0.365	0.470	0.430	0.79	
M-11.-09	11.32	0.516	0.111	0.068	0.214	2.079	1.919	2.614	2.835	0.344	0.411	0.379	0.93	
M-11.-10	11.28	0.452	0.098	0.066	0.217	1.835	1.793	2.296	2.536	0.334	0.361	0.353	1.10	
M-11.-11	11.25	0.403	0.088	0.061	0.219	1.591	1.553	2.055	2.294	0.312	0.312	0.305	1.40	
M-11.-12	11.22	0.355	0.080	0.059	0.225	1.363	1.349	1.815	2.082	0.302	0.267	0.264	1.75	
M-11.-13	11.19	0.315	0.071	0.054	0.225	1.069	1.059	1.612	1.860	0.279	0.209	0.207	2.80	
M-11.-14	11.18	0.298	0.068	0.053	0.226	0.947	0.941	1.529	1.772	0.272	0.185	0.184	3.25	
M-11.-15	11.48	0.770	0.114	0.151	0.148	-----	-----	3.846	2.851	0.754	-----	-----	----	PC (TW)
M-11.-16	11.46	0.750	0.115	0.148	0.154	-----	-----	3.747	2.881	0.742	-----	-----	----	PC (TW)
M-11.-17	11.45	0.722	0.115	0.138	0.159	-----	-----	3.615	2.878	0.689	-----	-----	----	FW
M-11.-18	11.44	0.718	0.115	0.134	0.161	-----	-----	3.596	2.894	0.673	-----	-----	----	FW
M-11.-19	11.42	0.704	0.111	0.138	0.158	-----	-----	3.530	2.798	0.694	-----	-----	----	FW

UNLESS OTHERWISE INDICATED, ALL DATA ARE FOR:
1. SUPERCAVITATING FLOW.
2. BOTH STATIC PRESSURE TAPS OPEN.

LEGEND
- * ONLY UPSTREAM STATIC PRESSURE TAP UTILIZED
- * ONLY DNSTREAM STATIC PRESSURE TAP UTILIZED
- PC PARTIALLY CAVITATING
- PC(TW) PARTIALLY CAVITATING (TAP WETTED)
- FW FULLY WETTED
- AT (ALPHAT) (TRUE) ANGLE OF ATTACK, CORRECTED FOR EFFECTS OF IMAGES OF TRAILING VORTICES
- AT2 ALPHAT**2
- SIGC CAVITATION NUMBER COMPUTED WITH MEASURED CAVITY PRESSURE
- SIGV CAVITATION NUMBER COMPUTED WITH CALCULATED VAPOR PRESSURE
- CD DRAG COEFFICIENT, CORRECTED FOR EFFECTS OF IMAGES OF TRAILING VORTICES
- (D/L) CORRECTED DRAG-TO-LIFT RATIO = CD/CL
- CAVLTH CAVITY LENGTH MEASURED FROM MIDCHORD AT CENTROID POSITION, NONDIMENSIONALIZED ON MEAN CHORD (OBTAINED FROM PHOTOGRAPHS)

EXPER INVES OF WALL EFFECTS ON SUPERCAVITATING HYDROFOILS OF FINITE SPAN

HYDROFOIL DATA IN NONDIMENSIONAL FORM (NO CORRECTIONS APPLIED)

RUN NO	ALPHA	CL	CDUNC	CM	L/D	D/L	RN*10**-6
A-12.-01	12.01	0.8883	0.1607	0.0982	5.5274	0.1809	1.1051
A-12.-02	12.01	0.8064	0.1577	0.0893	5.1143	0.1955	1.1011
A-12.-03	12.01	0.7386	0.1502	0.0847	4.9178	0.2033	1.0992
A-12.-04	12.01	0.6427	0.1375	0.0801	4.6738	0.2140	1.0972
A-12.-05	12.01	0.5552	0.1244	0.0752	4.4636	0.2240	1.0968
A-12.-06	12.01	0.4774	0.1098	0.0705	4.3459	0.2301	1.0948
A-12.-07	12.01	0.4431	0.1014	0.0680	4.3719	0.2287	1.0944
A-12.-08	12.01	0.3843	0.0903	0.0644	4.2567	0.2349	1.0952
A-12.-09	12.01	0.3451	0.0817	0.0604	4.2238	0.2368	1.0952
A-12.-10	12.01	0.3271	0.0773	0.0578	4.2308	0.2364	1.0960
A-12.-11	12.01	0.3615	0.0855	0.0612	4.2292	0.2365	1.0932
A-12.-12	12.01	0.3225	0.0764	0.0574	4.2218	0.2369	1.0964
A-12.-13	12.01	0.3110	0.0734	0.0561	4.2342	0.2362	1.0976
A-12.-14	12.01	0.3229	0.0759	0.0571	4.2560	0.2350	1.0956

LEGEND
- ALPHA GEOMETRIC ANGLE OF ATTACK CORRECTED FOR SHAFT TWIST
- CL LIFT COEFFICIENT, NONDIMENSIONALIZED ON UPSTREAM VELOCITY AND MODEL PLANFORM AREA
- CDUNC CD(UNCORRECTED), THE UNCORRECTED DRAG COEFFICIENT AS COMPUTED FROM MEASURED DRAG, AND NONDIMENSIONALIZED ON UPSTREAM VELOCITY AND MODEL PLANFORM AREA
- CM MOMENT COEFFICIENT, NONDIMENSIONALIZED ON UPSTREAM VELOCITY, MODEL PLANFORM AREA, AND MEAN CHORD
- L/D LIFT-TO-DRAG RATIO = CL/CDUNC
- D/L DRAG-TO-LIFT RATIO = CDUNC/CL
- RN REYNOLDS NUMBER, BASED ON MEAN CHORD

EXPER INVES OF WALL EFFECTS ON SUPERCAVITATING HYDROFOILS OF FINITE SPAN

PRIOR DATA CORRECTED FOR EFFECTS OF IMAGES OF TRAILING VORTEX SYSTEM

RUN NO	ALPHAT	CL	CD	CM	(D/L)	SIGV/AT	SIGC/AT	CL/AT	CD/AT2	CM/AT	SIGV	SIGC	CAVLTH	COMMENTS/REMARKS
H-12.-01	12.54	0.888	0.169	0.098	0.190	3.384	2.975	4.059	3.526	0.448	0.741	0.651	0.65	
H-12.-02	12.49	0.806	0.164	0.089	0.204	3.138	2.804	3.699	3.460	0.409	0.684	0.611	0.69	
H-12.-03	12.45	0.739	0.156	0.085	0.211	2.837	2.579	3.399	3.301	0.390	0.616	0.560	0.71	
H-12.-04	12.39	0.643	0.142	0.080	0.221	2.440	2.222	2.972	3.032	0.370	0.528	0.480	0.82	
H-12.-05	12.34	0.555	0.128	0.075	0.230	2.068	1.928	2.578	2.751	0.349	0.445	0.415	0.98	
H-12.-06	12.29	0.477	0.112	0.071	0.235	1.792	1.751	2.225	2.438	0.329	0.384	0.376	1.12	
H-12.-07	12.27	0.443	0.103	0.068	0.233	1.542	1.524	2.069	2.254	0.318	0.330	0.326	1.55	
H-12.-08	12.24	0.384	0.092	0.064	0.239	1.271	1.257	1.799	2.013	0.302	0.271	0.268	1.62	
H-12.-09	12.21	0.345	0.083	0.060	0.240	1.077	1.067	1.619	1.826	0.283	0.230	0.227	2.69	
H-12.-10+	12.20	0.327	0.078	0.058	0.240	1.073	1.047	1.536	1.729	0.271	0.228	0.223	3.57	
H-12.-11*	12.22	0.361	0.087	0.061	0.240	1.053	1.031	1.694	1.908	0.287	0.225	0.220	----	
H-12.-12	12.20	0.322	0.077	0.057	0.240	0.910	0.892	1.515	1.709	0.269	0.194	0.190	----	
H-12.-13	12.19	0.311	0.074	0.056	0.239	0.693	0.679	1.461	1.644	0.264	0.147	0.144	4.65	
H-12.-14*	12.20	0.323	0.077	0.057	0.238	0.672	0.662	1.517	1.698	0.268	0.143	0.141	----	

UNLESS OTHERWISE INDICATED, ALL DATA ARE FOR:
1. SUPERCAVITATING FLOW.
2. BOTH STATIC PRESSURE TAPS OPEN.

LEGEND
+ ONLY UPSTREAM STATIC PRESSURE TAP UTILIZED
* ONLY DNSTREAM STATIC PRESSURE TAP UTILIZED
PC PARTIALLY CAVITATING
PC(TW) PARTIALLY CAVITATING (TAP WETTED)
FW FULLY WETTED
AT (ALPHAT) (TRUE) ANGLE OF ATTACK, CORRECTED FOR EFFECTS OF IMAGES OF TRAILING VORTICES
AT2 ALPHAT**2
SIGC CAVITATION NUMBER COMPUTED WITH MEASURED CAVITY PRESSURE
SIGV CAVITATION NUMBER COMPUTED WITH CALCULATED VAPOR PRESSURE
CD DRAG COEFFICIENT, CORRECTED FOR EFFECTS OF IMAGES OF TRAILING VORTICES
(D/L) CORRECTED DRAG-TO-LIFT RATIO = CD/CL
CAVLTH CAVITY LENGTH MEASURED FROM MIDCHORD AT CENTROID POSITION, NONDIMENSIONALIZED ON MEAN CHORD (OBTAINED FROM PHOTOGRAPHS)

EXPER INVES OF WALL EFFECTS ON SUPERCAVITATING HYDROFOILS OF FINITE SPAN

HIDROFOIL DATA IN NONDIMENSIONAL FORM (NO CORRECTIONS APPLIED)

RUN NO	ALPHA	CL	CDUNC	CM	L/D	D/L	RN*10**-6
M-14.-01	14.01	0.9415	0.1643	0.1973	5.7296	0.1745	0.8493
M-14.-02	14.02	0.9422	0.1652	0.1986	5.7028	0.1754	1.0176
M-14.-03	14.02	0.9376	0.1652	0.1989	5.6767	0.1762	1.1456
M-14.-04	14.02	0.9561	0.1648	0.2029	5.8031	0.1723	1.1115
M-14.-05	14.02	0.9774	0.1658	0.2010	5.8954	0.1696	1.1053
M-14.-06	14.02	1.0075	0.1780	0.1865	5.6595	0.1767	1.1039
M-14.-07	14.02	1.0666	0.2049	0.1462	5.2055	0.1921	1.0995
M-14.-08	14.01	1.0533	0.2130	0.1215	4.9455	0.2022	1.0932
M-14.-09	14.01	1.0128	0.2137	0.1110	4.7388	0.2110	1.0936
M-14.-10	14.01	0.9616	0.2117	0.1027	4.5416	0.2202	1.0914
M-14.-11	14.01	0.9032	0.2071	0.0985	4.3612	0.2293	1.0903
M-14.-12	14.01	0.8443	0.2009	0.0946	4.2032	0.2379	1.0881
M-14.-13	14.01	0.7724	0.1894	0.0906	4.0776	0.2452	1.0862
M-14.-14	14.01	0.7136	0.1792	0.0884	3.9830	0.2511	1.0866
M-14.-15	14.01	0.6587	0.1691	0.0847	3.8953	0.2567	1.0851
M-14.-16	14.01	0.5957	0.1566	0.0820	3.8039	0.2629	1.0855
M-14.-17	14.01	0.5520	0.1462	0.0800	3.7745	0.2649	1.0847
M-14.-18	14.01	0.4698	0.1268	0.0736	3.7061	0.2698	1.0832
M-14.-19	14.01	0.4129	0.1118	0.0693	3.6936	0.2707	1.0829
M-14.-20	14.01	0.3821	0.1039	0.0671	3.6758	0.2720	1.0832
M-14.-21	14.00	0.7396	0.1802	0.0923	4.1048	0.2436	0.6524
M-14.-22	14.01	0.8280	0.1974	0.0967	4.1950	0.2384	0.9358
M-14.-23	14.02	0.9333	0.1630	0.1984	5.7249	0.1747	0.9376

LEGEND
- ALPHA GEOMETRIC ANGLE OF ATTACK CORRECTED FOR SHAFT TWIST
- CL LIFT COEFFICIENT, NONDIMENSIONALIZED ON UPSTREAM VELOCITY AND MODEL PLANFORM AREA
- CDUNC CD(UNCORRECTED), THE UNCORRECTED DRAG COEFFICIENT AS COMPUTED FROM MEASURED DRAG, AND NONDIMENSIONALIZED ON UPSTREAM VELOCITY AND MODEL PLANFORM AREA
- CM MOMENT COEFFICIENT, NONDIMENSIONALIZED ON UPSTREAM VELOCITY, MODEL PLANFORM AREA, AND MEAN CHORD
- L/D LIFT-TO-DRAG RATIO = CL/CDUNC
- D/L DRAG-TO-LIFT RATIO = CDUNC/CL
- RN REYNOLDS NUMBER, BASED ON MEAN CHORD

EXPER INVES OF WALL EFFECTS ON SUPERCAVITATING HYDROFOILS OF FINITE SPAN

PRIOR DATA CORRECTED FOR EFFECTS OF IMAGES OF TRAILING VORTEX SYSTEM

RUN NO	ALPHAT	CL	CD	CM	(D/L)	SIGV/AT	SIGC/AT	CL/AT	CD/AT2	CM/AT	SIGV	SIGC	CAVLTH	COMMENTS/REMARKS
B-14.-01	14.57	0.942	0.174	0.197	0.184	-----	-----	3.701	2.682	0.776	-----	-----	----	FW
B-14.-02	14.58	0.942	0.174	0.199	0.185	-----	-----	3.702	2.694	0.780	-----	-----	----	FW
B-14.-03	14.58	0.938	0.174	0.199	0.186	-----	-----	3.684	2.691	0.782	-----	-----	----	FW
B-14.-04	14.59	0.956	0.174	0.203	0.182	-----	-----	3.754	2.686	0.797	-----	-----	----	PC (TW)
B-14.-05	14.61	0.977	0.176	0.201	0.180	-----	-----	3.834	2.704	0.788	-----	-----	----	PC (TW)
B-14.-06	14.62	1.008	0.189	0.186	0.187	-----	-----	3.918	2.896	0.731	-----	-----	----	PC (TW)
B-14.-07	14.65	1.067	0.217	0.146	0.203	4.020	2.522	4.171	3.314	0.572	1.028	0.645	0.65	
B-14.-08	14.64	1.053	0.225	0.122	0.213	3.693	2.911	4.122	3.438	0.476	0.944	0.744	0.62	
B-14.-09	14.62	1.013	0.224	0.111	0.222	3.484	2.854	3.970	3.448	0.435	0.889	0.728	0.63	
B-14.-10	14.58	0.962	0.221	0.103	0.230	3.277	2.767	3.778	3.416	0.403	0.834	0.704	0.64	
B-14.-11	14.55	0.903	0.216	0.099	0.239	3.047	2.614	3.557	3.343	0.388	0.774	0.664	0.68	
B-14.-12	14.51	0.844	0.208	0.095	0.247	2.850	2.448	3.333	3.246	0.373	0.722	0.620	0.70	
B-14.-13	14.47	0.772	0.196	0.091	0.253	2.590	2.296	3.058	3.067	0.359	0.654	0.580	0.90	
B-14.-14	14.44	0.714	0.184	0.088	0.258	2.391	2.132	2.832	2.906	0.351	0.602	0.537	0.88	
B-14.-15	14.40	0.659	0.174	0.085	0.264	2.184	1.973	2.620	2.748	0.337	0.549	0.496	0.90	
B-14.-16	14.36	0.596	0.160	0.082	0.269	1.938	1.792	2.376	2.550	0.327	0.486	0.449	1.15	
B-14.-17	14.34	0.552	0.149	0.080	0.271	1.739	1.674	2.206	2.386	0.320	0.435	0.419	1.30	
B-14.-18	14.29	0.470	0.129	0.074	0.275	1.372	1.342	1.884	2.075	0.295	0.342	0.335	1.75	
B-14.-19	14.25	0.413	0.114	0.069	0.275	1.092	1.066	1.660	1.835	0.278	0.272	0.265	2.65	
B-14.-20	14.24	0.382	0.105	0.067	0.276	0.947	0.926	1.538	1.709	0.270	0.235	0.230	3.50	
B-14.-21	14.44	0.740	0.186	0.092	0.251	2.605	2.303	2.934	2.924	0.366	0.657	0.581	0.75	
B-14.-22	14.50	0.828	0.204	0.097	0.247	2.796	2.450	3.271	3.192	0.382	0.708	0.620	0.75	
B-14.-23	14.57	0.933	0.172	0.198	0.184	-----	-----	3.670	2.660	0.780	-----	-----	----	FW

UNLESS OTHERWISE INDICATED, ALL DATA ARE FOR:
1. SUPERCAVITATING FLOW.
2. BOTH STATIC PRESSURE TAPS OPEN.

LEGEND
- * ONLY UPSTREAM STATIC PRESSURE TAP UTILIZED
- * ONLY DNSTREAM STATIC PRESSURE TAP UTILIZED
- PC PARTIALLY CAVITATING
- PC(TW) PARTIALLY CAVITATING (TAP WETTED)
- FW FULLY WETTED
- AT (ALPHAT) (TRUE) ANGLE OF ATTACK, CORRECTED FOR EFFECTS OF IMAGES OF TRAILING VORTICES
- AT2 ALPHAT**2
- SIGC CAVITATION NUMBER COMPUTED WITH MEASURED CAVITY PRESSURE
- SIGV CAVITATION NUMBER COMPUTED WITH CALCULATED VAPOR PRESSURE
- CD DRAG COEFFICIENT, CORRECTED FOR EFFECTS OF IMAGES OF TRAILING VORTICES
- (D/L) CORRECTED DRAG-TO-LIFT RATIO = CD/CL
- CAVLTH CAVITY LENGTH MEASURED FROM MIDCHORD AT CENTROID POSITION, NONDIMENSIONALIZED ON MEAN CHORD (OBTAINED FROM PHOTOGRAPHS)

EIFER INVES OF WALL EFFECTS ON SUPERCAVITATING HYDROFOILS OF FINITE SPAN

HYDROFOIL DATA IN NONDIMENSIONAL FORM (NO CORRECTIONS APPLIED)

RUN NO	ALPHA	CL	CDUNC	CM	L/D	D/L	RN*10**-6
A-16.-01	16.01	1.0657	0.2664	0.1186	3.9997	0.2500	1.1378
A-16.-02	16.01	1.0033	0.2621	0.1113	3.8277	0.2613	1.1382
A-16.-03	16.01	0.9591	0.2573	0.1071	3.7273	0.2683	1.1371
A-16.-04	16.01	0.9055	0.2505	0.1047	3.6153	0.2766	1.1312
A-16.-05	16.01	0.8610	0.2425	0.1022	3.5505	0.2817	1.1275
A-16.-06	16.01	0.8059	0.2308	0.1005	3.4921	0.2864	1.1242
A-16.-07	16.01	0.7519	0.2197	0.0981	3.4228	0.2922	1.1224
A-16.-08	16.01	0.7107	0.2094	0.0951	3.3934	0.2947	1.1160
A-16.-09	16.01	0.6861	0.2038	0.0953	3.3667	0.2970	1.1138
A-16.-10	16.01	0.6229	0.1878	0.0911	3.3172	0.3015	1.1116
A-16.-11	16.01	0.5651	0.1704	0.0869	3.3155	0.3016	1.1093
A-16.-12	16.01	0.5351	0.1623	0.0824	3.2972	0.3033	1.1086
A-16.-13	16.01	0.4976	0.1525	0.0801	3.2625	0.3065	1.1078
A-16.-14	16.01	0.4634	0.1417	0.0778	3.2693	0.3059	1.1078
A-16.-15	16.01	0.4233	0.1295	0.0732	3.2676	0.3060	1.1070
A-16.-16	16.01	0.6743	0.2017	0.0904	3.3435	0.2991	1.1179
A-16.-17	16.01	0.8301	0.2358	0.0969	3.5208	0.2840	1.1175
A-16.-18	16.01	0.8101	0.2315	0.0971	3.4996	0.2857	1.1179
A-16.-19	16.01	0.8523	0.2411	0.0994	3.5347	0.2829	1.1160
A-16.-20	16.00	0.4784	0.1489	0.0799	3.2123	0.3113	0.7657
A-16.-21	16.00	0.7981	0.2168	0.1025	3.6807	0.2717	0.5285
A-16.-22	16.01	0.9036	0.2438	0.1060	3.7058	0.2698	0.7248
A-16.-23	16.01	0.8997	0.2457	0.1052	3.6609	0.2732	0.8231
A-16.-24	16.01	0.8866	0.2450	0.1022	3.6188	0.2763	0.9419
A-16.-25	16.01	0.8781	0.2450	0.1024	3.5846	0.2790	1.0342
A-16.-26	16.01	0.8892	0.2476	0.1024	3.5912	0.2785	1.1316
A-16.-27	16.01	1.0307	0.2103	0.1034	4.9019	0.2040	1.1301
A-16.-28	16.01	1.0549	0.2109	0.2157	5.0012	0.2000	0.8226

LEGEND

ALPHA GEOMETRIC ANGLE OF ATTACK CORRECTED FOR SHAFT TWIST
CL LIFT COEFFICIENT, NONDIMENSIONALIZED ON UPSTREAM VELOCITY AND MODEL PLANFORM AREA
CDUNC CD(UNCORRECTED), THE UNCORRECTED DRAG COEFFICIENT AS COMPUTED FROM MEASURED DRAG, AND NONDIMENSIONALIZED ON UPSTREAM VELOCITY AND MODEL PLANFORM AREA
CM MOMENT COEFFICIENT, NONDIMENSIONALIZED ON UPSTREAM VELOCITY, MODEL PLANFORM AREA, AND MEAN CHORD
L/D LIFT-TO-DRAG RATIO = CL/CDUNC
D/L DRAG-TO-LIFT RATIO = CDUNC/CL
RN REYNOLDS NUMBER, BASED ON MEAN CHORD

EXPER INVES OF WALL EFFECTS ON SUPERCAVITATING HYDROFOILS OF FINITE SPAN

PRIOR DATA CORRECTED FOR EFFECTS OF IMAGES OF TRAILING VORTEX SYSTEM

RUN NO	ALPHAT	CL	CD	CM	(D/L)	SIGV/AT	SIGC/AT	CL/AT	CD/AT2	CM/AT	SIGV	SIGC	CAVLTH	COMMENTS/REMARKS
B-16.-01	16.65	1.066	0.278	0.119	0.261	3.286	2.618	3.667	3.295	0.408	0.955	0.761	0.69	
B-16.-02	16.61	1.003	0.273	0.111	0.272	3.088	2.547	3.461	3.243	0.384	0.895	0.738	0.72	
B-16.-03	16.58	0.959	0.267	0.107	0.278	2.920	2.455	3.313	3.185	0.370	0.845	0.711	0.77	
B-16.-04	16.55	0.905	0.259	0.105	0.286	2.725	2.333	3.134	3.103	0.362	0.787	0.674	0.82	
B-16.-05	16.52	0.861	0.250	0.102	0.291	2.564	2.249	2.985	3.008	0.354	0.740	0.649	0.98	
B-16.-06	16.49	0.806	0.238	0.100	0.295	2.375	2.112	2.800	2.867	0.349	0.684	0.608	0.96	
B-16.-07	16.46	0.752	0.226	0.098	0.300	2.215	1.993	2.617	2.733	0.341	0.636	0.573	1.00	
B-16.-08	16.43	0.711	0.215	0.095	0.302	2.043	1.927	2.478	2.610	0.331	0.586	0.553	1.10	
B-16.-09	16.42	0.686	0.209	0.095	0.304	1.944	1.791	2.394	2.541	0.333	0.557	0.513	1.15	
B-16.-10	16.38	0.623	0.192	0.091	0.308	1.740	1.642	2.179	2.346	0.319	0.498	0.469	1.17	
B-16.-11	16.35	0.565	0.174	0.087	0.307	1.507	1.451	1.981	2.135	0.305	0.430	0.414	1.62	
B-16.-12	16.33	0.535	0.165	0.082	0.309	1.386	1.347	1.878	2.035	0.289	0.395	0.384	1.89	
B-16.-13	16.31	0.498	0.155	0.080	0.312	1.239	1.216	1.749	1.915	0.282	0.352	0.346	2.17	
B-16.-14	16.28	0.463	0.144	0.078	0.311	1.075	1.043	1.630	1.782	0.274	0.306	0.296	2.75	
B-16.-15	16.26	0.423	0.131	0.073	0.310	0.831	0.789	1.492	1.632	0.258	0.236	0.224	4.35	
B-16.-16	16.41	0.674	0.206	0.090	0.306	1.895	1.857	2.354	2.515	0.316	0.543	0.532	1.10	
B-16.-17	16.51	0.830	0.243	0.097	0.293	2.445	2.135	2.881	2.927	0.336	0.704	0.615	----	
B-16.-18*	16.49	0.810	0.238	0.097	0.294	2.455	2.162	2.814	2.876	0.337	0.707	0.622	----	
B-16.-19*	16.52	0.852	0.249	0.099	0.292	2.456	2.166	2.956	2.992	0.345	0.708	0.624	----	
B-16.-20	16.29	0.478	0.151	0.080	0.316	1.191	1.081	1.683	1.872	0.281	0.339	0.307	----	
B-16.-21	16.48	0.798	0.223	0.103	0.280	2.515	2.301	2.775	2.701	0.357	0.723	0.662	----	
B-16.-22	16.54	0.504	0.252	0.106	0.279	2.658	2.212	3.130	3.027	0.367	0.768	0.639	----	
B-16.-23	16.54	0.900	0.254	0.105	0.283	2.584	2.196	3.116	3.049	0.364	0.746	0.634	----	
B-16.-24	16.54	0.887	0.253	0.102	0.286	2.539	2.174	3.072	3.039	0.354	0.733	0.627	----	
B-16.-25	16.53	0.878	0.253	0.102	0.288	2.529	2.200	3.043	3.038	0.355	0.730	0.635	----	
B-16.-26	16.54	0.889	0.256	0.102	0.288	2.554	2.256	3.080	3.069	0.355	0.737	0.651	----	
B-16.-27	16.63	1.031	0.221	0.103	0.215	-----	-----	3.552	2.628	0.356	-----	-----	----	FW
B-16.-28	16.64	1.055	0.223	0.216	0.211	-----	-----	3.632	2.637	0.743	-----	-----	----	FW

UNLESS OTHERWISE INDICATED, ALL DATA ARE FOR:
1. SUPERCAVITATING FLOW.
2. BOTH STATIC PRESSURE TAPS OPEN.

LEGEND
+ ONLY UPSTREAM STATIC PRESSURE TAP UTILIZED
* ONLY DNSTREAM STATIC PRESSURE TAP UTILIZED
PC PARTIALLY CAVITATING
PC(TW) PARTIALLY CAVITATING (TAP WETTED)
FW FULLY WETTED
AT (ALPHAT) (TRUE) ANGLE OF ATTACK, CORRECTED FOR EFFECTS OF IMAGES OF TRAILING VORTICES
AT2 ALPHAT**2
SIGC CAVITATION NUMBER COMPUTED WITH MEASURED CAVITY PRESSURE
SIGV CAVITATION NUMBER COMPUTED WITH CALCULATED VAPOR PRESSURE
CD DRAG COEFFICIENT, CORRECTED FOR EFFECTS OF IMAGES OF TRAILING VORTICES
(D/L) CORRECTED DRAG-TO-LIFT RATIO = CD/CL
CAVLTH CAVITY LENGTH MEASURED FROM MIDCHORD AT CENTROID POSITION, NONDIMENSIONALIZED ON MEAN CHORD (OBTAINED FROM PHOTOGRAPHS)

EXPER INVES OF WALL EFFECTS ON SUPERCAVITATING HYDROFOILS OF FINITE SPAN

HYDROFOIL DATA IN NONDIMENSIONAL FORM (NO CORRECTIONS APPLIED)

RUN NO	ALPHA	CL	CDUNC	CM	L/D	D/L	RN*10**-6
M-18.-01	18.02	1.1390	0.3065	0.1431	3.7158	0.2691	1.1811
M-18.-02	18.02	1.1204	0.3059	0.1356	3.6622	0.2731	1.1814
M-18.-03	18.02	1.1018	0.3078	0.1274	3.5792	0.2794	1.1778
M-18.-04	18.01	1.0598	0.3067	0.1173	3.4552	0.2894	1.1767
M-18.-05	18.01	1.0344	0.3051	0.1139	3.3900	0.2950	1.1731
M-18.-06	18.01	0.9963	0.3030	0.1094	3.2884	0.3041	1.1702
M-18.-07	18.01	0.9483	0.2941	0.1064	3.2247	0.3101	1.1676
M-18.-08	18.01	0.8827	0.2820	0.1034	3.1307	0.3194	1.1654
M-18.-09	18.01	0.8241	0.2697	0.0997	3.0558	0.3273	1.1618
M-18.-10	18.01	0.7607	0.2531	0.0968	3.0051	0.3328	1.1584
M-18.-11	18.01	0.7024	0.2374	0.0932	2.9592	0.3379	1.1595
M-18.-12	18.01	0.6446	0.2190	0.0909	2.9430	0.3398	1.1573
M-18.-13	18.01	0.6015	0.2041	0.0878	2.9477	0.3393	1.1547
M-18.-14	18.01	0.5542	0.1875	0.0852	2.9563	0.3383	1.1544
M-18.-15	18.01	0.5113	0.1740	0.0830	2.9380	0.3404	1.1510
M-18.-16	18.01	0.4843	0.1664	0.0807	2.9109	0.3435	1.1510
M-18.-17	18.01	0.4692	0.1602	0.0786	2.9281	0.3415	1.1503
M-18.-18	18.01	0.4825	0.1631	0.0791	2.9580	0.3381	1.0315
M-18.-19	18.01	0.4527	0.1587	0.0774	2.8520	0.3506	1.0273
M-18.-20	18.01	0.4857	0.1664	0.0802	2.9195	0.3425	1.0387

LEGEND
- ALPHA GEOMETRIC ANGLE OF ATTACK CORRECTED FOR SHAFT TWIST
- CL LIFT COEFFICIENT, NONDIMENSIONALIZED ON UPSTREAM VELOCITY AND MODEL PLANFORM AREA
- CDUNC CD(UNCORRECTED), THE UNCORRECTED DRAG COEFFICIENT AS COMPUTED FROM MEASURED DRAG, AND NONDIMENSIONALIZED ON UPSTREAM VELOCITY AND MODEL PLANFORM AREA
- CM MOMENT COEFFICIENT, NONDIMENSIONALIZED ON UPSTREAM VELOCITY, MODEL PLANFORM AREA, AND MEAN CHORD
- L/D LIFT-TO-DRAG RATIO = CL/CDUNC
- D/L DRAG-TO-LIFT RATIO = CDUNC/CL
- RN REYNOLDS NUMBER, BASED ON MEAN CHORD

RIPER INVES OF WALL EFFECTS ON SUPERCAVITATING HYDROFOILS OF FINITE SPAN

PRIOR DATA CORRECTED FOR EFFECTS OF IMAGES OF TRAILING VORTEX SYSTEM

RUN NO	ALPHAT	CL	CD	CM	(D/L)	SIGV/AT	SIGC/AT	CL/AT	CD/AT2	CM/AT	SIGV	SIGC	CAVLTH	COMMENTS/REMARKS
R-18.-01	18.70	1.139	0.320	0.143	0.281	3.562	2.158	3.490	3.005	0.438	1.162	0.704	0.72	
R-18.-02	18.68	1.120	0.319	0.136	0.285	3.400	2.179	3.436	3.000	0.416	1.109	0.711	0.76	
R-18.-03	18.67	1.102	0.320	0.127	0.291	3.249	2.237	3.381	3.017	0.391	1.059	0.729	0.75	
R-18.-04	18.65	1.060	0.318	0.117	0.300	3.031	2.223	3.257	3.007	0.361	0.987	0.723	0.71	
R-18.-05	18.63	1.034	0.316	0.114	0.306	2.877	2.206	3.181	2.991	0.350	0.935	0.717	0.75	
R-18.-06	18.61	0.996	0.313	0.109	0.314	2.674	2.209	3.068	2.971	0.337	0.869	0.717	0.70	
R-18.-07	18.58	0.948	0.303	0.106	0.320	2.480	2.101	2.925	2.886	0.328	0.804	0.681	0.80	
R-18.-08	18.54	0.883	0.290	0.103	0.329	2.249	1.970	2.728	2.771	0.320	0.728	0.637	0.88	
R-18.-09	18.50	0.824	0.277	0.100	0.336	2.043	1.808	2.552	2.654	0.309	0.660	0.584	0.89	
R-18.-10	18.46	0.761	0.259	0.097	0.341	1.854	1.676	2.360	2.495	0.300	0.598	0.540	1.01	
R-18.-11	18.43	0.702	0.243	0.093	0.345	1.650	1.575	2.184	2.344	0.290	0.531	0.507	1.15	
R-18.-12	18.39	0.645	0.223	0.091	0.346	1.454	1.381	2.008	2.167	0.283	0.467	0.443	1.60	
R-18.-13	18.37	0.601	0.208	0.088	0.346	1.278	1.242	1.876	2.022	0.274	0.410	0.398	1.65	
R-18.-14	18.34	0.554	0.191	0.085	0.344	1.097	1.073	1.731	1.861	0.266	0.351	0.344	2.12	
R-18.-15	18.31	0.511	0.177	0.083	0.346	0.908	0.886	1.600	1.730	0.260	0.290	0.283	3.28	
R-18.-16	18.30	0.484	0.169	0.081	0.349	0.791	0.772	1.516	1.655	0.253	0.253	0.247	3.50	
R-18.-17	18.29	0.469	0.163	0.079	0.346	0.698	0.682	1.470	1.595	0.246	0.223	0.218	4.60	
R-18.-18	18.29	0.483	0.166	0.079	0.343	0.865	0.847	1.511	1.624	0.248	0.276	0.271	----	
R-18.-19+	18.28	0.453	0.161	0.077	0.355	0.870	0.855	1.419	1.581	0.243	0.278	0.273	----	
R-18.-20*	18.30	0.486	0.169	0.080	0.348	0.848	0.836	1.521	1.655	0.251	0.271	0.267	----	

UNLESS OTHERWISE INDICATED, ALL DATA ARE FOR:
1. SUPERCAVITATING FLOW.
2. BOTH STATIC PRESSURE TAPS OPEN.

LEGEND
+ ONLY UPSTREAM STATIC PRESSURE TAP UTILIZED
* ONLY DNSTREAM STATIC PRESSURE TAP UTILIZED
PC PARTIALLY CAVITATING
PC(TW) PARTIALLY CAVITATING (TAP WETTED)
FW FULLY WETTED
AT (ALPHAT) (TRUE) ANGLE OF ATTACK, CORRECTED FOR EFFECTS OF IMAGES OF TRAILING VORTICES
AT2 ALPHAT**2
SIGC CAVITATION NUMBER COMPUTED WITH MEASURED CAVITY PRESSURE
SIGV CAVITATION NUMBER COMPUTED WITH CALCULATED VAPOR PRESSURE
CD DRAG COEFFICIENT, CORRECTED FOR EFFECTS OF IMAGES OF TRAILING VORTICES
(D/L) CORRECTED DRAG-TO-LIFT RATIO = CD/CL
CAVLTH CAVITY LENGTH MEASURED FROM MIDCHORD AT CENTROID POSITION, NONDIMENSIONALIZED ON MEAN CHORD (OBTAINED FROM PHOTOGRAPHS)

RIPER INVES OF WALL EFFECTS ON SUPERCAVITATING HYDROFOILS OF FINITE SPAN

HYDROFOIL DATA IN NONDIMENSIONAL FORM (NO CORRECTIONS APPLIED)

RUN NO	ALPHA	CL	CDUNC	CM	L/D	D/L	RN*10**-6
A-21.-01	21.01	1.0606	0.3740	0.1238	2.8355	0.3527	1.1750
A-21.-02	21.01	1.0460	0.3716	0.1178	2.8148	0.3553	1.1686
A-21.-03	21.01	1.0159	0.3683	0.1130	2.7582	0.3625	1.1667
A-21.-04	21.01	0.9974	0.3633	0.1098	2.7457	0.3642	1.1648
A-21.-05	21.01	0.9560	0.3566	0.1070	2.6805	0.3731	1.1629
A-21.-06	21.01	0.9497	0.3565	0.1065	2.6642	0.3753	1.1583
A-21.-07	21.01	0.9739	0.3603	0.1075	2.7032	0.3699	1.1614
A-21.-08	21.01	0.9045	0.3433	0.1029	2.6351	0.3795	1.1621
A-21.-09	21.01	0.8539	0.3322	0.1004	2.5702	0.3891	1.1610
A-21.-10	21.01	0.8127	0.3209	0.0990	2.5328	0.3948	1.1614
A-21.-11	21.01	0.7571	0.3045	0.0969	2.4864	0.4022	1.1625
A-21.-12	21.01	0.7102	0.2839	0.0953	2.5018	0.3998	1.1614
A-21.-13	21.01	0.6585	0.2637	0.0928	2.4967	0.4005	1.1625
A-21.-14	21.01	0.6277	0.2505	0.0923	2.5058	0.3991	1.1625
A-21.-15	21.01	0.6056	0.2409	0.0909	2.5140	0.3978	1.1595
A-21.-16	21.01	0.5758	0.2301	0.0888	2.5019	0.3997	1.1579
A-21.-17	21.01	0.5524	0.2208	0.0873	2.5021	0.3997	1.1556
A-21.-18	21.01	0.5441	0.2172	0.0870	2.5053	0.3992	1.1541

LEGEND

ALPHA GEOMETRIC ANGLE OF ATTACK CORRECTED FOR SHAFT TWIST
CL LIFT COEFFICIENT, NONDIMENSIONALIZED ON UPSTREAM VELOCITY AND MODEL PLANFORM AREA
CDUNC CD(UNCORRECTED), THE UNCORRECTED DRAG COEFFICIENT AS COMPUTED FROM MEASURED DRAG, AND NONDIMENSIONALIZED ON UPSTREAM VELOCITY AND MODEL PLANFORM AREA
CM MOMENT COEFFICIENT, NONDIMENSIONALIZED ON UPSTREAM VELOCITY, MODEL PLANFORM AREA, AND MEAN CHORD
L/D LIFT-TO-DRAG RATIO = CL/CDUNC
D/L DRAG-TO-LIFT RATIO = CDUNC/CL
RN REYNOLDS NUMBER, BASED ON MEAN CHORD

EXPER INVES OF WALL EFFECTS ON SUPERCAVITATING HYDROFOILS OF FINITE SPAN

PRIOR DATA CORRECTED FOR EFFECTS OF IMAGES OF TRAILING VORTEX SYSTEM

RUN NO	ALPHAT	CL	CD	CM	(D/L)	SIGV/AT	SIGC/AT	CL/AT	CD/AT2	CM/AT	SIGV	SIGC	CAVLTH	COMMENTS/REMARKS
R-21.-01	21.65	1.061	0.386	0.124	0.364	3.299	1.999	2.807	2.702	0.328	1.246	0.755	0.80	
R-21.-02	21.64	1.046	0.383	0.118	0.366	3.112	2.022	2.770	2.686	0.312	1.175	0.763	0.85	
R-21.-03	21.62	1.016	0.379	0.113	0.373	2.899	2.011	2.692	2.662	0.299	1.094	0.759	0.89	
R-21.-04	21.61	0.997	0.374	0.110	0.375	2.683	1.969	2.645	2.627	0.291	1.012	0.743	0.96	
R-21.-05	21.58	0.956	0.366	0.107	0.383	2.506	1.949	2.538	2.581	0.284	0.944	0.734	1.03	
R-21.-06*	21.58	0.950	0.366	0.106	0.385	2.495	1.994	2.522	2.579	0.283	0.939	0.751	----	
R-21.-07*	21.59	0.974	0.370	0.108	0.380	2.488	1.992	2.584	2.606	0.285	0.938	0.751	----	
R-21.-08	21.55	0.905	0.352	0.103	0.389	2.251	1.836	2.405	2.486	0.274	0.847	0.690	1.10	
R-21.-09	21.52	0.854	0.340	0.100	0.398	2.019	1.703	2.273	2.409	0.267	0.759	0.640	1.25	
R-21.-10	21.50	0.813	0.328	0.099	0.403	1.840	1.625	2.166	2.328	0.264	0.690	0.610	1.40	
R-21.-11	21.46	0.757	0.310	0.097	0.410	1.660	1.506	2.021	2.212	0.259	0.622	0.564	1.42	
R-21.-12	21.43	0.710	0.289	0.095	0.407	1.485	1.382	1.898	2.066	0.255	0.555	0.517	1.75	
R-21.-13	21.40	0.658	0.268	0.093	0.407	1.284	1.222	1.763	1.922	0.248	0.480	0.457	2.10	
R-21.-14	21.38	0.628	0.255	0.092	0.406	1.164	1.134	1.682	1.828	0.247	0.434	0.423	2.40	
R-21.-15	21.37	0.606	0.245	0.091	0.404	1.079	1.051	1.623	1.759	0.244	0.402	0.392	2.80	
R-21.-16	21.35	0.576	0.234	0.089	0.406	0.960	0.934	1.545	1.682	0.238	0.358	0.348	3.55	
R-21.-17	21.34	0.552	0.224	0.087	0.405	0.882	0.858	1.483	1.615	0.234	0.329	0.320	3.78	
R-21.-18	21.33	0.548	0.220	0.087	0.405	0.832	0.810	1.461	1.589	0.234	0.310	0.302	----	

UNLESS OTHERWISE INDICATED, ALL DATA ARE FOR:
1. SUPERCAVITATING FLOW.
2. BOTH STATIC PRESSURE TAPS OPEN.

LEGEND
- * ONLY UPSTREAM STATIC PRESSURE TAP UTILIZED
- * ONLY DNSTREAM STATIC PRESSURE TAP UTILIZED
- PC PARTIALLY CAVITATING
- PC(TW) PARTIALLY CAVITATING (TAP WETTED)
- FW FULLY WETTED
- AT (ALPHAT) (TRUE) ANGLE OF ATTACK, CORRECTED FOR EFFECTS OF IMAGES OF TRAILING VORTICES
- AT2 ALPHAT**2
- SIGC CAVITATION NUMBER COMPUTED WITH MEASURED CAVITY PRESSURE
- SIGV CAVITATION NUMBER COMPUTED WITH CALCULATED VAPOR PRESSURE
- CD DRAG COEFFICIENT, CORRECTED FOR EFFECTS OF IMAGES OF TRAILING VORTICES
- (D/L) CORRECTED DRAG-TO-LIFT RATIO = CD/CL
- CAVLTH CAVITY LENGTH MEASURED FROM MIDCHORD AT CENTROID POSITION, NONDIMENSIONALIZED ON MEAN CHORD (OBTAINED FROM PHOTOGRAPHS)

EXPER INVES OF WALL EFFECTS ON SUPERCAVITATING HYDROFOILS OF FINITE SPAN

HYDROFOIL DATA IN NONDIMENSIONAL FORM (NO CORRECTIONS APPLIED)

RUN NO	ALPHA	CL	CDUNC	CM	L/D	D/L	RN*10**-6
L-8.0-01	8.02	0.6219	0.0831	0.0605	7.4828	0.1336	1.6185
L-8.0-02	8.02	0.5270	0.0771	0.0557	6.8382	0.1462	1.6129
L-8.0-03	8.02	0.4999	0.0748	0.0549	6.6807	0.1497	1.6129
L-8.0-04	8.02	0.5484	0.0790	0.0566	6.9428	0.1440	1.6111
L-8.0-05	8.02	0.4240	0.0667	0.0519	6.3581	0.1573	1.6136
L-8.0-06	8.02	0.3375	0.0558	0.0474	6.0438	0.1655	1.6148
L-8.0-07	8.01	0.2863	0.0472	0.0427	6.0645	0.1649	1.6148
L-8.0-08	8.01	0.2599	0.0437	0.0405	5.9516	0.1680	1.6010
L-8.0-09	8.01	0.2955	0.0491	0.0437	6.0155	0.1662	1.6148
L-8.0-10	8.01	0.2624	0.0438	0.0414	5.9967	0.1668	1.6104
L-8.0-11	8.01	0.2620	0.0444	0.0394	5.8960	0.1696	1.5334
L-8.0-12	8.01	0.2761	0.0463	0.0425	5.9686	0.1675	1.6061

LEGEND

ALPHA GEOMETRIC ANGLE OF ATTACK CORRECTED FOR SHAFT TWIST
CL LIFT COEFFICIENT, NONDIMENSIONALIZED ON UPSTREAM VELOCITY AND MODEL PLANFORM AREA
CDUNC CD(UNCORRECTED), THE UNCORRECTED DRAG COEFFICIENT AS COMPUTED FROM MEASURED DRAG, AND NONDIMENSIONALIZED ON UPSTREAM VELOCITY AND MODEL PLANFORM AREA
CM MOMENT COEFFICIENT, NONDIMENSIONALIZED ON UPSTREAM VELOCITY, MODEL PLANFORM AREA, AND MEAN CHORD
L/D LIFT-TO-DRAG RATIO = CL/CDUNC
D/L DRAG-TO-LIFT RATIO = CDUNC/CL
RN REYNOLDS NUMBER, BASED ON MEAN CHORD

EIPER INVES OF WALL EFFECTS ON SUPERCAVITATING HYDROFOILS OF FINITE SPAN

PRIOR DATA CORRECTED FOR EFFECTS OF IMAGES OF TRAILING VORTEX SYSTEM

RUN NO	ALPHAT	CL	CD	CM	(D/L)	SIGV/AT	SIGC/AT	CL/AT	CD/AT2	CM/AT	SIGV	SIGC	CAVLTH	COMMENTS/REMARKS
L-8.0-01	8.76	0.622	0.091	0.060	0.147	3.444	3.297	4.069	3.900	0.396	0.526	0.504	0.68	
L-8.0-02	8.64	0.527	0.083	0.056	0.157	2.992	2.876	3.493	3.639	0.369	0.451	0.434	0.78	
L-8.0-03+	8.61	0.500	0.080	0.055	0.160	2.969	2.830	3.326	3.542	0.366	0.446	0.425	----	
L-8.0-04*	8.67	0.548	0.085	0.057	0.155	2.951	2.817	3.625	3.722	0.374	0.446	0.426	----	
L-8.0-05	8.52	0.424	0.070	0.052	0.166	2.435	2.363	2.851	3.184	0.349	0.362	0.351	0.96	
L-8.0-06	8.42	0.337	0.058	0.047	0.172	1.956	1.889	2.297	2.697	0.323	0.287	0.277	1.38	
L-8.0-07	8.35	0.286	0.049	0.043	0.171	1.580	1.518	1.963	2.300	0.293	0.230	0.221	2.15	
L-8.0-08+	8.32	0.260	0.045	0.041	0.173	1.578	1.520	1.790	2.137	0.279	0.229	0.221	2.65	
L-8.0-09*	8.37	0.296	0.051	0.044	0.172	1.508	1.427	2.024	2.390	0.299	0.220	0.208	----	
L-8.0-10	8.33	0.262	0.045	0.041	0.172	1.249	1.173	1.806	2.140	0.285	0.182	0.170	----	
L-8.0-11+	8.32	0.262	0.046	0.039	0.175	1.669	1.591	1.804	2.173	0.271	0.242	0.231	----	QUESTIONABLE
L-8.0-12*	8.34	0.276	0.048	0.043	0.173	1.152	0.907	1.897	2.257	0.292	0.168	0.132	----	QUESTIONABLE

UNLESS OTHERWISE INDICATED, ALL DATA ARE FOR:
1. SUPERCAVITATING FLOW.
2. BOTH STATIC PRESSURE TAPS OPEN.

LEGEND
+ ONLY UPSTREAM STATIC PRESSURE TAP UTILIZED
* ONLY DNSTREAM STATIC PRESSURE TAP UTILIZED
PC PARTIALLY CAVITATING
PC(TW) PARTIALLY CAVITATING (TAP WETTED)
FW FULLY WETTED
AT (ALPHAT) (TRUE) ANGLE OF ATTACK, CORRECTED FOR EFFECTS OF IMAGES OF TRAILING VORTICES
AT2 ALPHAT**2
SIGC CAVITATION NUMBER COMPUTED WITH MEASURED CAVITY PRESSURE
SIGV CAVITATION NUMBER COMPUTED WITH CALCULATED VAPOR PRESSURE
CD DRAG COEFFICIENT, CORRECTED FOR EFFECTS OF IMAGES OF TRAILING VORTICES
(D/L) CORRECTED DRAG-TO-LIFT RATIO = CD/CL
CAVLTH CAVITY LENGTH MEASURED FROM MIDCHORD AT CENTROID POSITION, NONDIMENSIONALIZED ON MEAN CHORD (OBTAINED FROM PHOTOGRAPHS)

EXPER INVES OF WALL EFFECTS ON SUPERCAVITATING HYDROFOILS OF FINITE SPAN

HYDROFOIL DATA IN NONDIMENSIONAL FORM (NO CORRECTIONS APPLIED)

RUN NO	ALPHA	CL	CDUNC	CM	L/D	D/L	RN*10**-6
L-9.5-01	9.51	0.6809	0.0925	0.1292	7.3628	0.1358	0.8639
L-9.5-02	9.54	0.6995	0.0963	0.1323	7.2612	0.1377	1.3444
L-9.5-03	9.55	0.6996	0.0959	0.1317	7.2963	0.1371	1.4989
L-9.5-04	9.55	0.7124	0.0931	0.1385	7.6493	0.1307	1.5000
L-9.5-05	9.55	0.7370	0.0903	0.1404	8.1635	0.1225	1.4989
L-9.5-06	9.54	0.7877	0.0974	0.1230	8.0898	0.1236	1.4950
L-9.5-07	9.53	0.8274	0.1112	0.0885	7.4403	0.1344	1.4922
L-9.5-08	9.53	0.7710	0.1128	0.0767	6.8374	0.1463	1.4866
L-9.5-09	9.53	0.7496	0.1123	0.0749	6.6729	0.1499	1.4849
L-9.5-10	9.52	0.6922	0.1092	0.0712	6.3406	0.1577	1.4843
L-9.5-11	9.52	0.6650	0.1068	0.0700	6.2255	0.1606	1.4883
L-9.5-12	9.52	0.5927	0.1005	0.0673	5.8953	0.1696	1.4939
L-9.5-13	9.52	0.5700	0.0978	0.0661	5.8267	0.1716	1.4967
L-9.5-14	9.52	0.5059	0.0899	0.0629	5.6282	0.1777	1.5006
L-9.5-15	9.52	0.4826	0.0867	0.0621	5.5667	0.1796	1.5006
L-9.5-16	9.52	0.4433	0.0903	0.0597	4.9092	0.2037	1.5011
L-9.5-17	9.52	0.4234	0.0773	0.0574	5.4776	0.1826	1.5011
L-9.5-18	9.52	0.4045	0.0745	0.0561	5.4268	0.1843	1.5017
L-9.5-19	[illegible]	0.3773	0.0711	0.0554	5.3049	0.1885	1.5022
L-9.5-20	9.[illegible]	0.3431	0.0651	0.0522	5.2685	0.1898	1.5017
L-9.5-21	9.52	0.3249	0.0621	0.0509	5.2295	0.1912	1.5006
L-9.5-22	9.52	0.3171	0.0604	0.0501	5.2452	0.1907	1.4933
L-9.5-23	9.52	0.3088	0.0587	0.0495	5.2593	0.1901	1.4593
L-9.5-24	9.53	0.8224	0.1097	0.0854	7.4971	0.1334	1.4995
L-9.5-25	9.52	0.8203	0.1061	0.0963	7.7306	0.1294	1.2888
L-9.5-26	9.52	0.7883	0.1089	0.0815	7.2369	0.1382	1.1283
L-9.5-27	9.51	0.7491	0.1094	0.0724	6.8500	0.1460	1.0554

LEGEND
- ALPHA GEOMETRIC ANGLE OF ATTACK CORRECTED FOR SHAFT TWIST
- CL LIFT COEFFICIENT, NONDIMENSIONALIZED ON UPSTREAM VELOCITY AND MODEL PLANFORM AREA
- CDUNC CD(UNCORRECTED), THE UNCORRECTED DRAG COEFFICIENT AS COMPUTED FROM MEASURED DRAG, AND NONDIMENSIONALIZED ON UPSTREAM VELOCITY AND MODEL PLANFORM AREA
- CM MOMENT COEFFICIENT, NONDIMENSIONALIZED ON UPSTREAM VELOCITY, MODEL PLANFORM AREA, AND MEAN CHORD
- L/D LIFT-TO-DRAG RATIO = CL/CDUNC
- D/L DRAG-TO-LIFT RATIO = CDUNC/CL
- RN REYNOLDS NUMBER, BASED ON MEAN CHORD

EXPER INVES OF WALL EFFECTS ON SUPERCAVITATING HYDROFOILS OF FINITE SPAN

PRIOR DATA CORRECTED FOR EFFECTS OF IMAGES OF TRAILING VORTEX SYSTEM

RUN NO	ALPHAT	CL	CD	CM	(D/L)	SIGV/AT	SIGC/AT	CL/AT	CD/AT2	CM/AT	SIGV	SIGC	CAVLTH	COMMENTS/REMARKS
L-9.5-01	10.32	0.681	0.102	0.129	0.150	-----	-----	3.779	3.185	0.717	-----	-----	----	FW
L-9.5-02	10.37	0.699	0.106	0.132	0.152	-----	-----	3.866	3.252	0.731	-----	-----	----	FW
L-9.5-03	10.38	0.700	0.106	0.132	0.152	-----	-----	3.863	3.233	0.727	-----	-----	----	FW
L-9.5-04	10.39	0.712	0.104	0.138	0.145	-----	-----	3.927	3.149	0.763	-----	-----	----	PC(TW)
L-9.5-05	10.42	0.737	0.102	0.140	0.138	-----	-----	4.051	3.068	0.772	-----	-----	----	PC(TW)
L-9.5-06	10.48	0.788	0.110	0.123	0.140	-----	-----	4.308	3.296	0.672	-----	-----	----	PC(TW)
L-9.5-07	10.51	0.827	0.125	0.089	0.152	3.938	3.698	4.510	3.725	0.482	0.722	0.678	----	
L-9.5-08	10.44	0.771	0.125	0.077	0.162	3.573	3.356	4.231	3.766	0.421	0.651	0.611	----	
L-9.5-09+	10.41	0.750	0.124	0.075	0.165	3.588	3.395	4.124	3.752	0.412	0.652	0.617	0.70	
L-9.5-10	10.35	0.692	0.119	0.071	0.172	3.188	3.020	3.834	3.653	0.394	0.576	0.545	----	
L-9.5-11+	10.31	0.665	0.116	0.070	0.174	3.178	3.014	3.694	3.580	0.389	0.572	0.542	0.74	
L-9.5-12	10.23	0.593	0.108	0.067	0.182	2.802	2.640	3.321	3.384	0.377	0.500	0.471	----	
L-9.5-13+	10.20	0.570	0.105	0.066	0.183	2.797	2.637	3.202	3.300	0.371	0.498	0.469	0.82	
L-9.5-14	10.12	0.506	0.095	0.063	0.188	2.424	2.290	2.863	3.050	0.356	0.428	0.405	----	
L-9.5-15+	10.09	0.483	0.092	0.062	0.190	2.428	2.344	2.739	2.949	0.353	0.428	0.413	1.11	
L-9.5-16	10.05	0.443	0.094	0.060	0.213	2.103	2.045	2.528	3.069	0.340	0.369	0.359	----	
L-9.5-17+	10.02	0.423	0.081	0.057	0.191	2.129	2.074	2.420	2.647	0.328	0.372	0.363	1.20	
L-9.5-18	10.00	0.405	0.078	0.056	0.193	1.868	1.815	2.318	2.559	0.322	0.326	0.317	----	
L-9.5-19+	9.97	0.377	0.074	0.055	0.196	1.870	1.819	2.169	2.448	0.319	0.325	0.317	1.68	
L-9.5-20	9.93	0.343	0.068	0.052	0.197	1.589	1.541	1.980	2.251	0.301	0.275	0.267	----	
L-9.5-21+	9.90	0.325	0.064	0.051	0.198	1.592	1.570	1.880	2.153	0.294	0.275	0.271	2.28	
L-9.5-22	9.89	0.317	0.063	0.050	0.197	1.363	1.344	1.836	2.097	0.290	0.235	0.232	----	
L-9.5-23+	9.88	0.309	0.061	0.050	0.197	1.477	1.460	1.790	2.040	0.287	0.255	0.252	3.80	
L-9.5-24	10.51	0.822	0.124	0.085	0.150	3.904	3.664	4.486	3.680	0.466	0.716	0.672	----	
L-9.5-25	10.50	0.820	0.120	0.096	0.146	4.022	3.732	4.477	3.576	0.525	0.737	0.684	----	
L-9.5-26	10.45	0.788	0.122	0.081	0.154	3.814	3.560	4.322	3.660	0.447	0.696	0.649	----	PC
L-9.5-27	10.40	0.749	0.121	0.072	0.161	3.495	3.255	4.127	3.671	0.399	0.634	0.591	----	PC

UNLESS OTHERWISE INDICATED, ALL DATA ARE FOR:
1. SUPERCAVITATING FLOW.
2. BOTH STATIC PRESSURE TAPS OPEN.

LEGEND
+ ONLY UPSTREAM STATIC PRESSURE TAP UTILIZED
* ONLY DNSTREAM STATIC PRESSURE TAP UTILIZED
PC PARTIALLY CAVITATING
PC(TW) PARTIALLY CAVITATING (TAP WETTED)
FW FULLY WETTED
AT (ALPHAT) (TRUE) ANGLE OF ATTACK, CORRECTED FOR EFFECTS OF IMAGES OF TRAILING VORTICES
AT2 ALPHAT**2
SIGC CAVITATION NUMBER COMPUTED WITH MEASURED CAVITY PRESSURE
SIGV CAVITATION NUMBER COMPUTED WITH CALCULATED VAPOR PRESSURE
CD DRAG COEFFICIENT, CORRECTED FOR EFFECTS OF IMAGES OF TRAILING VORTICES
(D/L) CORRECTED DRAG-TO-LIFT RATIO = CD/CL
CAVLTH CAVITY LENGTH MEASURED FROM MIDCHORD AT CENTROID POSITION, NONDIMENSIONALIZED ON MEAN CHORD
(OBTAINED FROM PHOTOGRAPHS)

HYDROFOIL DATA IN NONDIMENSIONAL FORM (NO CORRECTIONS APPLIED)

RUN NO	ALPHA	CL	CDUNC	CM	L/D	D/L	RN*10**-6
L-11.-01	11.03	0.9067	0.1493	0.0917	6.0749	0.1646	1.4427
L-11.-02	11.03	0.8179	0.1462	0.0829	5.5931	0.1788	1.4427
L-11.-03	11.03	0.7425	0.1397	0.0788	5.3152	0.1881	1.4416
L-11.-04	11.03	0.6650	0.1298	0.0748	5.1248	0.1951	1.4449
L-11.-05	11.03	0.6365	0.1265	0.0740	5.0330	0.1987	1.4438
L-11.-06	11.03	0.6868	0.1335	0.0759	5.1425	0.1945	1.4438
L-11.-07	11.03	0.6027	0.1211	0.0722	4.9753	0.2010	1.4487
L-11.-08	11.02	0.5755	0.1172	0.0707	4.9122	0.2036	1.4481
L-11.-09	11.02	0.5302	0.1100	0.0684	4.8216	0.2074	1.4481
L-11.-10	11.02	0.5094	0.1060	0.0675	4.8042	0.2082	1.4498
L-11.-11	11.02	0.4637	0.0969	0.0635	4.7840	0.2090	1.4498
L-11.-12	11.02	0.4345	0.0931	0.0628	4.6657	0.2143	1.4514
L-11.-13	11.02	0.4213	0.0905	0.0617	4.6560	0.2148	1.4503
L-11.-14	11.02	0.3931	0.0849	0.0599	4.6286	0.2160	1.4514
L-11.-15	11.02	0.3793	0.0817	0.0586	4.6396	0.2155	1.4530
L-11.-16	11.02	0.3552	0.0770	0.0560	4.6148	0.2167	1.4492
L-11.-17	11.02	0.3627	0.0787	0.0574	4.6077	0.2170	1.4487
L-11.-18	11.02	0.3618	0.0785	0.0559	4.6112	0.2169	1.3741
L-11.-19	11.02	0.5309	0.1103	0.0679	4.8136	0.2077	1.3274
L-11.-20	11.02	0.5170	0.1071	0.0671	4.8278	0.2071	1.3287

LEGEND
- ALPHA GEOMETRIC ANGLE OF ATTACK CORRECTED FOR SHAFT TWIST
- CL LIFT COEFFICIENT, NONDIMENSIONALIZED ON UPSTREAM VELOCITY AND MODEL PLANFORM AREA
- CDUNC CD(UNCORRECTED), THE UNCORRECTED DRAG COEFFICIENT AS COMPUTED FROM MEASURED DRAG, AND NONDIMENSIONALIZED ON UPSTREAM VELOCITY AND MODEL PLANFORM AREA
- CM MOMENT COEFFICIENT, NONDIMENSIONALIZED ON UPSTREAM VELOCITY, MODEL PLANFORM AREA, AND MEAN CHORD
- L/D LIFT-TO-DRAG RATIO = CL/CDUNC
- D/L DRAG-TO-LIFT RATIO = CDUNC/CL
- RN REYNOLDS NUMBER, BASED ON MEAN CHORD

EXPER INVES OF WALL EFFECTS ON SUPERCAVITATING HYDROFOILS OF FINITE SPAN

PRIOR DATA CORRECTED FOR EFFECTS OF IMAGES OF TRAILING VORTEX SYSTEM

RUN NO	ALPHAT	CL	CD	CM	(D/L)	SIGV/AT	SIGC/AT	CL/AT	CD/AT2	CM/AT	SIGV	SIGC	CAVLTH	COMMENTS/REMARKS
L-11.-01	12.11	0.907	0.166	0.092	0.183	3.720	3.440	4.291	3.724	0.434	0.786	0.727	0.72	
L-11.-02	12.00	0.818	0.160	0.083	0.196	3.326	3.086	3.906	3.650	0.396	0.697	0.646	0.82	
L-11.-03	11.91	0.743	0.151	0.079	0.204	3.007	2.807	3.573	3.499	0.379	0.625	0.583	0.92	
L-11.-04	11.81	0.665	0.139	0.075	0.209	2.688	2.529	3.225	3.267	0.363	0.554	0.522	0.95	
L-11.-05+	11.78	0.636	0.135	0.074	0.212	2.698	2.540	3.096	3.190	0.360	0.555	0.522	----	
L-11.-06*	11.84	0.687	0.143	0.076	0.209	2.683	2.528	3.323	3.356	0.367	0.554	0.522	----	
L-11.-07	11.74	0.603	0.129	0.072	0.213	2.460	2.306	2.942	3.065	0.353	0.504	0.472	1.03	
L-11.-08+	11.71	0.576	0.124	0.071	0.215	2.467	2.335	2.817	2.971	0.346	0.504	0.477	1.08	
L-11.-09	11.65	0.530	0.116	0.068	0.218	2.187	2.139	2.607	2.800	0.337	0.445	0.435	----	
L-11.-10+	11.63	0.509	0.111	0.067	0.219	2.165	2.138	2.510	2.705	0.332	0.439	0.434	1.30	
L-11.-11	11.57	0.464	0.101	0.063	0.219	1.820	1.795	2.296	2.485	0.314	0.368	0.363	----	
L-11.-12+	11.54	0.438	0.097	0.063	0.223	1.820	1.796	2.158	2.393	0.312	0.366	0.362	1.68	
L-11.-13	11.52	0.421	0.094	0.062	0.223	1.636	1.613	2.095	2.329	0.307	0.329	0.324	----	
L-11.-14+	11.49	0.393	0.088	0.060	0.224	1.637	1.616	1.961	2.192	0.299	0.328	0.324	2.05	
L-11.-15	11.47	0.379	0.085	0.059	0.223	1.425	1.405	1.895	2.114	0.292	0.285	0.281	----	
L-11.-16+	11.44	0.355	0.080	0.056	0.224	1.414	1.395	1.779	1.996	0.280	0.282	0.279	3.20	
L-11.-17	11.45	0.363	0.081	0.057	0.225	1.243	1.227	1.815	2.039	0.287	0.248	0.245	3.12	
L-11.-18+	11.45	0.362	0.081	0.056	0.224	1.451	1.434	1.811	2.034	0.280	0.290	0.287	4.10	QUESTIONABLE
L-11.-19	11.65	0.531	0.116	0.068	0.219	2.167	2.102	2.611	2.809	0.334	0.441	0.427	----	
L-11.-20+	11.63	0.517	0.113	0.067	0.218	2.189	2.150	2.547	2.732	0.331	0.444	0.437	----	

UNLESS OTHERWISE INDICATED, ALL DATA ARE FOR:
1. SUPERCAVITATING FLOW.
2. BOTH STATIC PRESSURE TAPS OPEN.

LEGEND
+ ONLY UPSTREAM STATIC PRESSURE TAP UTILIZED
* ONLY DNSTREAM STATIC PRESSURE TAP UTILIZED
PC PARTIALLY CAVITATING
PC(TW) PARTIALLY CAVITATING (TAP WETTED)
FW FULLY WETTED
AT (ALPHAT) (TRUE) ANGLE OF ATTACK, CORRECTED FOR EFFECTS OF IMAGES OF TRAILING VORTICES
AT2 ALPHAT**2
SIGC CAVITATION NUMBER COMPUTED WITH MEASURED CAVITY PRESSURE
SIGV CAVITATION NUMBER COMPUTED WITH CALCULATED VAPOR PRESSURE
CD DRAG COEFFICIENT, CORRECTED FOR EFFECTS OF IMAGES OF TRAILING VORTICES
(D/L) CORRECTED DRAG-TO-LIFT RATIO = CD/CL
CAVLTH CAVITY LENGTH MEASURED FROM MIDCHORD AT CENTROID POSITION, NONDIMENSIONALIZED ON MEAN CHORD (OBTAINED FROM PHOTOGRAPHS)

EXPER INVES OF WALL EFFECTS ON SUPERCAVITATING HYDROFOILS OF FINITE SPAN

HYDROFOIL DATA IN NONDIMENSIONAL FORM (NO CORRECTIONS APPLIED)

RUN NO	ALPHA	CL	CDUNC	CM	L/D	D/L	RN*10**-6
L-12.-01	12.03	0.8829	0.1293	0.1814	6.8299	0.1464	0.9650
L-12.-02	12.04	0.8929	0.1318	0.1830	6.7764	0.1476	1.2099
L-12.-03	12.06	0.8986	0.1322	0.1836	6.7988	0.1471	1.4605
L-12.-04	12.06	0.9736	0.1417	0.1759	6.8700	0.1456	1.4634
L-12.-05	12.05	1.0164	0.1576	0.1494	6.4480	0.1551	1.4623
L-12.-06	12.04	1.0301	0.1702	0.1230	6.0528	0.1652	1.4646
L-12.-07	12.03	0.9915	0.1747	0.1033	5.6745	0.1762	1.4640
L-12.-08	12.03	0.9685	0.1745	0.0980	5.5516	0.1801	1.4646
L-12.-09	12.03	0.9159	0.1725	0.0914	5.3089	0.1884	1.4640
L-12.-10	12.03	0.8895	0.1713	0.0891	5.1942	0.1925	1.4640
L-12.-11	12.03	0.8444	0.1674	0.0858	5.0437	0.1983	1.4640
L-12.-12	12.03	0.8173	0.1648	0.0843	4.9588	0.2017	1.4640
L-12.-13	12.03	0.7514	0.1572	0.0813	4.7801	0.2092	1.4634
L-12.-14	12.03	0.7242	0.1528	0.0798	4.7397	0.2110	1.4646
L-12.-15	12.03	0.6780	0.1454	0.0778	4.6618	0.2145	1.4652
L-12.-16	12.03	0.6484	0.1410	0.0764	4.5995	0.2174	1.4658
L-12.-17	12.02	0.6120	0.1347	0.0745	4.5444	0.2200	1.4658
L-12.-18	12.02	0.5861	0.1301	0.0733	4.5041	0.2220	1.4658
L-12.-19	12.02	0.5455	0.1221	0.0708	4.4682	0.2238	1.4658
L-12.-20	12.02	0.5232	0.1168	0.0697	4.4794	0.2232	1.4664
L-12.-21	12.02	0.4986	0.1122	0.0674	4.4451	0.2250	1.4669
L-12.-22	12.02	0.4685	0.1079	0.0667	4.3414	0.2303	1.4658
L-12.-23	12.02	0.4553	0.1048	0.0650	4.3427	0.2303	1.4669
L-12.-24	12.02	0.4348	0.1005	0.0645	4.3270	0.2311	1.4664
L-12.-25	12.02	0.4186	0.0960	0.0628	4.3622	0.2292	1.4669
L-12.-26	12.02	0.3914	0.0905	0.0607	4.3251	0.2312	1.4669
L-12.-27	12.02	0.3914	0.0906	0.0607	4.3214	0.2314	1.4669
L-12.-28	12.02	0.3591	0.0829	0.0559	4.3326	0.2308	1.4605
L-12.-29	12.03	0.7497	0.1556	0.0809	4.8184	0.2075	1.4629
L-12.-30	12.02	0.7406	0.1546	0.0804	4.7907	0.2087	1.2979
L-12.-31	12.01	0.6861	0.1452	0.0779	4.7253	0.2116	1.0847
L-12.-32	12.01	0.7361	0.1490	0.0795	4.9411	0.2024	0.8774

LEGEND
- ALPHA GEOMETRIC ANGLE OF ATTACK CORRECTED FOR SHAFT TWIST
- CL LIFT COEFFICIENT, NONDIMENSIONALIZED ON UPSTREAM VELOCITY AND MODEL PLANFORM AREA
- CDUNC CD(UNCORRECTED), THE UNCORRECTED DRAG COEFFICIENT AS COMPUTED FROM MEASURED DRAG, AND NONDIMENSIONALIZED ON UPSTREAM VELOCITY AND MODEL PLANFORM AREA
- CM MOMENT COEFFICIENT, NONDIMENSIONALIZED ON UPSTREAM VELOCITY, MODEL PLANFORM AREA, AND MEAN CHORD
- L/D LIFT-TO-DRAG RATIO = CL/CDUNC
- D/L DRAG-TO-LIFT RATIO = CDUNC/CL
- RN REYNOLDS NUMBER, BASED ON MEAN CHORD

EXPER INVES OF WALL EFFECTS ON SUPERCAVITATING HYDROFOILS OF FINITE SPAN

PRIOR DATA CORRECTED FOR EFFECTS OF IMAGES OF TRAILING VORTEX SYSTEM

RUN NO	ALPHAT	CL	CD	CM	(D/L)	SIGV/AT	SIGC/AT	CL/AT	CD/AT2	CM/AT	SIGV	SIGC	CAVLTH	COMMENTS/REMARKS
L-12.-01	13.07	0.883	0.145	0.181	0.165	-----	-----	3.870	2.793	0.795	-----	-----	----	FW
L-12.-02	13.10	0.893	0.148	0.183	0.166	-----	-----	3.906	2.837	0.800	-----	-----	----	FW
L-12.-03	13.13	0.899	0.149	0.184	0.166	-----	-----	3.922	2.837	0.802	-----	-----	----	FW
L-12.-04	13.21	0.974	0.161	0.176	0.166	-----	-----	4.222	3.034	0.763	-----	-----	----	PC(TW)
L-12.-05	13.25	1.016	0.179	0.149	0.176	-----	-----	4.394	3.345	0.646	-----	-----	----	PC(TW)
L-12.-06	13.26	1.030	0.192	0.123	0.187	-----	-----	4.450	3.586	0.531	-----	-----	----	PC(TW)
L-12.-07	13.21	0.991	0.195	0.103	0.197	3.814	3.424	4.300	3.670	0.448	0.879	0.789	----	
L-12.-08*	13.18	0.969	0.194	0.098	0.200	3.818	3.428	4.210	3.663	0.426	0.878	0.789	0.61	
L-12.-09	13.12	0.916	0.190	0.091	0.207	3.488	3.156	4.001	3.623	0.399	0.798	0.723	----	
L-12.-10*	13.08	0.890	0.188	0.089	0.211	3.495	3.183	3.895	3.598	0.390	0.798	0.727	0.64	
L-12.-11	13.03	0.844	0.182	0.086	0.216	3.194	2.903	3.713	3.523	0.377	0.726	0.660	----	
L-12.-12*	11.00	0.817	0.179	0.084	0.219	3.201	2.930	3.603	3.472	0.372	0.726	0.665	0.74	
L-12.-13	12.92	0.751	0.169	0.081	0.225	2.866	2.634	3.333	3.322	0.361	0.646	0.594	----	
L-12.-14*	12.89	0.724	0.164	0.080	0.226	2.867	2.636	3.220	3.236	0.355	0.645	0.593	1.00	
L-12.-15	12.83	0.678	0.155	0.078	0.229	2.557	2.348	3.028	3.090	0.348	0.573	0.526	----	
L-12.-16*	12.79	0.648	0.150	0.076	0.231	2.561	2.372	2.904	3.002	0.342	0.572	0.530	1.05	
L-12.-17	12.75	0.612	0.142	0.074	0.233	2.288	2.121	2.750	2.876	0.335	0.509	0.472	----	
L-12.-18*	12.72	0.586	0.137	0.073	0.234	2.292	2.166	2.640	2.785	0.330	0.509	0.481	1.18	
L-12.-19	12.67	0.545	0.128	0.071	0.235	2.039	1.974	2.467	2.622	0.320	0.451	0.436	----	
L-12.-20*	12.64	0.523	0.122	0.070	0.234	2.039	1.976	2.371	2.515	0.316	0.450	0.436	1.30	
L-12.-21	12.61	0.499	0.117	0.067	0.235	1.819	1.758	2.265	2.421	0.306	0.400	0.387	----	
L-12.-22*	12.58	0.468	0.112	0.067	0.240	1.805	1.745	2.134	2.334	0.304	0.396	0.383	1.73	
L-12.-23	12.56	0.455	0.109	0.066	0.240	1.641	1.583	2.077	2.270	0.300	0.360	0.347	----	
L-12.-24*	12.54	0.435	0.104	0.065	0.240	1.644	1.587	1.987	2.180	0.295	0.360	0.347	2.10	
L-12.-25	12.52	0.419	0.100	0.063	0.238	1.440	1.386	1.916	2.087	0.288	0.315	0.303	----	
L-12.-26*	12.48	0.391	0.094	0.061	0.239	1.463	1.410	1.796	1.973	0.279	0.319	0.307	3.55	
L-12.-27	12.48	0.391	0.094	0.061	0.240	1.237	1.186	1.796	1.975	0.279	0.270	0.258	----	
L-12.-28*	12.44	0.359	0.086	0.056	0.238	1.312	1.262	1.653	1.814	0.257	0.285	0.274	4.10	QUESTIONABLE
L-12.-29	12.92	0.750	0.167	0.081	0.223	2.842	2.617	3.326	3.291	0.359	0.641	0.590	----	
L-12.-30	12.90	0.741	0.166	0.080	0.224	2.782	2.573	3.290	3.274	0.357	0.626	0.579	----	
L-12.-31	12.83	0.686	0.155	0.078	0.226	2.625	2.400	3.065	3.091	0.348	0.588	0.537	----	
L-12.-32	12.88	0.736	0.160	0.080	0.218	2.886	2.550	3.274	3.169	0.354	0.649	0.573	----	

UNLESS OTHERWISE INDICATED, ALL DATA ARE FOR:
1. SUPERCAVITATING FLOW.
2. BOTH STATIC PRESSURE TAPS OPEN.

LEGEND
* ONLY UPSTREAM STATIC PRESSURE TAP UTILIZED
* ONLY DNSTREAM STATIC PRESSURE TAP UTILIZED
PC PARTIALLY CAVITATING
PC(TW) PARTIALLY CAVITATING (TAP WETTED)
FW FULLY WETTED
AT (ALPHAT) (TRUE) ANGLE OF ATTACK, CORRECTED FOR EFFECTS OF IMAGES OF TRAILING VORTICES
AT2 ALPHAT**2
SIGC CAVITATION NUMBER COMPUTED WITH MEASURED CAVITY PRESSURE
SIGV CAVITATION NUMBER COMPUTED WITH CALCULATED VAPOR PRESSURE
CD DRAG COEFFICIENT, CORRECTED FOR EFFECTS OF IMAGES OF TRAILING VORTICES
(D/L) CORRECTED DRAG-TO-LIFT RATIO = CD/CL
CAVLTH CAVITY LENGTH MEASURED FROM MIDCHORD AT CENTROID POSITION, NONDIMENSIONALIZED ON MEAN CHORD (OBTAINED FROM PHOTOGRAPHS)

EXPER INVES OF WALL EFFECTS ON SUPERCAVITATING HYDROFOILS OF FINITE SPAN

HYDROFOIL DATA IN NONDIMENSIONAL FORM (NO CORRECTIONS APPLIED)

RUN NO	ALPHA	CL	CDUNC	CM	L/D	D/L	RN*10**-6
L-14.-01	14.03	1.0755	0.2288	0.1101	4.7013	0.2127	1.3457
L-14.-02	14.03	1.0408	0.2259	0.1054	4.6075	0.2170	1.3457
L-14.-03	14.03	1.0074	0.2244	0.1021	4.4897	0.2227	1.3451
L-14.-04	14.03	0.9758	0.2221	0.0992	4.3936	0.2276	1.3457
L-14.-05	14.03	0.9372	0.2183	0.0967	4.2935	0.2329	1.3457
L-14.-06	14.03	0.9056	0.2138	0.0944	4.2357	0.2361	1.3457
L-14.-07	14.03	0.8454	0.2055	0.0910	4.1129	0.2431	1.3463
L-14.-08	14.03	0.8134	0.2002	0.0899	4.0635	0.2461	1.3469
L-14.-09	14.03	0.7719	0.1924	0.0878	4.0121	0.2492	1.3487
L-14.-10	14.03	0.7446	0.1873	0.0863	3.9755	0.2515	1.3493
L-14.-11	14.02	0.7068	0.1792	0.0842	3.9440	0.2536	1.3499
L-14.-12	14.02	0.6749	0.1733	0.0823	3.8939	0.2568	1.3505
L-14.-13	14.02	0.6293	0.1629	0.0798	3.8633	0.2588	1.3511
L-14.-14	14.02	0.6041	0.1561	0.0792	3.8690	0.2585	1.3511
L-14.-15	14.02	0.5714	0.1480	0.0779	3.8608	0.2590	1.3517
L-14.-16	14.02	0.5402	0.1432	0.0760	3.7719	0.2651	1.3517
L-14.-17	14.02	0.5306	0.1409	0.0759	3.7656	0.2656	1.3523
L-14.-18	14.02	0.4987	0.1329	0.0742	3.7520	0.2665	1.3517
L-14.-19	14.02	0.4962	0.1313	0.0737	3.7789	0.2646	1.3535
L-14.-20	14.02	0.4642	0.1236	0.0714	3.7568	0.2662	1.3511
L-14.-21	14.02	0.4729	0.1250	0.0714	3.7817	0.2644	1.3517
L-14.-22	14.02	0.4367	0.1158	0.0674	3.7698	0.2653	1.3457
L-14.-23	14.02	0.6394	0.1639	0.0803	3.9016	0.2563	1.1126
L-14.-24	14.02	0.6070	0.1561	0.0787	3.8883	0.2572	1.1126

LEGEND
- ALPHA GEOMETRIC ANGLE OF ATTACK CORRECTED FOR SHAFT TWIST
- CL LIFT COEFFICIENT, NONDIMENSIONALIZED ON UPSTREAM VELOCITY AND MODEL PLANFORM AREA
- CDUNC CD(UNCORRECTED), THE UNCORRECTED DRAG COEFFICIENT AS COMPUTED FROM MEASURED DRAG, AND NONDIMENSIONALIZED ON UPSTREAM VELOCITY AND MODEL PLANFORM AREA
- CM MOMENT COEFFICIENT, NONDIMENSIONALIZED ON UPSTREAM VELOCITY, MODEL PLANFORM AREA, AND MEAN CHORD
- L/D LIFT-TO-DRAG RATIO = CL/CDUNC
- D/L DRAG-TO-LIFT RATIO = CDUNC/CL
- RN REYNOLDS NUMBER, BASED ON MEAN CHORD

EXPER INVES OF WALL EFFECTS ON SUPERCAVITATING HYDROFOILS OF FINITE SPAN

PRIOR DATA CORRECTED FOR EFFECTS OF IMAGES OF TRAILING VORTEX SYSTEM

RUN NO	ALPHAT	CL	CD	CM	(D/L)	SIGV/AT	SIGC/AT	CL/AT	CD/AT2	CM/AT	SIGV	SIGC	CAVLTH	COMMENTS/REMARKS
L-14.-01	15.31	1.076	0.253	0.110	0.235	3.611	3.153	4.026	3.540	0.412	0.965	0.842	----	
L-14.-02*	15.27	1.041	0.248	0.105	0.239	3.620	3.199	3.906	3.498	0.396	0.964	0.852	0.70	
L-14.-03	15.22	1.007	0.245	0.102	0.244	3.350	2.967	3.791	3.475	0.384	0.890	0.788	----	
L-14.-04*	15.19	0.976	0.242	0.099	0.248	3.355	2.991	3.681	3.442	0.374	0.889	0.793	0.80	
L-14.-05	15.14	0.937	0.236	0.097	0.252	3.100	2.792	3.547	3.387	0.366	0.819	0.738	----	
L-14.-06*	15.10	0.906	0.231	0.094	0.255	3.107	2.818	3.436	3.322	0.358	0.819	0.743	0.83	
L-14.-07	15.03	0.845	0.220	0.091	0.261	2.777	2.545	3.223	3.202	0.347	0.728	0.668	----	
L-14.-08*	14.99	0.813	0.214	0.090	0.263	2.761	2.549	3.109	3.124	0.343	0.722	0.667	0.92	
L-14.-09	14.94	0.772	0.205	0.088	0.265	2.534	2.342	2.960	3.011	0.337	0.661	0.611	----	
L-14.-10*	14.91	0.745	0.199	0.086	0.267	2.536	2.364	2.862	2.936	0.332	0.660	0.615	0.95	
L-14.-11	14.86	0.707	0.190	0.084	0.268	2.292	2.140	2.725	2.817	0.324	0.595	0.555	----	
L-14.-12*	14.82	0.675	0.183	0.082	0.271	2.295	2.163	2.609	2.730	0.318	0.594	0.560	1.10	
L-14.-13	14.77	0.629	0.171	0.080	0.272	2.013	1.958	2.441	2.575	0.310	0.519	0.505	----	
L-14.-14*	14.74	0.604	0.164	0.079	0.271	2.016	1.982	2.348	2.473	0.308	0.519	0.510	1.43	
L-14.-15	14.70	0.571	0.155	0.078	0.271	1.749	1.716	2.227	2.351	0.304	0.449	0.440	----	
L-14.-16*	14.66	0.540	0.149	0.076	0.276	1.752	1.740	2.111	2.279	0.297	0.448	0.445	1.80	
L-14.-17	14.65	0.531	0.147	0.076	0.277	1.635	1.604	2.075	2.244	0.297	0.418	0.410	1.88	
L-14.-18*	14.61	0.499	0.138	0.074	0.277	1.640	1.629	1.955	2.123	0.291	0.418	0.416	2.20	
L-14.-19	14.61	0.496	0.136	0.074	0.275	1.499	1.490	1.946	2.098	0.289	0.382	0.380	----	
L-14.-20*	14.57	0.464	0.128	0.071	0.276	1.508	1.500	1.825	1.979	0.281	0.383	0.381	2.95	
L-14.-21	14.58	0.473	0.130	0.071	0.274	1.349	1.342	1.858	2.002	0.281	0.343	0.342	----	
L-14.-22*	14.54	0.437	0.120	0.067	0.274	1.364	1.358	1.721	1.861	0.266	0.346	0.345	4.50	QUESTIONABLE
L-14.-23	14.77	0.639	0.172	0.080	0.270	2.075	2.012	2.480	2.592	0.311	0.535	0.519	----	
L-14.-24*	14.74	0.607	0.164	0.079	0.270	2.078	2.017	2.360	2.476	0.306	0.535	0.519	----	

UNLESS OTHERWISE INDICATED, ALL DATA ARE FOR:
1. SUPERCAVITATING FLOW.
2. BOTH STATIC PRESSURE TAPS OPEN.

LEGEND
* ONLY UPSTREAM STATIC PRESSURE TAP UTILIZED
* ONLY DNSTREAM STATIC PRESSURE TAP UTILIZED
PC PARTIALLY CAVITATING
PC(TW) PARTIALLY CAVITATING (TAP WETTED)
FW FULLY WETTED
AT (ALPHAT) (TRUE) ANGLE OF ATTACK, CORRECTED FOR EFFECTS OF IMAGES OF TRAILING VORTICES
AT2 ALPHAT**2
SIGC CAVITATION NUMBER COMPUTED WITH MEASURED CAVITY PRESSURE
SIGV CAVITATION NUMBER COMPUTED WITH CALCULATED VAPOR PRESSURE
CD DRAG COEFFICIENT, CORRECTED FOR EFFECTS OF IMAGES OF TRAILING VORTICES
(D/L) CORRECTED DRAG-TO-LIFT RATIO = CD/CL
CAVLTH CAVITY LENGTH MEASURED FROM MIDCHORD AT CENTROID POSITION, NONDIMENSIONALIZED ON MEAN CHORD (OBTAINED FROM PHOTOGRAPHS)

EFFECTS OF WALL EFFECTS ON SUPERCAVITATING HYDROFOILS OF FINITE SPAN

HYDROFOIL DATA IN NONDIMENSIONAL FORM (NO CORRECTIONS APPLIED)

RUN NO	ALPHA	CL	CDUNC	CM	L/D	D/L	RN*10**-6
L-16.-01	16.03	1.1380	0.2393	0.1947	4.7547	0.2103	0.9787
L-16.-02	16.04	1.1532	0.2448	0.1950	4.7107	0.2123	1.1831
L-16.-03	16.05	1.1499	0.2456	0.1953	4.6816	0.2136	1.3820
L-16.-04	16.05	1.2418	0.2703	0.1786	4.5945	0.2176	1.3766
L-16.-05	16.04	1.2294	0.2768	0.1626	4.4412	0.2252	1.3786
L-16.-06	16.04	1.2059	0.2795	0.1437	4.3143	0.2318	1.3780
L-16.-07	16.04	1.1902	0.2809	0.1414	4.2366	0.2360	1.3760
L-16.-08	16.04	1.1639	0.2845	0.1294	4.0905	0.2445	1.3747
L-16.-09	16.03	1.1389	0.2818	0.1238	4.0421	0.2474	1.3753
L-16.-10	16.03	1.0835	0.2765	0.1149	3.9183	0.2552	1.3760
L-16.-11	16.03	1.0595	0.2743	0.1096	3.8625	0.2589	1.3753
L-16.-12	16.03	1.0145	0.2672	0.1058	3.7962	0.2634	1.3760
L-16.-13	16.03	0.9805	0.2645	0.1021	3.7073	0.2697	1.3766
L-16.-14	16.03	0.9353	0.2574	0.0984	3.6333	0.2752	1.3766
L-16.-15	16.03	0.8929	0.2506	0.0960	3.5626	0.2807	1.3806
L-16.-16	16.03	0.8283	0.2363	0.0938	3.5049	0.2853	1.3813
L-16.-17	16.03	0.7950	0.2290	0.0921	3.4722	0.2880	1.3813
L-16.-18	16.02	0.7440	0.2181	0.0889	3.4111	0.2932	1.3826
L-16.-19	16.02	0.7075	0.2083	0.0870	3.3963	0.2944	1.3846
L-16.-20	16.02	0.6712	0.1986	0.0865	3.3796	0.2959	1.3833
L-16.-21	16.02	0.6412	0.1909	0.0856	3.3582	0.2978	1.3826
L-16.-22	16.02	0.6183	0.1839	0.0838	3.3621	0.2974	1.3846
L-16.-23	16.02	0.5861	0.1767	0.0828	3.3176	0.3014	1.3853
L-16.-24	16.02	0.5680	0.1709	0.0818	3.3244	0.3008	1.3879
L-16.-25	16.02	0.5383	0.1621	0.0799	3.3217	0.3011	1.3866
L-16.-26	16.02	0.5348	0.1614	0.0795	3.3131	0.3018	1.3846
L-16.-27	16.02	0.5345	0.1618	0.0801	3.3029	0.3028	1.3853
L-16.-28	16.03	0.8457	0.2394	0.0945	3.5317	0.2831	1.3853
L-16.-29	16.02	0.8067	0.2300	0.0911	3.5079	0.2851	1.1925
L-16.-30	16.01	0.8719	0.2448	0.0972	3.5613	0.2808	0.8739

LEGEND
- ALPHA GEOMETRIC ANGLE OF ATTACK CORRECTED FOR SHAFT TWIST
- CL LIFT COEFFICIENT, NONDIMENSIONALIZED ON UPSTREAM VELOCITY AND MODEL PLANFORM AREA
- CDUNC CD(UNCORRECTED), THE UNCORRECTED DRAG COEFFICIENT AS COMPUTED FROM MEASURED DRAG, AND NONDIMENSIONALIZED ON UPSTREAM VELOCITY AND MODEL PLANFORM AREA
- CM MOMENT COEFFICIENT, NONDIMENSIONALIZED ON UPSTREAM VELOCITY, MODEL PLANFORM AREA, AND MEAN CHORD
- L/D LIFT-TO-DRAG RATIO = CL/CDUNC
- D/L DRAG-TO-LIFT RATIO = CDUNC/CL
- RN REYNOLDS NUMBER, BASED ON MEAN CHORD

EXPER INVES OF WALL EFFECTS ON SUPERCAVITATING HYDROFOILS OF FINITE SPAN

PRIOR DATA CORRECTED FOR EFFECTS OF IMAGES OF TRAILING VORTEX SYSTEM

RUN NO	ALPHAT	CL	CD	CM	(D/L)	SIGV/AT	SIGC/AT	CL/AT	CD/AT2	CM/AT	SIGV	SIGC	CAVLTH	COMMENTS/REMARKS
L-16.-01	17.38	1.138	0.266	0.195	0.234	-----	-----	3.752	2.894	0.642	-----	-----	----	FW
L-16.-02	17.41	1.153	0.272	0.195	0.236	-----	-----	3.796	2.951	0.642	-----	-----	----	FW
L-16.-03	17.42	1.150	0.273	0.195	0.237	-----	-----	3.783	2.954	0.643	-----	-----	----	FW
L-16.-04	17.52	1.242	0.302	0.179	0.243	-----	-----	4.061	3.231	0.584	-----	-----	----	PC(TW)
L-16.-05	17.50	1.229	0.308	0.163	0.251	4.423	2.987	4.024	3.302	0.532	1.351	0.913	----	PC
L-16.-06	17.47	1.206	0.310	0.144	0.257	4.104	3.135	3.955	3.330	0.471	1.251	0.956	----	
L-16.-07*	17.45	1.190	0.310	0.141	0.261	4.120	3.148	3.908	3.345	0.464	1.255	0.959	0.60	
L-16.-08	17.42	1.164	0.313	0.129	0.269	3.749	2.932	3.829	3.383	0.426	1.139	0.891	----	
L-16.-09*	17.38	1.139	0.309	0.126	0.271	3.750	3.040	3.754	3.352	0.408	1.138	0.922	0.69	
L-16.-10	17.32	1.094	0.301	0.115	0.278	3.373	2.785	3.585	3.293	0.380	1.019	0.842	----	
L-16.-11*	17.29	1.059	0.298	0.110	0.281	3.381	2.863	3.512	3.269	0.363	1.020	0.864	0.85	
L-16.-12	17.23	1.014	0.289	0.106	0.284	3.051	2.604	3.373	3.190	0.352	0.918	0.783	----	
L-16.-13*	17.19	0.981	0.284	0.102	0.290	3.054	2.661	3.268	3.159	0.340	0.916	0.798	0.86	
L-16.-14	17.14	0.935	0.276	0.098	0.295	2.760	2.456	3.127	3.080	0.329	0.826	0.735	----	
L-16.-15*	17.09	0.893	0.267	0.096	0.299	2.751	2.484	2.994	3.004	0.322	0.820	0.741	0.82	
L-16.-16	17.01	0.828	0.251	0.094	0.302	2.422	2.209	2.790	2.843	0.316	0.719	0.656	----	
L-16.-17*	16.97	0.795	0.242	0.092	0.304	2.426	2.232	2.684	2.760	0.311	0.719	0.661	0.92	
L-16.-18	16.91	0.748	0.230	0.089	0.309	2.126	1.968	2.521	2.636	0.301	0.627	0.581	----	
L-16.-19*	16.86	0.708	0.219	0.087	0.309	2.124	2.003	2.404	2.525	0.296	0.625	0.590	1.40	
L-16.-20	16.82	0.671	0.208	0.086	0.310	1.881	1.797	2.286	2.413	0.295	0.552	0.528	----	
L-16.-21*	16.78	0.641	0.199	0.086	0.311	1.885	1.821	2.189	2.324	0.292	0.552	0.533	1.71	
L-16.-22	16.76	0.618	0.192	0.084	0.310	1.666	1.621	2.114	2.243	0.286	0.487	0.474	----	
L-16.-23*	16.72	0.586	0.184	0.083	0.314	1.667	1.623	2.009	2.158	0.284	0.486	0.474	2.17	
L-16.-24	16.70	0.568	0.178	0.082	0.313	1.500	1.457	1.949	2.091	0.281	0.437	0.425	----	
L-16.-25*	16.66	0.538	0.168	0.080	0.312	1.487	1.445	1.851	1.988	0.275	0.432	0.420	2.94	
L-16.-26	16.66	0.535	0.167	0.079	0.313	1.291	1.251	1.840	1.980	0.273	0.375	0.364	----	
L-16.-27*	16.66	0.535	0.168	0.080	0.314	1.288	1.250	1.839	1.985	0.276	0.375	0.363	2.98	
L-16.-28	17.03	0.846	0.254	0.094	0.301	2.459	2.247	2.845	2.878	0.318	0.731	0.668	----	
L-16.-29	16.98	0.807	0.243	0.091	0.302	2.300	2.085	2.723	2.773	0.307	0.681	0.618	----	
L-16.-30	17.04	0.872	0.261	0.097	0.299	2.621	2.360	2.931	2.944	0.327	0.780	0.702	----	

UNLESS OTHERWISE INDICATED, ALL DATA ARE FOR:
1. SUPERCAVITATING FLOW.
2. BOTH STATIC PRESSURE TAPS OPEN.

LEGEND
* ONLY UPSTREAM STATIC PRESSURE TAP UTILIZED
* ONLY DNSTREAM STATIC PRESSURE TAP UTILIZED
PC PARTIALLY CAVITATING
PC(TW) PARTIALLY CAVITATING (TAP WETTED)
FW FULLY WETTED
AT (ALPHAT) (TRUE) ANGLE OF ATTACK, CORRECTED FOR EFFECTS OF IMAGES OF TRAILING VORTICES
AT2 ALPHAT**2
SIGC CAVITATION NUMBER COMPUTED WITH MEASURED CAVITY PRESSURE
SIGV CAVITATION NUMBER COMPUTED WITH CALCULATED VAPOR PRESSURE
CD DRAG COEFFICIENT, CORRECTED FOR EFFECTS OF IMAGES OF TRAILING VORTICES
(D/L) CORRECTED DRAG-TO-LIFT RATIO = CD/CL
CAVLTH CAVITY LENGTH MEASURED FROM MIDCHORD AT CENTROID POSITION, NONDIMENSIONALIZED ON MEAN CHORD
(OBTAINED FROM PHOTOGRAPHS)

EXPER INVES OF WALL EFFECTS ON SUPERCAVITATING HYDROFOILS OF FINITE SPAN

HYDROFOIL DATA IN NONDIMENSIONAL FORM (NO CORRECTIONS APPLIED)

RUN NO	ALPHA	CL	CDUNC	CM	L/D	D/L	RN*10**-6
L-18.-01	18.04	1.1011	0.3260	0.1192	3.3780	0.2960	1.4298
L-18.-02	18.04	1.0821	0.3223	0.1149	3.3575	0.2978	1.4298
L-18.-03	18.04	1.0682	0.3197	0.1146	3.3416	0.2993	1.4286
L-18.-04	18.04	1.0430	0.3162	0.1112	3.2983	0.3032	1.4280
L-18.-05	18.04	1.0300	0.3138	0.1100	3.2819	0.3047	1.4275
L-18.-06	18.03	1.0066	0.3122	0.1068	3.2240	0.3102	1.4263
L-18.-07	18.03	0.9864	0.3072	0.1048	3.2114	0.3114	1.4234
L-18.-08	18.03	0.9712	0.3039	0.1047	3.1954	0.3129	1.4211
L-18.-09	18.03	0.9970	0.3104	0.1057	3.2116	0.3114	1.3194
L-18.-10	18.03	0.9670	0.3037	0.1047	3.1842	0.3140	1.3194
L-18.-11	18.03	0.9465	0.3012	0.1016	3.1426	0.3182	1.3194
L-18.-12	18.03	0.9219	0.2932	0.1007	3.1444	0.3180	1.3194
L-18.-13	18.03	0.8699	0.2827	0.0999	3.0771	0.3250	1.3181
L-18.-14	18.03	0.8348	0.2745	0.0965	3.0413	0.3288	1.3200
L-18.-15	18.03	0.8122	0.2679	0.0948	3.0317	0.3298	1.3181
L-18.-16	18.03	0.7705	0.2579	0.0926	2.9873	0.3348	1.3200
L-18.-17	18.03	0.7582	0.2542	0.0922	2.9827	0.3353	1.3200
L-18.-18	18.03	0.7222	0.2429	0.0916	2.9727	0.3364	1.3207
L-18.-19	18.03	0.7112	0.2401	0.0912	2.9620	0.3376	1.3207
L-18.-20	18.02	0.6873	0.2309	0.0903	2.9768	0.3359	1.3200
L-18.-21	18.02	0.6848	0.2299	0.0901	2.9792	0.3357	1.3200
L-18.-22	18.02	0.6575	0.2214	0.0900	2.9694	0.3368	1.3207
L-18.-23	18.02	0.6459	0.2177	0.0897	2.9670	0.3370	1.3200
L-18.-24	18.02	0.6129	0.2073	0.0884	2.9565	0.3382	1.3226
L-18.-25	18.02	0.6237	0.2101	0.0884	2.9694	0.3368	1.3226
L-18.-26	18.02	0.5717	0.1933	0.0853	2.9569	0.3382	1.3111

LEGEND
ALPHA GEOMETRIC ANGLE OF ATTACK CORRECTED FOR SHAFT TWIST
CL LIFT COEFFICIENT, NONDIMENSIONALIZED ON UPSTREAM VELOCITY AND MODEL PLANFORM AREA
CDUNC CD(UNCORRECTED), THE UNCORRECTED DRAG COEFFICIENT AS COMPUTED FROM MEASURED DRAG, AND NONDIMENSIONALIZED ON UPSTREAM VELOCITY AND MODEL PLANFORM AREA
CM MOMENT COEFFICIENT, NONDIMENSIONALIZED ON UPSTREAM VELOCITY, MODEL PLANFORM AREA, AND MEAN CHORD
L/D LIFT-TO-DRAG RATIO = CL/CDUNC
D/L DRAG-TO-LIFT RATIO = CDUNC/CL
RN REYNOLDS NUMBER, BASED ON MEAN CHORD

EXPER INVES OF WALL EFFECTS ON SUPERCAVITATING HYDROFOILS OF FINITE SPAN

PRIOR DATA CORRECTED FOR EFFECTS OF IMAGES OF TRAILING VORTEX SYSTEM

RUN NO	ALPHAT	CL	CD	CH	(D/L)	SIGV/AT	SIGC/AT	CL/AT	CD/AT2	CH/AT	SIGV	SIGC	CAVLTH	COMMENTS/REMARKS
L-18.-01	19.34	1.101	0.351	0.119	0.319	3.314	2.587	3.261	3.080	0.353	1.119	0.873	----	
L-18.-02+	19.32	1.082	0.347	0.115	0.320	3.304	2.630	3.209	3.048	0.341	1.114	0.887	0.92	
L-18.-03	19.30	1.068	0.343	0.115	0.321	3.138	2.516	3.170	3.024	0.340	1.057	0.848	----	
L-18.-04+	19.27	1.043	0.339	0.111	0.325	3.158	2.589	3.101	2.994	0.331	1.062	0.871	1.10	
L-18.-05	19.26	1.030	0.336	0.110	0.326	2.975	2.473	3.064	2.973	0.327	1.000	0.831	----	
L-18.-06+	19.23	1.007	0.333	0.107	0.331	2.983	2.507	2.999	2.958	0.318	1.001	0.841	0.87	QUESTIONABLE
L-18.-07	19.20	0.986	0.327	0.105	0.332	2.782	2.399	2.943	2.914	0.313	0.932	0.804	----	
L-18.-08+	19.19	0.971	0.323	0.105	0.333	2.793	2.423	2.900	2.885	0.313	0.935	0.811	0.92	
L-18.-09	19.21	0.997	0.331	0.106	0.332	2.825	2.445	2.973	2.944	0.315	0.947	0.820	----	
L-18.-10+	19.18	0.967	0.323	0.105	0.334	2.814	2.449	2.889	2.884	0.313	0.942	0.820	0.90	
L-18.-11	19.15	0.947	0.320	0.102	0.338	2.627	2.294	2.832	2.862	0.304	0.878	0.767	----	
L-18.-12+	19.12	0.922	0.311	0.101	0.337	2.630	2.345	2.762	2.790	0.302	0.878	0.783	0.95	
L-18.-13	19.06	0.870	0.298	0.100	0.343	2.357	2.135	2.615	2.696	0.300	0.784	0.710	----	
L-18.-14+	19.02	0.835	0.289	0.097	0.346	2.354	2.118	2.515	2.623	0.291	0.781	0.703	1.20	
L-18.-15	18.99	0.812	0.282	0.095	0.347	2.140	1.935	2.451	2.563	0.286	0.709	0.641	----	
L-18.-16+	18.94	0.770	0.270	0.093	0.351	2.139	1.967	2.331	2.473	0.280	0.707	0.650	1.27	
L-18.-17	18.92	0.758	0.266	0.092	0.351	1.964	1.808	2.296	2.439	0.279	0.649	0.597	----	
L-18.-18+	18.88	0.722	0.254	0.092	0.351	1.949	1.843	2.191	2.336	0.278	0.642	0.607	1.68	
L-18.-19	18.87	0.711	0.251	0.091	0.352	1.806	1.780	2.159	2.310	0.277	0.595	0.586	----	
L-18.-20+	18.84	0.687	0.241	0.090	0.350	1.809	1.752	2.090	2.226	0.275	0.595	0.576	1.82	
L-18.-21	18.84	0.685	0.240	0.090	0.350	1.680	1.608	2.083	2.216	0.274	0.552	0.529	----	
L-18.-22+	18.80	0.657	0.230	0.090	0.350	1.681	1.642	2.003	2.139	0.274	0.552	0.539	2.22	
L-18.-23	18.79	0.646	0.226	0.090	0.350	1.538	1.500	1.969	2.104	0.273	0.504	0.492	----	
L-18.-24+	18.75	0.613	0.215	0.088	0.351	1.534	1.497	1.873	2.008	0.270	0.502	0.490	2.70	
L-18.-25	18.76	0.624	0.218	0.088	0.350	1.420	1.384	1.905	2.034	0.270	0.465	0.453	3.90	
L-18.-26+	18.70	0.572	0.200	0.085	0.350	1.465	1.429	1.751	1.878	0.261	0.478	0.466	----	QUESTIONABLE

UNLESS OTHERWISE INDICATED, ALL DATA ARE FOR:
1. SUPERCAVITATING FLOW.
2. BOTH STATIC PRESSURE TAPS OPEN.

LEGEND
+ ONLY UPSTREAM STATIC PRESSURE TAP UTILIZED
* ONLY DNSTREAM STATIC PRESSURE TAP UTILIZED
PC PARTIALLY CAVITATING
PC(TW) PARTIALLY CAVITATING (TAP WETTED)
FW FULLY WETTED
AT (ALPHAT) (TRUE) ANGLE OF ATTACK, CORRECTED FOR EFFECTS OF IMAGES OF TRAILING VORTICES
AT2 ALPHAT**2
SIGC CAVITATION NUMBER COMPUTED WITH MEASURED CAVITY PRESSURE
SIGV CAVITATION NUMBER COMPUTED WITH CALCULATED VAPOR PRESSURE
CD DRAG COEFFICIENT, CORRECTED FOR EFFECTS OF IMAGES OF TRAILING VORTICES
(D/L) CORRECTED DRAG-TO-LIFT RATIO = CD/CL
CAVLTH CAVITY LENGTH MEASURED FROM MIDCHORD AT CENTROID POSITION, NONDIMENSIONALIZED ON MEAN CHORD (OBTAINED FROM PHOTOGRAPHS)

EXPER INVES OF WALL EFFECTS ON SUPERCAVITATING HYDROFOILS OF FINITE SPAN

HYDROFOIL DATA IN NONDIMENSIONAL FORM (NO CORRECTIONS APPLIED)

RUN NO	ALPHA	CL	CDUNC	CM	L/D	D/L	RN*10**-6
L-21.-01	21.03	1.1244	0.4099	0.1257	2.7435	0.3645	1.2848
L-21.-02	21.03	1.1092	0.4053	0.1231	2.7366	0.3654	1.2861
L-21.-03	21.03	1.0950	0.4013	0.1207	2.7288	0.3665	1.2904
L-21.-04	21.03	1.0822	0.3966	0.1181	2.7288	0.3665	1.2911
L-21.-05	21.03	1.0558	0.3907	0.1164	2.7020	0.3701	1.2935
L-21.-06	21.03	1.0264	0.3851	0.1140	2.6655	0.3752	1.2948
L-21.-07	21.03	1.0025	0.3799	0.1121	2.6386	0.3790	1.2942
L-21.-08	21.03	0.9698	0.3720	0.1085	2.6072	0.3836	1.2942
L-21.-09	21.03	0.9616	0.3676	0.1075	2.6161	0.3823	1.2954
L-21.-10	21.03	0.9357	0.3614	0.1060	2.5888	0.3863	1.2954
L-21.-11	21.03	0.9288	0.3594	0.1064	2.5841	0.3870	1.2979
L-21.-12	21.03	0.9044	0.3515	0.1055	2.5729	0.3887	1.2979
L-21.-13	21.03	0.8937	0.3472	0.1039	2.5745	0.3884	1.2991
L-21.-14	21.03	0.8616	0.3384	0.1026	2.5464	0.3927	1.2985
L-21.-15	21.03	0.8498	0.3346	0.1018	2.5397	0.3938	1.3010
L-21.-16	21.03	0.8185	0.3231	0.1015	2.5333	0.3947	1.3010
L-21.-17	21.03	0.8113	0.3191	0.1007	2.5419	0.3934	1.3028
L-21.-18	21.03	0.7844	0.3089	0.1015	2.5398	0.3937	1.3003
L-21.-19	21.03	0.7844	0.3076	0.1015	2.5501	0.3921	1.3003
L-21.-20	21.03	0.7471	0.2955	0.1010	2.5281	0.3955	1.3003
L-21.-21	21.03	0.7471	0.2935	0.1005	2.5460	0.3928	1.3034
L-21.-22	21.03	0.6995	0.2759	0.0973	2.5354	0.3944	1.3022
L-21.-23	21.02	0.8495	0.3319	0.1038	2.5595	0.3907	1.1471
L-21.-24	21.02	0.8148	0.3202	0.1029	2.5450	0.3929	1.1485

LEGEND
- ALPHA GEOMETRIC ANGLE OF ATTACK CORRECTED FOR SHAFT TWIST
- CL LIFT COEFFICIENT, NONDIMENSIONALIZED ON UPSTREAM VELOCITY AND MODEL PLANFORM AREA
- CDUNC CD(UNCORRECTED), THE UNCORRECTED DRAG COEFFICIENT AS COMPUTED FROM MEASURED DRAG, AND NONDIMENSIONALIZED ON UPSTREAM VELOCITY AND MODEL PLANFORM AREA
- CM MOMENT COEFFICIENT, NONDIMENSIONALIZED ON UPSTREAM VELOCITY, MODEL PLANFORM AREA, AND MEAN CHORD
- L/D LIFT-TO-DRAG RATIO = CL/CDUNC
- D/L DRAG-TO-LIFT RATIO = CDUNC/CL
- RN REYNOLDS NUMBER, BASED ON MEAN CHORD

EXPER INVES OF WALL EFFECTS ON SUPERCAVITATING HYDROFOILS OF FINITE SPAN

PRIOR DATA CORRECTED FOR EFFECTS OF IMAGES OF TRAILING VORTEX SYSTEM

RUN NO	ALPHAT	CL	CD	CM	(D/L)	SIGV/AT	SIGC/AT	CL/AT	CD/AT2	CM/AT	SIGV	SIGC	CAVLTH	COMMENTS/REMARKS
L-21.-01	22.37	1.124	0.436	0.126	0.389	3.347	2.471	2.880	2.861	0.322	1.307	0.965	----	
L-21.-02*	22.35	1.109	0.431	0.123	0.388	3.342	2.509	2.844	2.831	0.316	1.304	0.979	1.22	
L-21.-03	22.33	1.095	0.426	0.121	0.389	3.104	2.317	2.810	2.805	0.310	1.210	0.903	----	
L-21.-04*	22.32	1.082	0.421	0.118	0.389	3.098	2.412	2.778	2.774	0.303	1.203	0.939	1.28	
L-21.-05	22.28	1.056	0.414	0.116	0.392	2.835	2.270	2.715	2.736	0.299	1.103	0.883	----	
L-21.-06*	22.25	1.026	0.407	0.114	0.396	2.833	2.351	2.643	2.698	0.294	1.100	0.913	1.30	
L-21.-07	22.22	1.002	0.401	0.112	0.400	2.580	2.152	2.585	2.664	0.289	1.001	0.835	----	
L-21.-08*	22.18	0.970	0.391	0.109	0.404	2.584	2.197	2.505	2.612	0.280	1.000	0.851	1.50	
L-21.-09	22.17	0.962	0.387	0.107	0.402	2.402	2.126	2.485	2.583	0.278	0.929	0.823	----	
L-21.-10*	22.14	0.936	0.380	0.106	0.406	2.404	2.129	2.422	2.542	0.274	0.929	0.823	1.30	
L-21.-11	22.13	0.929	0.377	0.106	0.406	2.273	1.999	2.404	2.529	0.275	0.878	0.772	----	
L-21.-12*	22.10	0.904	0.368	0.105	0.407	2.275	2.056	2.344	2.476	0.273	0.877	0.793	1.25	
L-21.-13	22.09	0.894	0.364	0.104	0.407	2.094	1.891	2.318	2.447	0.269	0.807	0.729	----	
L-21.-14*	22.05	0.862	0.354	0.103	0.411	2.112	1.950	2.239	2.388	0.267	0.813	0.751	1.30	
L-21.-15	22.04	0.850	0.350	0.102	0.411	1.969	1.822	2.210	2.363	0.265	0.757	0.701	----	
L-21.-16*	22.00	0.819	0.337	0.102	0.412	1.971	1.852	2.132	2.286	0.264	0.757	0.711	1.55	
L-21.-17	21.99	0.811	0.333	0.101	0.410	1.816	1.712	2.114	2.259	0.262	0.697	0.657	----	
L-21.-18*	21.96	0.784	0.322	0.101	0.410	1.825	1.776	2.047	2.189	0.265	0.699	0.680	1.65	
L-21.-19	21.96	0.784	0.320	0.101	0.408	1.687	1.653	2.047	2.181	0.265	0.647	0.633	----	
L-21.-20*	21.91	0.747	0.307	0.101	0.411	1.689	1.656	1.953	2.099	0.264	0.646	0.633	1.80	
L-21.-21	21.91	0.747	0.305	0.101	0.408	1.531	1.499	1.953	2.085	0.263	0.586	0.573	----	
L-21.-22*	21.86	0.700	0.286	0.097	0.409	1.550	1.519	1.834	1.965	0.255	0.591	0.580	3.15	
L-21.-23	22.03	0.849	0.347	0.104	0.408	1.981	1.943	2.209	2.346	0.270	0.762	0.747	----	
L-21.-24*	21.99	0.815	0.334	0.103	0.410	1.961	1.924	2.123	2.267	0.268	0.752	0.738	1.50	

UNLESS OTHERWISE INDICATED, ALL DATA ARE FOR:
1. SUPERCAVITATING FLOW.
2. BOTH STATIC PRESSURE TAPS OPEN.

LEGEND
* ONLY UPSTREAM STATIC PRESSURE TAP UTILIZED
* ONLY DNSTREAM STATIC PRESSURE TAP UTILIZED
PC PARTIALLY CAVITATING
PC(TW) PARTIALLY CAVITATING (TAP WETTED)
FW FULLY WETTED
AT (ALPHAT) (TRUE) ANGLE OF ATTACK, CORRECTED FOR EFFECTS OF IMAGES OF TRAILING VORTICES
AT2 ALPHAT**2
SIGC CAVITATION NUMBER COMPUTED WITH MEASURED CAVITY PRESSURE
SIGV CAVITATION NUMBER COMPUTED WITH CALCULATED VAPOR PRESSURE
CD DRAG COEFFICIENT, CORRECTED FOR EFFECTS OF IMAGES OF TRAILING VORTICES
(D/L) CORRECTED DRAG-TO-LIFT RATIO = CD/CL
CAVLTH CAVITY LENGTH MEASURED FROM MIDCHORD AT CENTROID POSITION, NONDIMENSIONALIZED ON MEAN CHORD (OBTAINED FROM PHOTOGRAPHS)

M.I.T., Department of Ocean Engineering,
Report 83481-3

An Experimental Investigation of Wall Effects on Supercavitating Hydrofoils of Finite Span, by Michael R. Maixner, July 1977, 130 pages, illustrated.

UNCLASSIFIED

A geometrically similar family of three supercavitating hydrofoils was tested in the M.I.T. variable pressure water tunnel. The half-span foils were of elliptical planform; the ratio of foil half-span to tunnel height was 1/4 for the small foil, 1/2 for the medium foil, and 3/4 for the largest foil. The tunnel was of square cross section. Lift, drag, moment, tunnel speed, ambient pressure, and cavity pressure were measured for attack angles from 8 to 21 degrees and a variety of ambient pressure settings; cavity length measurements were obtained from photographs. Results were compared with theoretical results obtained by Leehey, and also with a more detailed numerical lifting surface procedure developed by Jiang and Leehey. For the small and medium foils it was sufficient to correct only for the effect on downwash of the images of the trailing vortices. The large foil data, however, required further correction; upon application of the same corrections which were applied to the data for the two smaller foils, the force and moment data for the large foil plotted slightly lower than did the data for the two smaller foils, while the cavity length data for the large foil indicated cavity lengths significantly larger than for either of the theoretical predictions or the cavity length data for the two smaller foils. Through the application of existing two-dimensional corrections, the force data for the large foil were brought into close agreement with the force data for the two smaller foils, but no suitable correction factors exist for the cavity length data.

Cavity Flow
Hydrofoils
Wall Effects

M.I.T., Department of Ocean Engineering,
Report 83481-3

An Experimental Investigation of Wall Effects on Supercavitating Hydrofoils of Finite Span, by Michael R. Maixner, July 1977, 130 pages, illustrated.

UNCLASSIFIED

A geometrically similar family of three supercavitating hydrofoils was tested in the M.I.T. variable pressure water tunnel. The half-span foils were of elliptical planform; the ratio of foil half-span to tunnel height was 1/4 for the small foil, 1/2 for the medium foil, and 3/4 for the largest foil. The tunnel was of square cross section. Lift, drag, moment, tunnel speed, ambient pressure, and cavity pressure were measured for attack angles from 8 to 21 degrees and a variety of ambient pressure settings; cavity length measurements were obtained from photographs. Results were compared with theoretical results obtained by Leehey, and also with a more detailed numerical lifting surface procedure developed by Jiang and Leehey. For the small and medium foils it was sufficient to correct only for the effect on downwash of the images of the trailing vortices. The large foil data, however, required further correction; upon application of the same corrections which were applied to the data for the two smaller foils, the force and moment data for the large foil plotted slightly lower than did the data for the two smaller foils, while the cavity length data for the large foil indicated cavity lengths significantly larger than for either of the theoretical predictions or the cavity length data for the two smaller foils. Through the application of existing two-dimensional corrections, the force data for the large foil were brought into close agreement with the force data for the two smaller foils, but no suitable correction factors exist for the cavity length data.

Cavity Flow
Hydrofoils
Wall Effects

M.I.T., Department of Ocean Engineering,
Report 83481-3

An Experimental Investigation of Wall Effects on Supercavitating Hydrofoils of Finite Span, by Michael R. Maixner, July 1977, 130 pages, illustrated.

UNCLASSIFIED

A geometrically similar family of three supercavitating hydrofoils was tested in the M.I.T. variable pressure water tunnel. The half-span foils were of elliptical planform; the ratio of foil half-span to tunnel height was 1/4 for the small foil, 1/2 for the medium foil, and 3/4 for the largest foil. The tunnel was of square cross section. Lift, drag, moment, tunnel speed, ambient pressure, and cavity pressure were measured for attack angles from 8 to 21 degrees and a variety of ambient pressure settings; cavity length measurements were obtained from photographs. Results were compared with theoretical results obtained by Leehey, and also with a more detailed numerical lifting surface procedure developed by Jiang and Leehey. For the small and medium foils it was sufficient to correct only for the effect on downwash of the images of the trailing vortices. The large foil data, however, required further correction; upon application of the same corrections which were applied to the data for the two smaller foils, the force and moment data for the large foil plotted slightly lower than did the data for the two smaller foils, while the cavity length data for the large foil indicated cavity lengths significantly larger than for either of the theoretical predictions or the cavity length data for the two smaller foils. Through the application of existing two-dimensional corrections, the force data for the large foil were brought into close agreement with the force data for the two smaller foils, but no suitable correction factors exist for the cavity length data.

Cavity Flow
Hydrofoils
Wall Effects

M.I.T., Department of Ocean Engineering,
Report 83481-3

An Experimental Investigation of Wall Effects on Supercavitating Hydrofoils of Finite Span, by Michael R. Maixner, July 1977, 130 pages, illustrated.

UNCLASSIFIED

A geometrically similar family of three supercavitating hydrofoils was tested in the M.I.T. variable pressure water tunnel. The half-span foils were of elliptical planform; the ratio of foil half-span to tunnel height was 1/4 for the small foil, 1/2 for the medium foil, and 3/4 for the largest foil. The tunnel was of square cross section. Lift, drag, moment, tunnel speed, ambient pressure, and cavity pressure were measured for attack angles from 8 to 21 degrees and a variety of ambient pressure settings; cavity length measurements were obtained from photographs. Results were compared with theoretical results obtained by Leehey, and also with a more detailed numerical lifting surface procedure developed by Jiang and Leehey. For the small and medium foils it was sufficient to correct only for the effect on downwash of the images of the trailing vortices. The large foil data, however, required further correction; upon application of the same corrections which were applied to the data for the two smaller foils, the force and moment data for the large foil plotted slightly lower than did the data for the two smaller foils, while the cavity length data for the large foil indicated cavity lengths significantly larger than for either of the theoretical predictions or the cavity length data for the two smaller foils. Through the application of existing two-dimensional corrections, the force data for the large foil were brought into close agreement with the force data for the two smaller foils, but no suitable correction factors exist for the cavity length data.

Cavity Flow
Hydrofoils
Wall Effects